



INSTITUTO DE  
TECNOLOGÍA  
QUÍMICA



EXCELENCIA  
SEVERO  
OCHOA



UNIVERSITAT  
POLITÈCNICA  
DE VALÈNCIA



UNIVERSITAT POLITÈCNICA DE VALÈNCIA

DEPARTAMENTO DE QUÍMICA

INSTITUTO UNIVERSITARIO MIXTO DE TECNOLOGÍA QUÍMICA (UPV-CSIC)

---

DOCTORAL THESIS

# 2'-Methoxyacetophenone as DNA Photosensitiser for Mono and Biphotonic Processes

---

Ofelia Rodríguez Alzueta

Supervisors:

Prof. Miguel Ángel Miranda Alonso

Dr. M<sup>a</sup> Consuelo Cuquerella Alabort

Valencia, September 2020



## CERTIFICATION

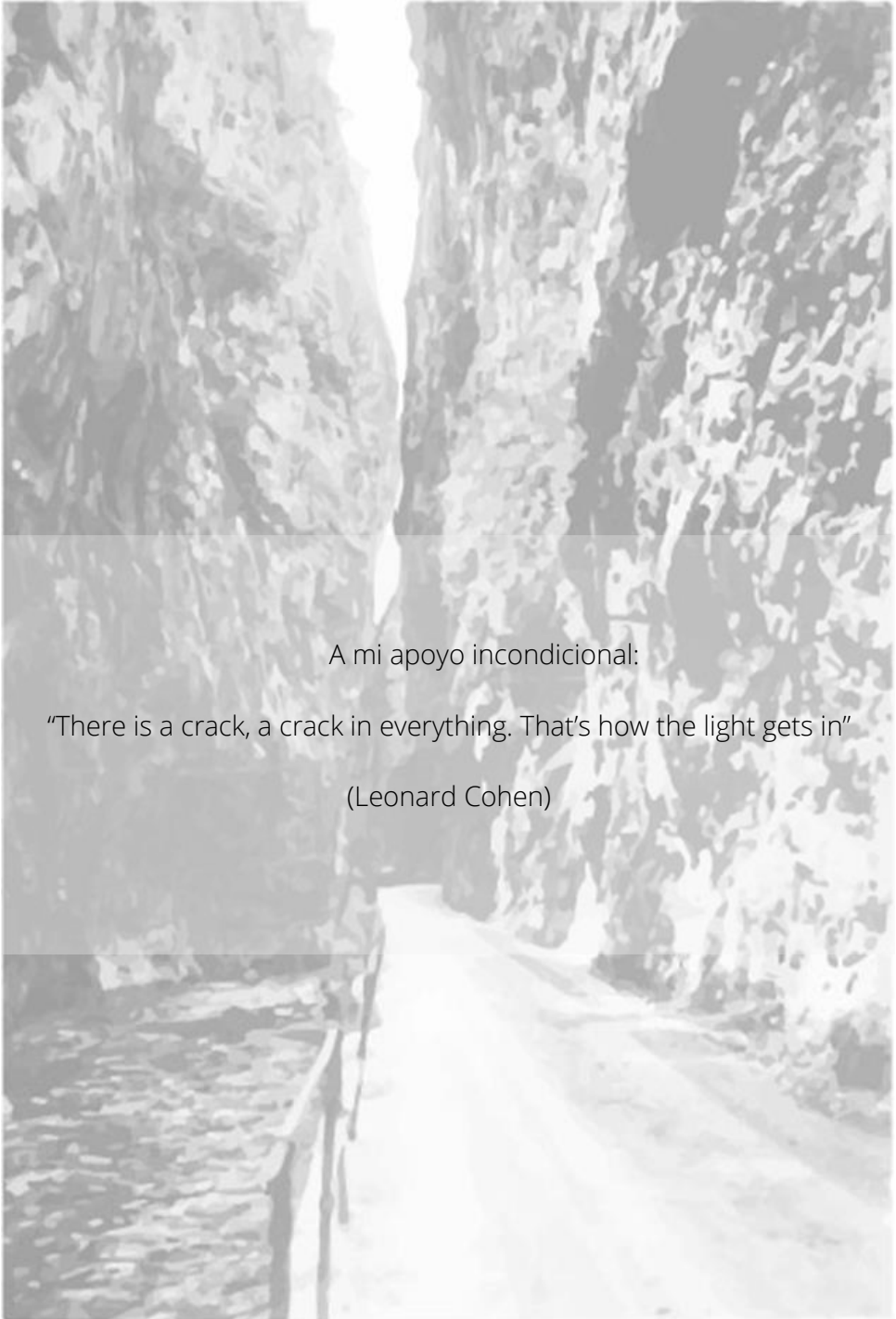
Miguel Ángel Miranda Alonso, Full Professor of the Universitat Politècnica de València (UPV) and M<sup>a</sup> Consuelo Cuquerella Alabort senior Researcher at UPV,

CERTIFY that the Doctoral Thesis entitled "2'-Methoxyacetophenone as DNA Photosensitiser for Mono and Biphotonic Processes" has been developed by Ofelia Rodríguez Alzueta under their supervision in the Instituto Universitario Mixto de Tecnología Química (UPV-CSIC).

Prof. Miguel Ángel Miranda Alonso

Dr. M<sup>a</sup> Consuelo Cuquerella Alabort





A mi apoyo incondicional:

“There is a crack, a crack in everything. That’s how the light gets in”

(Leonard Cohen)



# Symbols and Abbreviations

---

A / Ade	Adenine
$\Delta A$	Absorbance variation
AC	Acetone
ACN	Acetonitrile
ANFX	4'-N-acetyl derivative of norfloxacin
AP	Acetophenone
BP	Benzophenone
BR	Biradical
BSC	Basal cell carcinoma
C / Cyt	Cytosine
c	Speed of light
$CDCl_3$	Deuterated chloroform
Cg	Cytosine glycol
CMM	Cutaneous malignant melanoma
CPDs	Cyclobutane pyrimidine dimers
$\delta$	Chemical shift
DEWs	Dewar valence isomers

## *Symbols and Abbreviations*

---

DMF	N, N'- Dimethylformamide
DMSO-d <sub>6</sub>	Deuterated dimethyl sulfoxide
DNA	Deoxyribonucleic acid
(d <sub>T</sub> ) <sub>18</sub>	Thymine oligonucleotide
E	Energy
$\epsilon$	Molar absorption coefficient
$\Delta E$	Energy gap
EA	Electron affinity
ESI	Electrospray ionization
E <sub>T</sub>	Triplet energy
EtOH	Ethanol
eV	Electronvoltio
F	Fluorescence emission
FapyG	2,6-Diamino-4-hydroxy-5-formamido-pyrimidine
FB	Fenofibrate
ForU	5-Formyluracil
fs	Femtosecond
$\Phi_{\Delta}$	Singlet oxygen quantum yield
$\Phi_{ISC}$	Intersystem crossing quantum yield
$\Phi_{Phos}$	Phosphorescence quantum yield
G / Gua	Guanine

$G^{\bullet+}$	Guanine radical cation
$\Delta G$	Gibbs free energy
$h$	Plancks' constant
HD	Hydrogen donor
HH	Head-to-head
HmUra	5-Hydroxymethyl-uracil
HOMO	Highest occupied molecular orbital
HPLC	High-performance liquid chromatography
HRMS	High-resolution mass spectroscopy
HT	Head-to-tail
Hz	Hertz
$h\nu$	Photon
I	Common reactive intermediate
IC	Internal conversion
IP	Ionisation potential
IR	Infrared
ISC	Intersystem crossing
J	Jules
$J$	Coupling constants
$k_D$	Diffusion rate constant
$k_{ET}$	Rate constant for energy transfer

## *Symbols and Abbreviations*

---

$k_q$	Quenching constant
$\lambda$	Wavelength of the radiation
$\lambda_{exc}$	Excitation wavelength
LC	Liquid chromatography
LFP	Laser flash photolysis
LUMO	Lowest unoccupied molecular orbital
M	Molecule in an initial state
$M^*$	Molecule in an excited state
2M	2'-Methoxyacetophenone
MeOH	Methanol
mM	Milimolar
MOs	Molecular orbitals
$\mu s$	Microsecond
ms	Milisecond
$\nu$	Frecuency
NADPH	Nicotinamide adenine dinucleotide phosphate
NFX	Norfloxacin
NIR	Near infrared
nm	Namometers
NMR	Nuclear magnetic resonance
NMSC	Non-melanoma skin cancers

ns	Nanosecond
NSAIDS	Non-steroidal anti-inflammatory drugs
$^1\text{O}_2$	Singlet oxygen
$\bullet\text{OH}$	Hydroxyl radical
8-oxoG	8-Oxo-7,8-dehydroguanine
P	Observed product
PAR	Photosynthetically active radiation
PB	Phosphate buffer solution
PE	Potential energy
Phos	Phosphorescence emission
Phs	Photosensitiser
PMT	Photomultiplier tube
6-4 PPs	(6-4 PPs) Pyrimidine (6-4) pyrimidone adducts
ppm	Parts per million
ps	Picosecond
PUVA	Psolaren and ultraviolet A therapy
Pyr	Pyrimidine
R	Second molecular species
R	Universal gas constant
$\text{R}_1\text{COR}_2^*$	Carbonyl excited state
RI	Radical ions intermediates

## *Symbols and Abbreviations*

---

RNA	Ribonucleic acid
ROS	Reactive oxygen species
RP	Radical pair
$S_0$	Molecule lowest-energy electronic ground state
SCC	Squamous cell carcinoma
S-FB	S-Flurbiprofen
$S_n$	Singlet excited states
T / Thy	Thymine
T	Temperature
$\tau$	Lifetime
$\tau_T$	Triplet lifetime
TAS	Transient absorption spectroscopy
<i>t</i> BU	<i>tert</i> -Butyluracil
Tg	Thymine glycol
Thd	Thymidine
TLC	Thin-layer liquid chromatography
TMP	Thymine nucleotide
$T_n$	Triplet excited states
TOF	Time of flight
TpT	Thymine dinucleotide
TTET	Triplet-triplet energy transfer

U / Ura	Uracil
UPLC-MS/MS	Ultra performance liquid chromatography tandem mass spectrometer
UV	Ultraviolet light
UVA	Ultraviolet A light (315-400 nm)
UVB	Ultraviolet B light (280-315 nm)
UVC	Ultraviolet C light (<280 nm)
UV-Vis	Ultraviolet-Visible



# Outline

---

---

<i>Preface</i>	<i>i</i>
<b>Chapter 1. Introduction</b>	<b>1</b>
1.1. Photochemistry of Organic Molecules	3
1.2. Photochemistry of Carbonyl Compounds	7
1.2.1. Hydrogen Abstraction	8
1.2.1.1. Intermolecular Hydrogen Abstraction	8
1.2.1.2. Intramolecular Hydrogen Abstraction	9
1.2.2. [2+2] Photocycloadditions	10
1.2.2.1. Cyclobutane Formation	10
1.2.2.2. Oxetane Formation	12
<b>1.3. Nucleic Acid Damage and Skin Cancer Induced by UV light.</b>	<b>13</b>
1.3.1. Solar Light Duality: Beneficial and Harmful	15
1.3.2. Photoinduced DNA Lesions	17
1.3.2.1. Direct DNA Damage	18
1.3.2.1.1. Cyclobutane Pyrimidine Dimers	18
1.3.2.1.2. Pyrimidine (6-4) Pyrimidone Adducts and Dewar Valence Isomers	22
1.3.2.1.3. Other Photoproducts	24
1.3.2.2. Indirect DNA Damage: Photosensitisation	25
1.3.2.2.1. Cyclobutane Pyrimidine Dimers	27

## Outline

---

1.3.2.2.2. Photosensitisers	30
<b>1.4. Photophysics</b>	<b>34</b>
1.4.1. Transient Absorption Spectroscopy	34
1.4.2. Upper Triplet Excited States: Two Photon Photochemistry	38
<b>1.5. References</b>	<b>41</b>
<b>Chapter 2. General Objectives</b>	<b>55</b>
<b>Chapter 3. Transient UV-Vis Absorption Spectroscopic Characterisation of 2'-Methoxyacetophenone as a DNA Photosensitiser</b>	<b>59</b>
3.1. Introduction	61
3.2. Results and Discussion	62
3.3. Conclusions	69
3.4. Experimental Section	70
3.4.1. Synthesis and Characterisation	70
3.4.2. Irradiation Procedures	73
3.4.3. Laser Flash Photolysis	73
3.5. References	74
<b>Chapter 4. Triplet Energy Transfer versus Excited State Cyclisation as the Controlling Step in Photosensitised Bipyrimidine Dimerisation</b>	<b>77</b>
4.1. Introduction	79
4.2. Results and Discussion	81
4.3. Conclusions	92
4.4. Experimental Section	93
4.4.1. Synthesis and Characterisation	93
4.4.1.1. Compounds 2 a-c	93
4.4.1.2. Compounds 3 and 3'	94
4.4.1.3. Compounds 4 a,b	98

---

4.4.1.4. Compounds 5	103
4.4.1.5. Compounds 6	110
4.4.2. Irradiation Procedures	118
4.4.2.1. Photosensitised Irradiation with Acetone in H <sub>2</sub> O	118
4.4.2.2. Analytical 2'-Methoxyacetophenone Photosensitised Irradiation	133
4.4.2.3. Preparative 2'-Methoxyacetophenone Photosensitised Irradiation	133
4.4.3. Absorption Spectra	133
4.4.4. Phosphorescence Spectroscopy	134
4.4.5. Phosphorescence Spectroscopy	134
4.5. Annex	135
4.6. References	144
<i>Chapter 5. Photosensitised Biphotonic Chemistry of Pyrimidine Derivatives</i>	<i>147</i>
5.1. Introduction	149
5.2. Results and Discussion	153
5.3. Conclusions	158
5.4. Experimental Section	158
5.4.1. Synthesis and Characterisation	158
5.4.2. Irradiation Procedures and Spectral Measurements	164
5.4.2.1. High Energy Photosensitised Irradiations	164
5.4.2.2. Control experiment: Irradiation in the absence of photosensitiser	164
5.4.2.3. Steady-State Monochromatic Irradiations	165
5.4.2.4. Securing equivalent photon fluxes in the laser and Xe-lamp irradiation	165
5.4.3. Spectral Measurements	166
5.5. References	167

<b>Chapter 6.</b>	<b><i>Instrumentation</i></b>	<b>171</b>
6.1.	<b>General Instrumentation</b>	<b>173</b>
6.1.1.	Nuclear Magnetic Resonance (NMR)	173
6.1.2.	Chromatography	173
6.1.2.1.	Thin-Layer Liquid Chromatography (TLC) and Liquid Chromatography (LC)	173
6.1.2.2.	Ultra Performance Liquid Chromatography Tandem Mass Spectrometer (UPLC-MS/MS)	173
6.2.	<b>Photochemical Instrumentation</b>	<b>174</b>
6.2.1.	UV-VIS Absorption Spectroscopy	174
6.2.2.	Steady-State Photolysis	174
6.2.3.	Laser Flash Photolysis Spectroscopy (LFP)	174
6.2.4.	Phosphorescence Emission Measurements	175
<b>Chapter 7.</b>	<b><i>General Conclusions</i></b>	<b>177</b>
<b>Chapter 8.</b>	<b><i>Summary-Resumen-Resum</i></b>	<b>183</b>
8.1.	Summary	185
8.2.	Resumen	187
8.3.	Resum	189
<b>Chapter 9.</b>	<b><i>Scientific Contribution</i></b>	<b>191</b>
9.1.	Contribution to Congresses	193
9.2.	Publications	193

# Preface

---

Since the beginning of time, the sun has been the object of cult and fascination due to its crucial importance for the maintenance and sustenance of life on Earth. This star is the heart of our solar system and represents our main source of energy, providing the heat and light necessary for survival.

Solar radiation reaching the Earth's surface comprises wavelengths ranging from 290 to 320 nm (UVB), 320 to 400 nm (UVA), visible light and infrared radiation. Both, UVB and UVA radiations, have been demonstrated to induce mutations in DNA that may be in the origin of cancer. This occurs when molecules in living cells absorb photons of these wavelengths and they are promoted to excited states, from which chemical transformations occur.

If these lesions are not effectively repaired or damaged cells are not eliminated by apoptosis or necrosis, deleterious processes as mutagenesis or carcinogenesis may be fostered, leading ultimately to cancer. In fact, skin cancer is one of the most common nowadays, being of special concern its severe increase all around the world.

This worrying tendency is associated in a great extend with our outdoor lifestyle, less clothing cover (more skin exposed), and tanning popularity. Despite awareness campaigns focused on prevention and early detection programs, individuals continue to experiment the drawbacks of excessive

sun exposure, having become skin cancer risk in a major public health problem.

The scientific community has joined government's efforts to reduce this cancer prevalence and mortality. Thus, an intense research work has been dedicated to unveil the mechanism responsible for DNA photolesions formation and repair together with proliferation to malignant tumours.

In this context, the present Thesis has been devoted to study DNA damage, more concretely photosensitised DNA damage, commonly related with UVA light absorption which is not directly absorbed by the biomolecule, but by endogenous or exogenous chromophores present in drugs, cosmetic agents, metabolites, etc. Following UVA light absorption, different excited states are populated from which chemical reactions can occur and may modify the chemical integrity of the DNA. Thus, the in principle less dangerous UVA-radiation (scarcely absorbed by DNA), has been related also with photocarcinogenesis.

For this purpose, different DNA models of increasing complexity have been synthesised in this Thesis, and their photosensitisation with acetophenone and benzophenone derivatives investigated through intermolecular approaches. In addition, the influence of low and high intensity irradiation has also been taken into account.

Thus, a good knowledge of the principles of organic (photo)chemistry, with special attention to the carbonyl/enone groups, which photoreactivity is intimately related to UV damage to pyrimidine DNA bases, is required. Therefore, a thorough review of direct and photosensitised damage to DNA will be presented along the following sections.

# CHAPTER 1

## Chapter 1. Introduction

---



## 1.1. Photochemistry of Organic Molecules

Over time, photochemistry has become a mature science that studies the net chemical and physical changes resulting from the interaction of matter with light ranging from ultraviolet (UV) to near infrared (200-800 nm).

The first law of photochemistry (Grotthuss-Draper) states that only absorbed light is effective in photochemical transformations. Furthermore, light is a form of energy which exhibits dual wave-particle nature and whose energy is quantised in small packets called photons ( $h\nu$ ). Thus, light absorption is a quantum process where usually one photon is absorbed by a single molecule as establishes the second law of photochemistry (Stark-Einstein).

The energy transferred to a molecule after absorption of light (photon energy) can be easily calculated by the Einstein equation (Equation 1.1):

$$E = h\nu = hc/\lambda$$

*Equation 1.1 Einstein equation where  $h$  is Plancks' constant,  $\lambda$  wavelength of the radiation and  $c$  the speed of light.*

Therefore, if this energy is higher than the energy gap ( $\Delta E$ ) between two states of a molecule ( $M$ ), a promotion to an electronically excited state ( $M^*$ ) can be achieved (Equation 1.2).

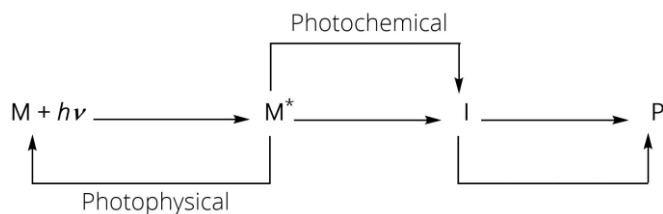
$$\Delta E = |E_2 - E_1| = |E_2(M^*) - E_1(M)| = h\nu = hc/\lambda$$

*Equation 1.2 Einstein's resonance condition for the absorption of light, where  $E_2$  and  $E_1$  are the energies of a molecule in an excited ( $M^*$ ) and an initial ( $M$ ) state, respectively.*

Excited states are formally isomers of the molecule lowest-energy electronic ground state ( $S_0$ ). They constitute the essential species universal to all photochemical and photophysical processes. Once an excited species

---

is populated (upon light absorption) it can either react leading to new products ( $P$ ) or just decay to the ground state with the regeneration of the starting material ( $M$ ), respectively (Scheme 1.1).<sup>1-4</sup>



*Scheme 1.1 Schematic representation of the overall photochemical ( $M^* \rightarrow P$ ) and photophysical ( $M^* \rightarrow M$ ) pathways of  $M$ , where  $I$  represents the common reactive intermediates (radical pairs, biradicals, zwitterionic species, carbenes, etc) that undergo conventional thermal processes leading to the observed product ( $P$ ).*

In order to understand the photochemistry of the common functional groups of organic chemistry (carbonyl, olefinic, enone, aromatic compounds, etc), which corresponds to the main chromophores where the absorption proceeds, two aspects need to be considered:

- 1) The electron configurations of the highest occupied molecular orbital (HOMO) and the lowest unoccupied molecular orbital (LUMO).
- 2) The spin configurations of the electrons in the HOMO and LUMO for the key structures:  $M$ ,  $M^*$ ,  $I$  and  $P$  (Scheme 1.1).

The electronic configuration of the ground states of  $M$  and  $P$  is generally  $(\text{HOMO})^2(\text{LUMO})^0$  for ordinary organic molecules with the two electrons' spin paired (Pauli exclusion principle), and is termed *singlet spin configuration* or *singlet state*.

However, in the case of  $M^*$  and  $I$ , the electronic configuration typically possesses one electron in each of the molecular orbitals (MOs) that can be either paired ( $\uparrow\downarrow$ , singlet states) or unpaired ( $\uparrow\uparrow$ , triplet states). In the case of

radicals or radical ions the unpaired electron represents a doublet. Transitions between any two electronic states can be rationalised with the help of state energy diagrams, that are sometimes referred as Jablonski diagrams (Figure 1.1).<sup>5</sup>

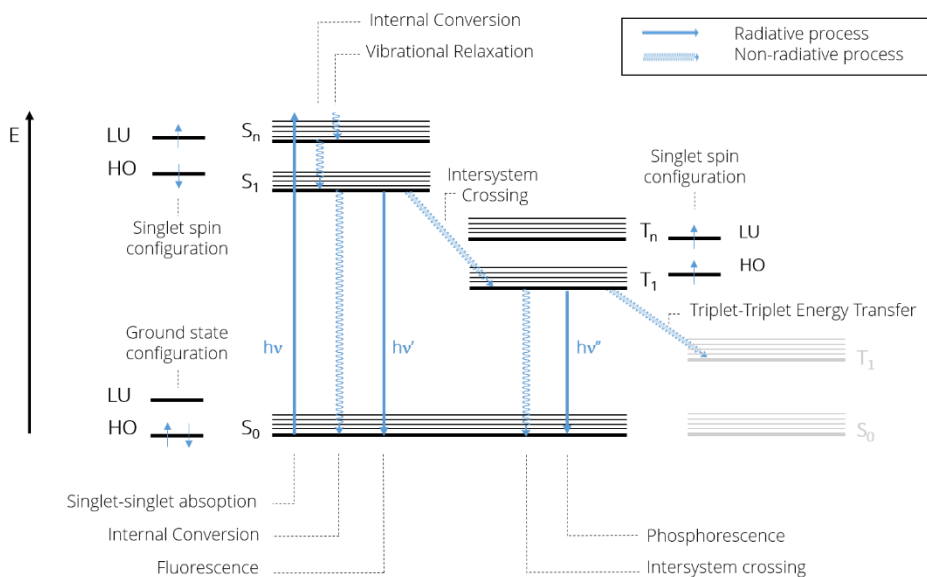


Figure 1.1 Simplified Jablonski Diagram.

In a state diagram the Y axis corresponds to the potential energy (PE) of the system in which relative energies are displayed. The different possible excited electronic states ( $S_1$ ,  $S_2$ ,  $T_1$ ,  $T_2$ ,  $T_n$ ) are then located in this diagram starting with the  $S_0$ , also known as the zero-point of the system. Then, all the transitions between states, that may be radiative or non-radiative, are represented through arrows, straight or wavy, respectively.

Thus, as shown by the diagram, the absorption of a photon by a molecule in its ground state, promotes an electron from the HOMO to the LUMO, reaching an excited electronic state,  $S_n$ . In the case of higher-energy

singlet states, excitation generally results in deactivation to  $S_1$  (Kasha's rule) through an internal conversion (IC). As this is an allowed transition typically happens in the order of a few pico to femtoseconds, due to the low energy gap between the different  $S_n$ , until the  $S_1$  is reached. Similarly, higher-energy triplet states  $T_n$  deactivate to  $T_1$  in the order of femto or picoseconds through IC.

At the same time, any of the vibrational levels in  $S_1$  can be reached by the electron, but an ultrafast process (picosecond range), called vibrational relaxation, favours preferably the lowest vibrational one. The lifetime ( $\tau$ ) of the molecule at the  $S_1$  is normally in the nanosecond scale and can deactivate to the ground state by non-radiative (IC) or radiative processes (fluorescence emission, F).

Another possible decay pathway involves spin-forbidden radiationless transitions between excited states of different spin ( $S_1 \rightarrow T_1$  or  $T_n$ ), in a process called intersystem crossing (ISC). Triplet excited states are longer-lived (with  $\tau$  ranging from  $\mu\text{s}$  to ms) than singlet excited states and can decay to the ground state also through non-emissive (ISC) or radiative deactivation (phosphorescence emission, Phos).

In addition, interaction between an electronically excited state ( $M^*$ ) and a second molecular species ( $R$ ) can lead to competitive photochemical processes. Electron and energy transfer, are two of the most important interactions that can take place along with other reactions as photocycloadditions.<sup>2,3,6</sup>

This Thesis will focus on the photosensitised damage to pyrimidine DNA bases, whose photochemistry is intimately related with that of the carbonyl group/enone moiety they possess. In this context, a deep knowledge of [2+2] photocycloadditions yielding cyclobutanes and oxetanes

(Paternò-Büchi reaction), as well as hydrogen abstraction, leading to Norrish-Yang photocycloadditions, is needed.

## 1.2. Photochemistry of Carbonyl Compounds

Often, carbonyl containing compounds have excellent UV absorption properties, thermal stability and wide reactivity, being popular starting materials in applied synthetic photochemistry to perform transformations through direct excitation, normally under UV-light irradiation. Nevertheless, they can also absorb visible-light, which makes them photosensitisers, photoinitiators and photocatalysts extensively used. As a result, their photochemistry, especially related to ketones and aldehydes, is well understood.<sup>2,7</sup>

The photoreactivity of the carbonyl compounds is markedly affected by the nature of their excited states. Some of the properties of these excited states, that normally lead to radical pairs (RP), biradicals (BR) or radical ion intermediates (RI), are enumerated below:<sup>2</sup>

- a) A  $R_1COR_2^*$  ( $n,\pi^*$ ) electronic state is generally much more reactive than the  $R_1COR_2^*$  ( $\pi,\pi^*$ ) electronic state of comparable energy for a given process:  $R_1COR_2^* \rightarrow I$ . Among all the states, the  $T_1^*$  ( $n,\pi^*$ ) is the most commonly observed.
- b) A  $R_1COR_2^*$  ( $\pi,\pi^*$ ) electronic state is usually more energetic than a  $R_1COR_2^*$  ( $n,\pi^*$ ), although this may change as in some cases both states lie close in energy. This may vary changing the polarity of the solvent or the substitution of aromatic ketones<sup>8</sup>.
- c) The  $R_1COR_2^*$  ( $n,\pi^*$ ) states may be localised on the C=O group, although depending on the substituent, the  $\pi^*$  electron may be delocalised over conjugated atoms.

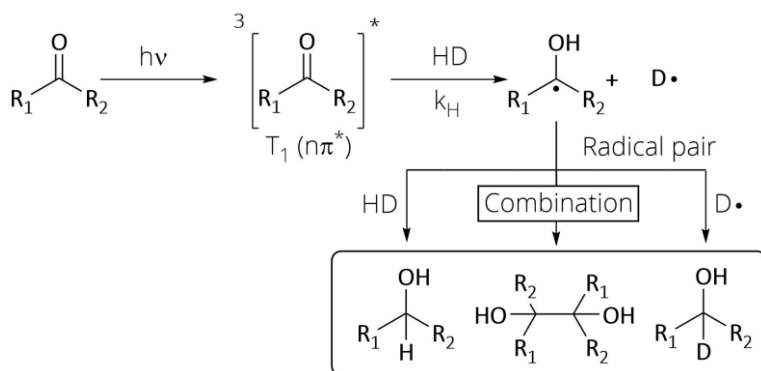
### 1.2.1. Hydrogen Abstraction

A vast variety of carbonyl compounds can be involved in intermolecular or intramolecular hydrogen atom abstraction from a hydrogen donor (HD). This reaction involves two consecutive intermediates: first an excited state and then a radical pair (intermolecular) or a biradical (intramolecular).

Although, two multiplicities of the carbonyl excited state have been shown to display reactivity (singlet and triplet), this process generally occurs from the  $T_1$  with  $n\pi^*$  electronic configuration.

#### 1.2.1.1. Intermolecular Hydrogen Abstraction

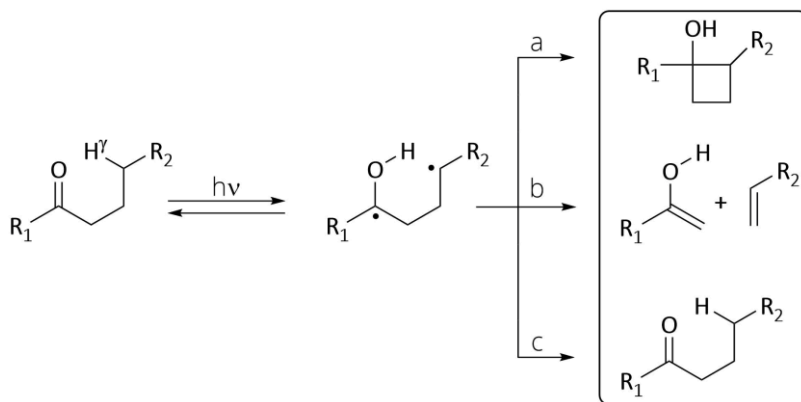
In the case of intermolecular hydrogen abstraction, a radical pair is formed by the ketyl and the donor radicals (Scheme 1.2) which in absence of other reactive molecules undergo combination or disproportionation processes. As a result, a wide range of products can be generated, being of special synthetic interest the pinacols yielded after two identical ketyl radicals combination. Besides, reduced species arising from a second hydrogen abstraction, or new compounds formed by reaction with other radicals present in the medium, are also frequently observed (Scheme 1.2).<sup>9</sup>



Scheme 1.2 General pathways for intermolecular hydrogen abstraction.

### 1.2.1.2. Intramolecular Hydrogen Abstraction

Remarkably, 1,4-biradicals (1,4-BR) are formed through intramolecular hydrogen abstraction. Carbonyls with accessible  $\gamma$ -hydrogen atoms undergo an unstrained six-membered cyclic transition state, which allows 1,5 hydrogen transfer from the  $\gamma$ -carbon atom to the carbonyl oxygen of the  $n\pi^*$  state. The secondary radical-radical competing processes derived from these 1,4-BR are termed *Norrish Type II* reactions and can lead to the following products (Scheme 1.3).<sup>2</sup>



Scheme 1.3 General pathways for intramolecular hydrogen abstraction. *Norrish Type II* reactions.

- Cyclobutanols arise from a ring closure process, termed *Yang photocyclisation*.
- Mixtures of enols and alkenes as a result of the 2,3-bond cleavage, process known as *Norrish Type II cleavage*.
- Ground-state starting material regenerated through reverse hydrogen transfer.

However, special attention has been paid in this Thesis to the Norrish-Yang photocyclisation and its two-photon photosensitised version will be addressed in Chapter 5.

### 1.2.2. [2+2] Photocycloadditions

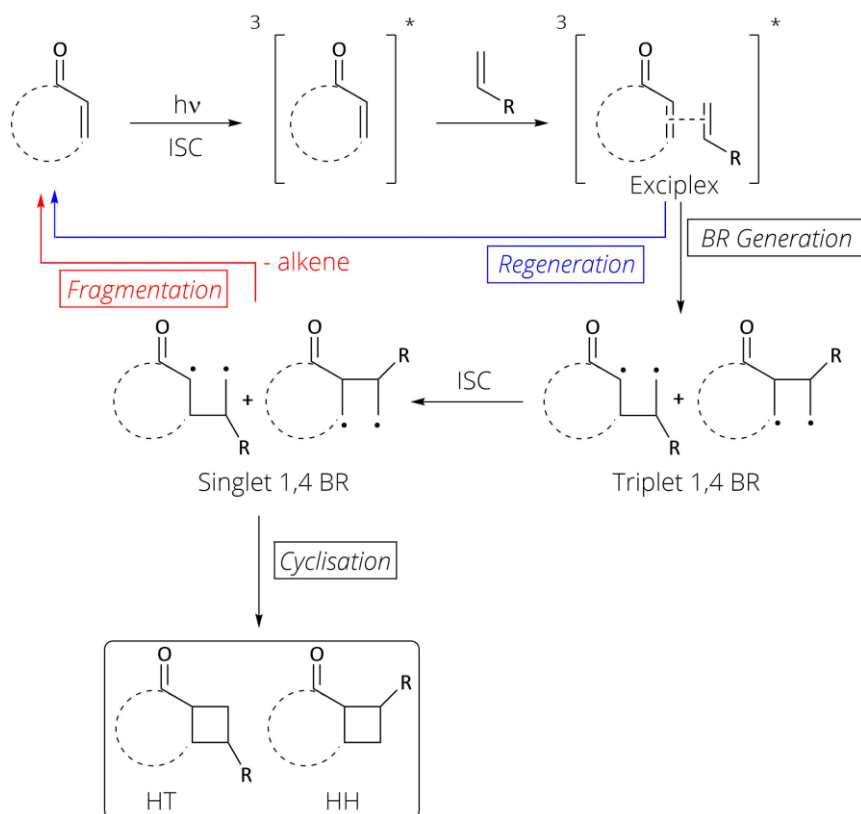
The [n + m] cycloaddition reactions consist of ring-forming addition of “m” number of atoms of one group to “n” number of atoms of another one, leading to a cycloadduct whose composition is the sum of the individual components. Among them, stereoselective [2+2] cycloaddition is one of the most commonly used photochemical reactions in synthetic organic chemistry, as strained four-membered ring compounds can readily be prepared. So, it constitutes a powerful carbon-carbon bond forming tool that affords a wide range of extremely useful and versatile building blocks through photochemical means.<sup>2</sup>

#### 1.2.2.1. Cyclobutane Formation

Analogously to photocycloaddition of simple alkenes, cyclobutanes can be synthesised by addition of excited  $\alpha,\beta$ -unsaturated carbonyls to alkenes. These [2+2] cycloadditions are favoured in cyclic enones, as *cis-trans* isomerisation is not allowed. In fact, the high efficiency and selectivity observed in the [2+2] cycloaddition of alkenes to cyclopentenone and cyclohexenone derivatives, has led to the use of this reaction in the synthesis of complex polycyclic natural products.<sup>2</sup>

The accepted mechanism involves, as a first step, population of the enone triplet excited state, that can be either  $n,\pi^*$  or  $\pi,\pi^*$ . Then, this excited enone forms an exciplex with a ground-state alkene, which in turn decays to form one or more of the possible ground-state 1,4-biradical intermediates. Then, these biradicals can cyclise and form the corresponding cyclobutanes

or revert to the ground-state regenerating the starting materials (Scheme 1.4).<sup>7</sup>



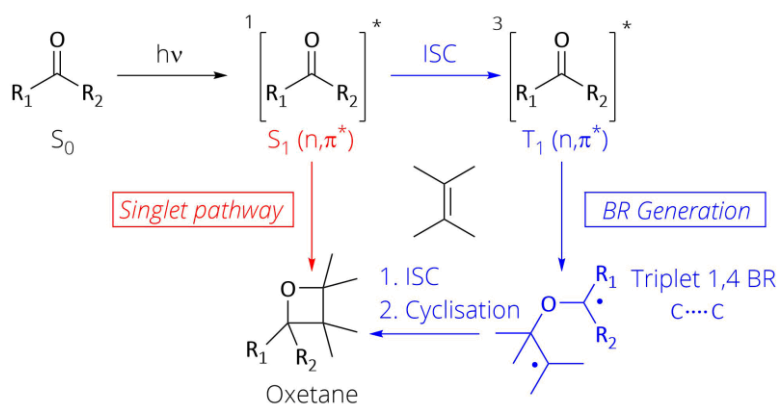
Scheme 1.4 Mechanism for the [2+2] photocycloaddition of cyclic  $\alpha,\beta$ -unsaturated carbonyls to alkenes.

When unsymmetrically substituted alkenes are used, mixtures of head-to-head (HH) and head-to-tail (HT) cyclobutanes are formed. The HT isomer is the favoured product with donor-substituents while the HH is preferably formed with electron-poor ethylenes. However, regioselectivity in [2+2] photocycloadditions does not follow a simple pattern which represents an important problem that limits its synthetic utility.<sup>10,11</sup>

## 1.2.2.2. Oxetane Formation

The addition of alkenes to excited carbonyl compounds is generally known as the Paternò-Büchi reaction and leads to oxetanes formation with both aldehydes and ketones (dialkyl, arylalkyl or diaryl ketones) when the oxygen atom of the  $n,\pi^*$  carbonyl state interacts with the ethylene's  $\pi$  bond.

It has been established that for aliphatic carbonyl compounds, the reaction can occur either through their singlet or the triplet excited states, whereas the triplet excited state pathway is the only one allowed in aromatic compounds (Scheme 1.5).<sup>7</sup>



Scheme 1.5 Mechanism for the [2+2] photocycloaddition of carbonyls to alkenes, Paternò-Büchi reaction.

It is worth noting that, in the case cycloadducts are produced from the singlet excited state, the reaction may involve a concerted process (red pathway of Scheme 1.5). However, in triplet excited species, a stepwise mechanism via 1,4 BR intermediates, with C-C initial attack, has been confirmed (blue pathway of Scheme 1.5). In addition, exciplex, radical ion pair and zwitterion intermediate formation, prior to oxetane cyclisation, has also been reported, although in a less significant manner.

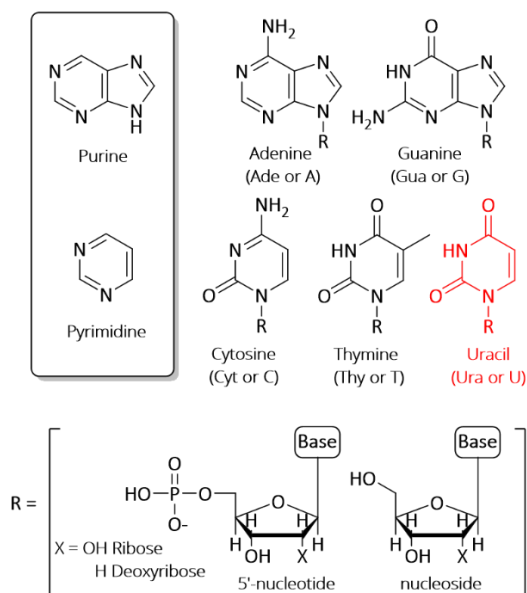
Regio- and stereoselectivity in oxetane formation, strongly depends on the reactant multiplicity. Thus, high stereoselectivity results when the photoreaction proceeds through the  $S_1 (n\pi^*)$  since C-C bond rotation takes longer than singlet deactivation (usually in the nanosecond timescale). However, when the process occurs through the  $T_1 (n\pi^*)$ , the C-C 1,4 BR bond rotation can take place, leading to the initial stereochemistry loss.<sup>7</sup>

Furthermore, electron-rich alkenes will preferentially interact with the electrophilic half-filled n-orbital on the oxygen atom whereas electron-deficient alkenes will attack indistinctly the oxygen atom or the nucleophilic carbon atom.<sup>7</sup>

### 1.3. Nucleic Acid Damage and Skin Cancer Induced by UV light.

The knowledge that UV radiation may have deleterious effects on organisms dates back to 1877, when Downes and Blunt discovered the bactericidal activity of sunlight.<sup>12</sup> The next milestone was established later on, in 1896, when Unna associated excessive exposure to solar radiation, especially UV, to skin cancer.<sup>13</sup> Since then, an intense effort has been dedicated to the characterisation of UV-induced carcinogenesis and also photoinduced repair.<sup>14-16</sup>

DNA is one of the main UV chromophores in the mammalian skin, together with proteins and melanin, due to their absorbance in the UVB region. This is a crucial macromolecule for the continuity of life as it encodes the genetic information in organisms, and it is composed by four nucleic acids bases which are merely substituted purines and pyrimidines (Scheme 1.6).<sup>7,9,14</sup>



*Scheme 1.6 Purine (adenine and guanine) and pyrimidine (thymine and cytosine) bases derivatives found in DNA. In RNA uracil (in red) replaces thymine (5-methyluracil). Attaching ribose or deoxyribose to the N<sub>1</sub> position of the pyrimidines, or to the N<sub>9</sub> position of the purines, ribonucleosides and 2'-deoxyribonucleosides are formed.*

These key building blocks have short S<sub>1</sub> excited-state lifetimes (ps or less) which gives them photochemical stability. This means they are protected against greater photochemical damage that would occur if they undergo intersystem crossing to their reactive triplet states.<sup>7,9</sup>

Purine bases such as adenine and guanine are quite stable to UV light, but not pyrimidine bases as thymine (uracil in RNA) and cytosine, which can experiment photodimerisation with another adjacent pyrimidine base in the same DNA strand. This is, undoubtedly, the most common photoreaction resulting from UV irradiation of DNA where the major process is the [2+2] photocycloaddition, addressed in the previous Section 1.2.2, to form a cyclobutane pyrimidine dimer via the excited triplet state or an oxetane

through the Paternò-Büchi reaction.<sup>9,14,17,18</sup> This kind of photoproducts among others will be deeply studied in the following sections.

### 1.3.1. Solar Light Duality: Beneficial and Harmful

Solar radiation is the portion of the electromagnetic spectrum, that provides the light and heat fundamental for the maintenance of life on Earth. However, as mentioned above, it also represents a constant threat to the living organisms, as prolonged exposure may result genotoxic.

Among the three separate wavelength ranges within solar spectrum, namely ultraviolet (100-400 nm), visible (400-700 nm) and infrared (700-10<sup>6</sup> nm), visible light represents the 42.3% of the total solar light that reaches the Earth's surface. This wavelength range also constitutes the Photosynthetically Active Radiation (PAR), the wavelength region where the vital photosynthesis process optimally occurs (Figure 1.2).

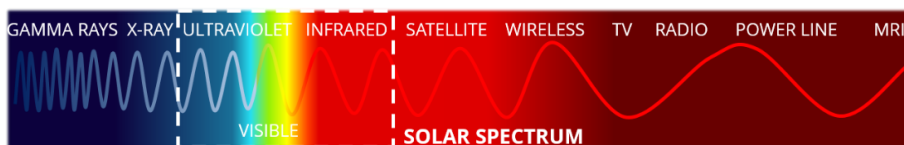


Figure 1.2 Solar spectrum within electromagnetic spectrum.

On the contrary, ultraviolet light comprises a minute portion of the total incident light (6,1%), but corresponds with the more harmful and mutagenic component of the solar radiation.<sup>19</sup> It is a double-edged sword: on one hand, it is necessary to produce vitamin D which is critical for human health, mediates the synthesis of endorphins in the skin and lowers blood pressure, reducing the risk of myocardial infarction, etc. On the other hand, UV is able to produce sunburn, skin aging, corneal damage and a long-term risk of both cutaneous malignant melanoma (CMM) and the non-melanoma skin cancers (NMSC), basal cell carcinoma (BSC) and squamous cell carcinoma (SCC).<sup>20</sup>

Ultraviolet light is sub-divided into three sections: UVC (<280 nm), UVB (280-315 nm) and UVA (315-400 nm). Among them, UVC presents the highest energy (>4.4 eV), being strongly mutagenic. Fortunately, it is completely blocked by the stratospheric ozone layer. Therefore, ultraviolet light reaching the Earth's surface is mainly UVA (90-95%) and to a minor extent UVB (5-10%). Besides, UVA rays have a deeper penetration depth (dermis) than UVB light, which is almost completely absorbed by the epidermis (Figure 1.3 A).<sup>15,19</sup>

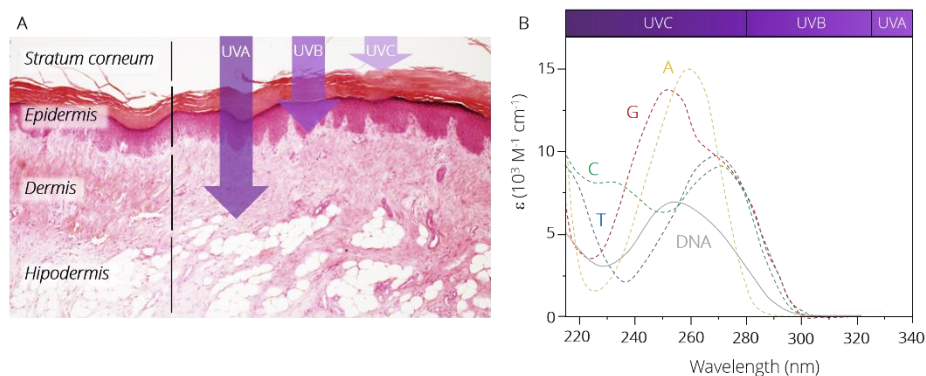


Figure 1.3 A) Human skin ultraviolet penetration depth. B) Absorption spectra of native human DNA and of DNA nucleobases in water.

It is important to note that, although UVA is predominant in the Earth's surface and is characterised by a deeper penetration in the skin, it is scarcely absorbed in contrast with UVB, as it can be observed in Figure 1.3 B. As a result, UVB radiation is by far more carcinogenic by direct absorption even at significantly lower doses than UVA radiation. Still, the latter can induce different types of DNA lesions through direct and indirect mechanisms, being of particular relevance for this Thesis the UVA photosensitised DNA damage mediated by other non-DNA chromophores (endogenous or exogenous). In this case a photosensitiser absorbs the UVA radiation and initiates damage through processes such as triplet energy transfer, photoadduct formation or the generation of reactive oxygen species (ROS, e.g. singlet oxygen).<sup>17</sup>

## 1.3.2. Photoinduced DNA Lesions

DNA photolesions can be induced by direct absorption of UV radiation or mediated by photosensitisers (normally absorbing in the UVA range). These two pathways, as well as the main photoproducts arisen, will be deeply studied in the following sections (Figure 1.4).

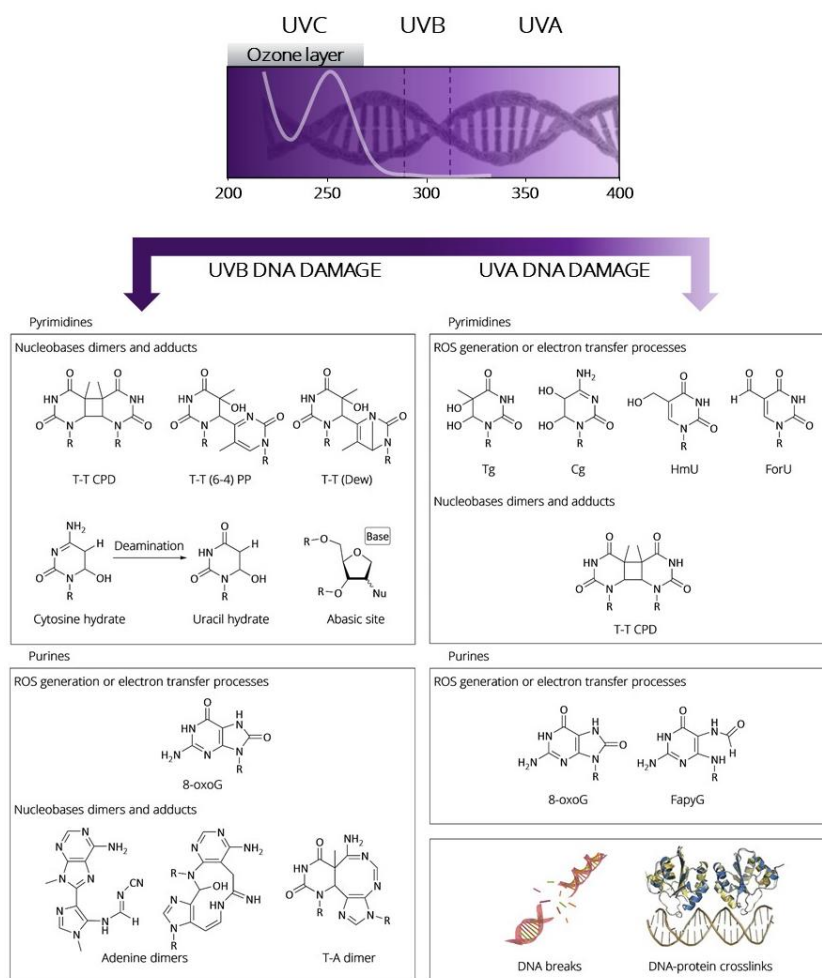


Figure 1.4 Pyrimidine and purine lesions induced by UVB (left) and UVA (right) light.

### 1.3.2.1. Direct DNA Damage

Absorption of UV light by the cellular DNA affects mainly the pyrimidine bases.<sup>17,19</sup> In terms of quantitative importance, the bipyrimidine lesions, cyclobutane pyrimidine dimers (CPDs) and pyrimidine (6-4) pyrimidone adducts (6-4 PPs), are the major photoproducts formed (Figure 1.5). Moreover, 6-4 PPs can easily convert into a third type of photoproducts known as the Dewar valence isomers (DEWs) upon exposure mainly to UVB radiation (Figure 1.4).<sup>21</sup>

The relation of these photolesions with skin cancers, both non-melanoma and melanoma, has been undoubtedly established as they appear massively in specific skin tumor genes.<sup>28,29,30</sup>

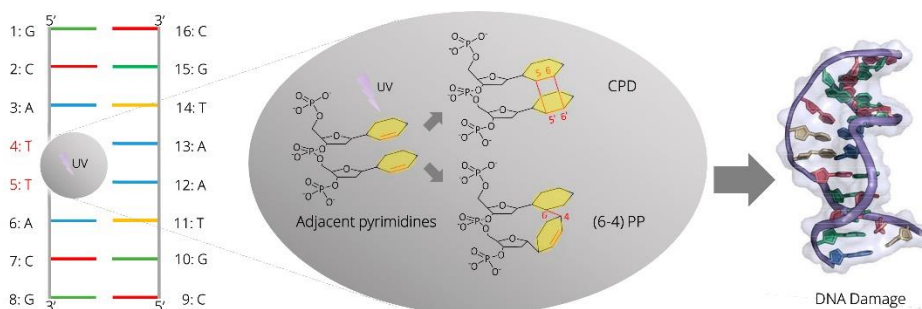


Figure 1.5 Cyclobutane pyrimidine dimers (CPDs) and pyrimidine (6-4) pyrimidone adducts (6-4 PPs).

#### 1.3.2.1.1. Cyclobutane Pyrimidine Dimers

Cyclobutane pyrimidine dimers are the result of a formal  $[2\pi+2\pi]$  photocycloaddition between the  $C(5)=C(6)$  double bonds of two pyrimidine bases. It is a very fast reaction reported to occur in less than 1 ps in single-stranded DNA, with a quite low quantum yield of around 2%.<sup>22,23</sup>

In solution, with monomeric derivatives, six diastereomers can be generated depending both, on the position of these bases with respect to the cyclobutane ring (*cis/trans* stereochemistry) and on the relative orientation of the two C5-C6 bonds (*syn/anti* regiochemistry) (Figure 1.6).<sup>16,17,24</sup>

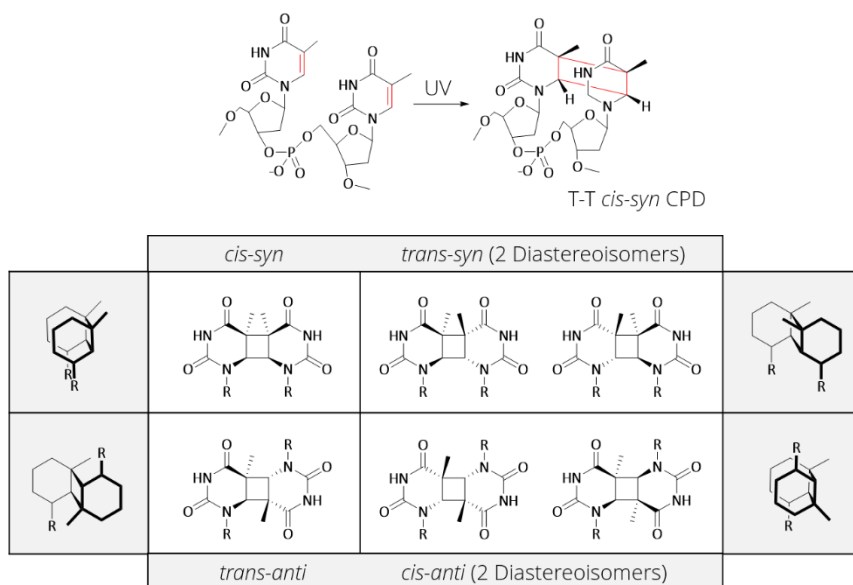


Figure 1.6 Up) Cyclobutane pyrimidine formation in thymine dinucleotide (TpT). Bottom) structure of the possible CPDs formed following Thy derivatives irradiation.

However, within DNA and oligonucleotides, as pyrimidine bases are attached to the sugar-phosphate backbone, some conformations are simply impossible due to steric constraints.<sup>22</sup> Thus, only *syn* isomers can be generated in double-stranded duplexes and the *cis-syn* form is produced in large excess with respect to the *trans-syn* diastereomers. Besides, the latter isomers are just present in single-stranded and denatured DNA.<sup>17</sup>

Cyclobutane pyrimidine dimers are mainly formed at TT sites although cytosine can react as well, leading to T<>T, C<>C or T<>C and C<>T CPDs. The

relative ratios of the *cis-syn* cyclobutane dimers are: 5'-TT-3', 5'-TC-3', 5'-CT-3' and 5'-CC-3' (2:1:0,4:0,1).<sup>25</sup> Among these bypyrimidine dimers, the thymine moieties are chemically stable under physiological conditions, while cytosine moieties can undergo deamination after their exocyclic amino function is replaced with a hydroxyl group. This converts cytosine rings into uracil, leading to uracil or mixed thymine-uracil photodimers<sup>26,27</sup>. Indeed, the presence of uracil-containing photoproducts codes for the predominant incorporation of adenine upon replication while the original cytosine should lead to the incorporation of guanine (Figure 1.7)<sup>6</sup>

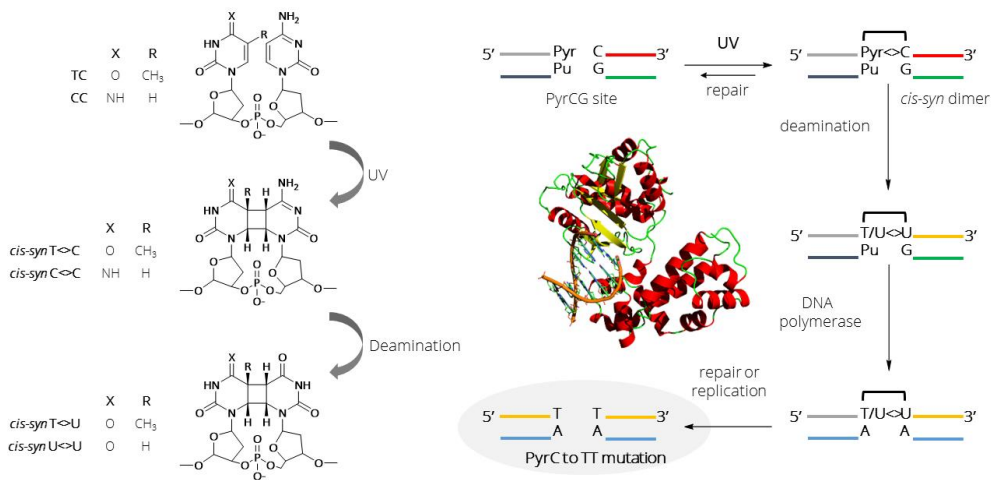


Figure 1.7 Deamination mechanism model of CC and TC dimer mutagenesis, used to explain C→T and CC→TT

As a consequence, this results in U-U: A-A mismatch sequences, highly mutagenic, because they force any repair system to replace the UU-lesion with two thymine units. In fact, this mechanism could be in the origin for the observed C→T and CC →TT transition in the genes of skin cancer cells. In

addition, as these transitions are found almost exclusively in the UVB-induced skin cancer, they are also referred to as *UVB fingerprint* or *signature mutations* (Figure 1.7).<sup>15</sup>

However, despite the fact that these damages have been widely found, the nature of the excited states giving rise to CPDs remains uncertain. It has been shown for TT sites that CPDs formation after direct UVB irradiation occurs nearly exclusively by the singlet channel.<sup>28,29</sup>

But, it must be borne in mind, that CPDs can also be induced by UVA irradiation, being much more carcinogenic than oxidative damage, which was long thought to be the hallmark of UVA genotoxicity.<sup>14,30,31</sup>

Even if this UVA-induced generation of CPDs is a well established fact, the mechanisms involved are still a matter of debate.<sup>32</sup> Thus, they could arise either by direct absorption of UVA photons by DNA or from photosensitisation (Figure 1.8).<sup>30</sup> In the former case, the direct absorption of UVA photons has been recently reported to be driven by the stacking of bases in the double helix. Moreover, it has been suggested that the weak absorption is due to delocalised states with pronounced charge transfer character. However, it is not clear if and how these states could contribute to the formation of CPDs in the UVA range.<sup>29,30,33,34</sup> In the case of CPDs, formation in TT sequences, and more recently at the mixed dipyrimidine sites TC and CT, has been demonstrated to occur by sensitisation from UVA radiation via the triplet channel.<sup>29,35,36</sup>

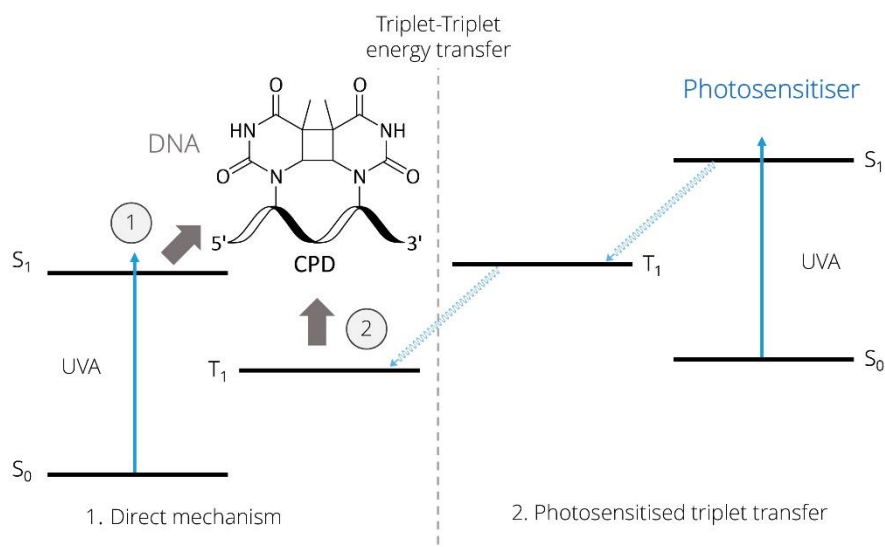
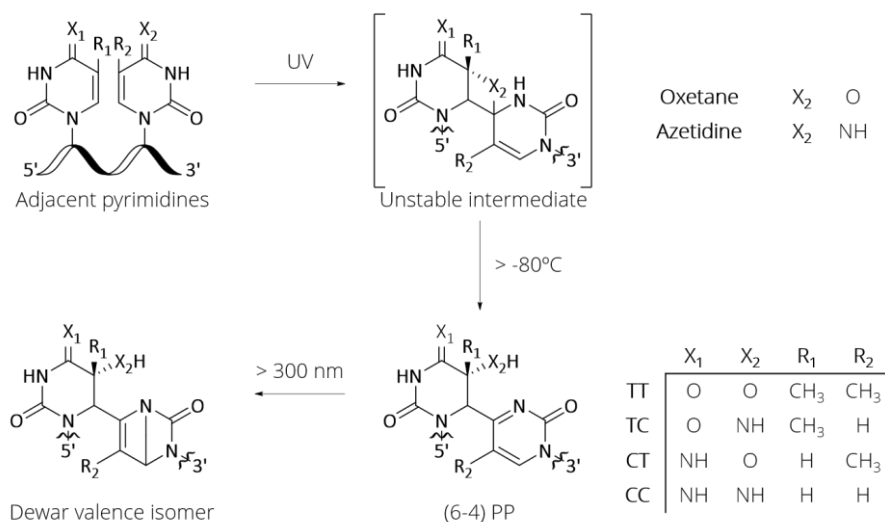


Figure 1.8 The two possible mechanisms to form cyclobutane pyrimidine dimers upon UVA irradiation. 1) Direct absorption by DNA bases 2) photosensitised energy transfer.

### 1.3.2.1.2. Pyrimidine (6-4) Pyrimidone Adducts and Dewar Valence Isomers

Pyrimidine (6-4) pyrimidone adducts are produced by a [2+2] cycloaddition between the C(5)=C(6) double bond of the 5'-end first pyrimidine and either the C(4)=O carbonyl group of a 3'-end thymine base or the C(4)=NH (*E*)-imino tautomeric form of a 3'-end cytosine. Thus, an unstable oxetane or azetidine heterocyclic intermediate is formed, respectively. Both are the photoproducts of a Paternò-Büchi reaction, and rapidly undergo a ring-opening reaction to the corresponding (6-4) photolesions only a few milliseconds after the UV excitation (Scheme 1.7).<sup>6,17,26,30</sup>



Scheme 1.7 Mechanism of (6-4) photoproducts formation and their rearrangement to the related Dewar valence isomers.

These photolesions are produced in lower yields than CPDs, in a ratio ranging between 1:2 and 1:8 depending on the detection methods used and the bipyrimidine sequence considered.<sup>17,37,38</sup> Among the possible sequences, the TC (6-4) PP is the most frequent, being the relative ratios determined by HPLC-MS/MS as follows: 5'-TC-3' > 5'-TT-3' > 5'-CC-3' > 5'-CT-3' (1:0.2:0.1:0.01) in cellular calf thymus DNA.<sup>6,25</sup>

Photophysically, (6-4) PPs are characterised by a strong absorption in the UVB/UVA region with a maximum at 314 nm, due to the presence of a substituted pyrimidone ring which also exhibits fluorescence with a band centered at 320 nm and a quantum yield of ca 0.09. Its triplet excited state has also been characterised with a broad band centered at 441 nm and a triplet excited state energy of 297 kJ mol<sup>-1</sup>.<sup>39</sup>

Indeed, upon absorption in the 310-350 nm range, the pyrimidone ring may further decompose through a 4 $\pi$  electrocyclicalisation leading to the related

Dewar valence isomers (Scheme 1.7).<sup>21</sup> Besides, the formation of these lesions is more efficient with simulated sunlight containing both UVB and UVA or by successive exposure to UVB and UVA. In fact, they have been detected in human cells exposed to natural sunlight, so their UV genotoxicity has been unambiguously established.<sup>17,30,38</sup>

In addition, (6-4) PPs have been obtained exclusively after direct UVC or UVB irradiation, in clear contrast to CPDs which were also induced by photosensitisation. Based on this fact, the widely accepted paradigm is that the (6-4) PPs are mediated via their singlet excited states.<sup>6,30</sup> However, the lower energy excited triplet state of pyrimidine is of  $\pi\pi^*$  nature, while the Paternò-Büchi type is a characteristic process of the  $n\pi^*$  triplets. Thus, it seems feasible that some of the generally accepted "singlet" photochemistry actually occurs from a triplet excited state with the appropriate electronic configuration, as it will be studied in more detail in Chapter 5.<sup>40,41</sup>

### 1.3.2.1.3. Other Photoproducts

Monomeric photolesions are also formed in DNA upon UV irradiation. In spite of being less abundant, these monoadducts should be taken into account as they also contribute significantly to mutagenic effects of UV. Their greatest exponent is 6-hydroxy-5,6-dihydrocytosine, the so-called cytosine photohydrate, which may persist in DNA after prolonged periods of time, and undergoes deamination to the more stable uracil hydrate (Figure 1.4).<sup>42,43,44</sup>

Thymine and 5-methylcytosine do not readily undergo photohydration, but instead they can experience cleavage of their N-glycosidic bonds leading to abasic sites upon UVB irradiation (Figure 1.4)

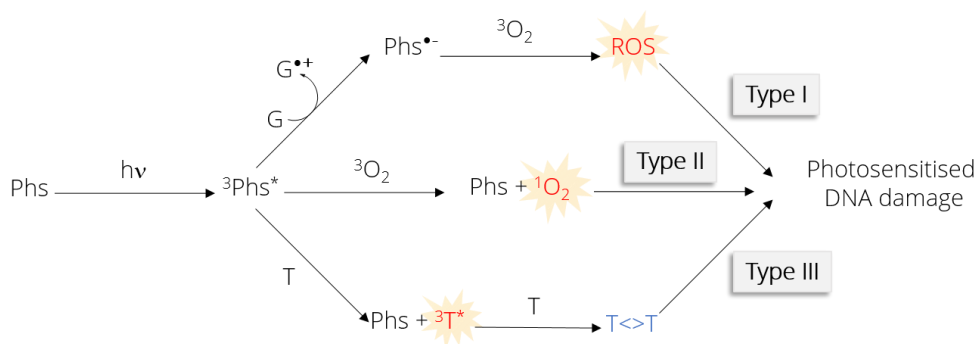
Even though tandem pyrimidine residues are the preferential targets of UV-induced DNA damage and mutation, purines are also photoreactive.

Thus, adenine dimers and thymine-adenine adducts (T-A) have also been observed but in very low yields (Figure 1.4).<sup>17,45-47</sup>

### 1.3.2.2. Indirect DNA Damage: Photosensitisation

Photosensitisation is the process by which a compound undergoes a physical or chemical alteration as a result of the initial absorption of light by another compound called photosensitiser (Phs). In the case of DNA, undesired photosensitised modifications are mediated by endogenous (flavins, NADPH oxidase, heme groups, porphyrins, melanin, and cytochromes) or exogenous agents present in dyes, fragrances, drugs, etc, able to absorb UV energy resulting in excited molecules (Scheme 1.10, Section 1.3.2.2.1).

The mechanisms involved in photosensitisations are classified as: i) electron or H transfer between the  $^3\text{Phs}^*$  and a suitable partner resulting in the formation of semireduced and semioxidised radical-type species (*Type I* reactions) and ii) energy transfer to any substrate whose triplet state lies at lower level compared with  $^3\text{Phs}^*$  (*Type II* and *Type III* reactions) (Scheme 1.8).<sup>6</sup>



Scheme 1.8 Photosensitised mechanisms (i) one-electron or H transfer reaction (*Type I*), (ii) addition of  ${}^1\text{O}_2$  (*Type II*) and (iii) triplet-triplet energy transfer (*Type III*).

The Type I mechanism involves a complex chain of events in which the photosensitiser in its excited state reacts directly with the substrate resulting in either hydrogen atom or one-electron transfer. Electron transfer can actually occur in both directions, but normally, the excited photosensitiser acts as an oxidant,<sup>48</sup> leading to DNA radical cation. Usually the interaction occurs with guanine since this nucleobase exhibits the lowest oxidation potential.<sup>49</sup> In DNA, guanine radical cation ( $G^{\bullet+}$ ) deprotonates giving rise mainly to 8-oxo-7,8-dehydroguanine (8-oxoG), but also to other products such as 2,6-diamino-4-hydroxy-5-formamido-pyrimidine (FapyG, Figure 1.4).<sup>30</sup>

Furthermore, the initially formed radical intermediate can react with solvent molecules or oxygen. Of particular importance is the latter case, when oxygen acts as the electron acceptor. It gives rise to reactive oxygen species such as the highly reactive hydroxyl radicals ( $\bullet\text{OH}$ ), which does not show any specificity and reacts with all the components of DNA (Scheme 1.8).<sup>50</sup> The reaction of this radical with purines leads also to the 8-oxoG and FapyG (Figure 1.4) <sup>17,19</sup>

Pyrimidine bases are less susceptible to oxidation than their purine analogues. Yet, reaction of  $\bullet\text{OH}$  with their C5-C6 double bond occurs leading to the 5,6-dihydroxy-5,6-dihydropyrimidines namely thymine and cytosine glycols (Tg and Cg, Figure 1.4). Besides, it can react with the methyl group of thymine generating the 5-hydroxymethyluracil (HmUra) and the 5-formyluracil (ForU).<sup>6,51</sup>

Type II involves an energy transfer from the photosensitiser to molecular oxygen, producing singlet oxygen ( $^1\text{O}_2$ ) (Scheme 1.8). This species' lifetime may be long in cells, allowing for its diffusion over large distances before being deactivated.<sup>52</sup> Hence, due to its high reactivity, it is able to oxidise the DNA leading mainly to the previously addressed 8-oxoG.<sup>6,26</sup>

Finally, a Type III mechanism consists of an energy transfer from the excited photosensitiser to the DNA bases. This is specially relevant as cyclobutane pyrimidine dimers are formed upon triplet sensitisation and are by far the most relevant Pyr photoproducts (Scheme 1.8). In fact, triplet-mediated pyrimidine dimerisation is a key process in photochemical damage to DNA.<sup>53-55</sup>

### 1.3.2.2.1. Cyclobutane Pyrimidine Dimers

In a photosensitised pyrimidine dimerisation process, the photosensitiser is excited upon light absorption and then transfers its energy usually from its triplet excited state to the pyrimidine base, giving rise to  $^3\text{Thy}^*$  or  $^3\text{Cyt}^*$ , which subsequently react with another Thy or Cyt in their ground state, leading to the final CPD (Figure 1.9).

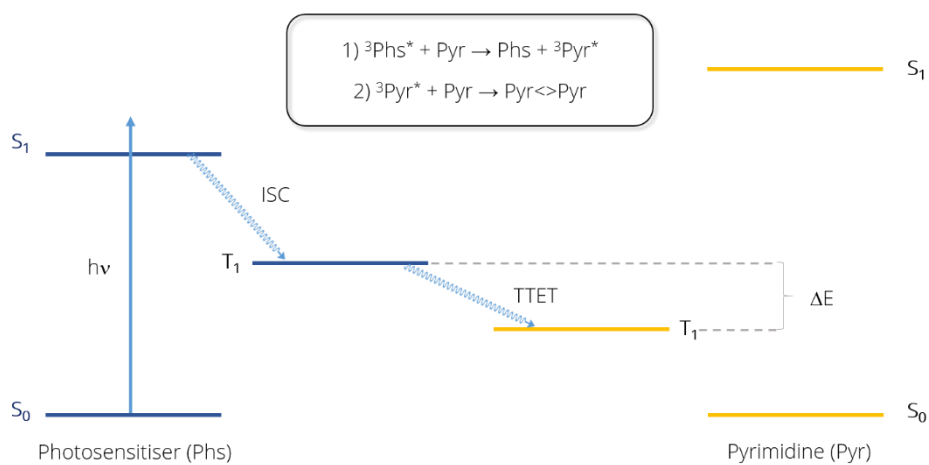
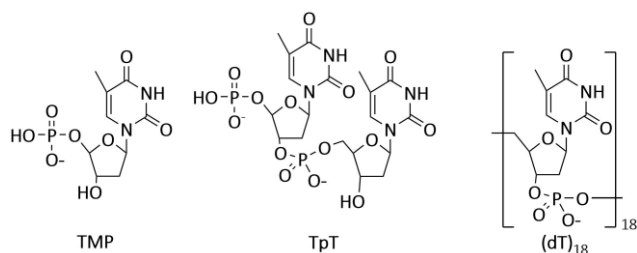


Figure 1.9 Interconversion between the excited states involved in pyrimidine (Pyr) photosensitisation.

As well as in the CPDs formation upon direct irradiation, the predominant photoproduct is found to be the T<->T, while the amounts of

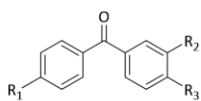
T<>C and C<>T produced are one order of magnitude lower.<sup>56</sup> It is important to note that photoproducts formation and their distribution are strongly influenced by the nature of both the pyrimidine (Pyr) and the photosensitiser lowest triplet excited state but also by neighbouring effects, the solvents used, etc.<sup>53,57-60</sup> In this context, the investigation of CPDs photosensitisation has been addressed using a wide range of pyrimidine models, as thymine nucleotide (TMP), thymine dinucleotide (TpT) and the thymine oligonucleotide (dT)<sub>18</sub> (Scheme 1.9).



*Scheme 1.9 Pyrimidine models widely used in investigation of CPDs photosensitisation.*

Aromatic ketones, fluoroquinolones and psoralens are relevant DNA-photosensitisers. Examples of aromatic ketones are non-steroidal anti-inflammatory drugs (NSAIDs)<sup>6,61</sup> like ketoprofen or antilipidemic agents like fenofibrate, well known to produce photoallergic and phototoxic side effects. Fluoroquinolones are phototoxic and photomutagenic antibacterial drugs<sup>62-65</sup> and psoralens are used in the UVA treatment against psoriasis (PUVA)<sup>66-69</sup>. The interaction of their triplet excited states with DNA have been thoroughly investigated by the scientific community.

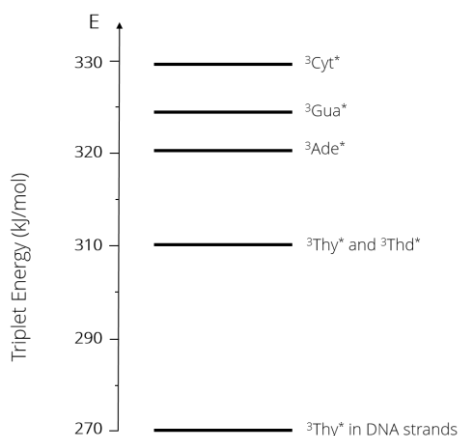
In the following sections, a more detailed analysis of the thymine derivatives and photosensitisers photophysical properties will be presented, with special emphasis on ketones since they have been key compounds in the present Thesis (Scheme 1.10).

	R <sub>1</sub>	R <sub>2</sub>		
Acetone	CH <sub>3</sub>	CH <sub>3</sub>		
Acetophenone	Ph	CH <sub>3</sub>		
Propiophenone	Ph	CH <sub>2</sub> CH <sub>3</sub>		
	R <sub>1</sub>	R <sub>2</sub>	R <sub>3</sub>	
Benzophenone	H	H	H	
Ketoprofen	H	CHCH <sub>3</sub> COOH	H	
Fenofibrate	Cl	H	OC(CH <sub>3</sub> ) <sub>2</sub> COOCH(CH <sub>3</sub> ) <sub>2</sub>	
Fenofibric acid	Cl	H	OC(CH <sub>3</sub> ) <sub>2</sub> COOH	

Scheme 1.10 Examples of Pyr<>Pyr ketone photosensitisers.

The energy of Pyr triplet excited states is a critical parameter to determine the feasibility of triplet-triplet energy transfer (TTET), intimately related with the photomutagenic potential of a photosensitiser. Accordingly, an important effort has been done by the researchers to establish these values.

It is well known that <sup>3</sup>Thy\* is the lowest lying among the Pyr triplet excited states. Conversely, the nucleobase with the highest manifold corresponds to cytosine (Scheme 1.11). Accordingly, T<>T CPDs predominate over the analogous cytosine derivatives.<sup>70,71</sup>



Scheme 1.11 Energies of DNA nucleobases triplet excited states.

Monomeric Thy and Thd 5'-monophosphate present a triplet energy ( $E_T$ ) of  $310 \text{ kJ mol}^{-1}$  in solution (Scheme 1.11).<sup>70,72-74</sup> Noteworthy, due to the base stacking, the  $E_T$  of thymine in DNA results much lower than that of the free base or the nucleoside. Thus, in DNA, the upper limit of thymine  $E_T$  has been progressively downshifted from  $297 \text{ kJ mol}^{-1}$  (estimated using methoxyacetophenones as Phs)<sup>72,73,75</sup> to  $290 \text{ kJ mol}^{-1}$  (using benzophenone and phthalimidine derivatives as Phs)<sup>76-79</sup> and finally, with the contribution of our group,  $267 \text{ kJ mol}^{-1}$  (in the range defined by triplet energies of fluoroquinolones NFX and ANFX, Scheme 1.11)<sup>70,80,81</sup>.

This value, can be considered as the “functional value” for the triplet energy of Thy in DNA. Thereby, it can be taken as the  $E_T$  required for a given compound to become a potential DNA photosensitiser.

### 1.3.2.2.2. Photosensitisers

When considering a compound as a triplet photosensitiser, a series of requirements have to be fulfilled, such as:

- a) To present a  $E_T$  higher than that of  $^3\text{Pyr}^*$ , as corresponds to thermodynamically favoured processes.
- b) To absorb light at longer wavelengths than Pyr, to allow for selective excitation of the photosensitiser in mixtures containing both.
- c) To have an efficient intersystem crossing quantum yield ( $\Phi_{ISC}$ ) and a long triplet lifetime ( $\tau_T$ ), to promote a large amount of photoexcited sensitiser molecules to the triplet excited state and to enhance the probability of energy transfer to the acceptor.
- d) To be inert under the reaction conditions, avoiding side reactions and photosensitiser degradation.
- e) To be spatially close to the Pyr unit to allow collisions.

- f) To have good water solubility for biological applications, in native environments.

Therefore, the most effective photosensitisers present a high  $E_T$ , with a long-lived triplet state and a high quantum yield. In other words, the time scale of the energy transfer process must be faster than the intrinsic lifetime of the  $^3\text{Phs}^*$ .<sup>6,53,56</sup>

The rate of a TTET ( $k_{ET}$ ) from a photosensitiser to a substrate depends on the  $\Delta E$  between their triplet excited states, and it is governed by the Sandro's equation (Equation 1.3):<sup>53,82</sup>

$$k_{ET} = k_D \frac{1}{(e^{-\Delta E/RT} + 1)}$$

*Equation 1.3 Sandro's equation where  $k_D$  is the diffusion rate constant in liquid solution,  $T$ , the temperature and  $R$  the universal gas constant.*

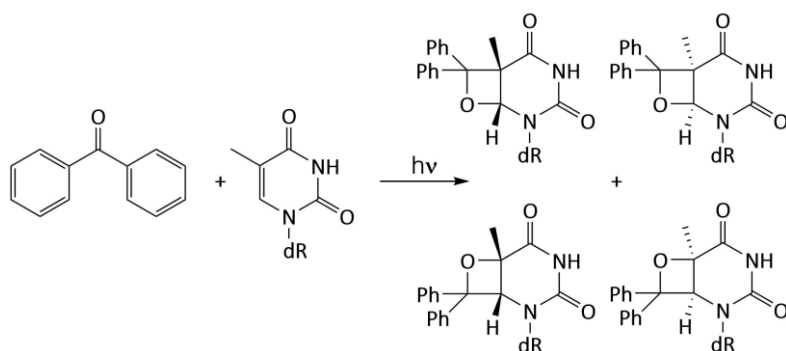
This  $k_{ET}$  is generally accepted to be nearly diffusion-controlled when donor triplet level is at least 8 kJ mol<sup>-1</sup> above that of the acceptor.<sup>83</sup> Thus, any chemical (cosmetics, drugs, pesticides, etc.) with  $E_T$  higher than 270 kJ mol<sup>-1</sup> has to be considered as potentially photogenotoxic.

Benzophenone (BP), acetone (Ac) and acetophenone (AP) are good examples of photosensitisers that fulfill the requirements stated above. They have been widely employed as triplet sensitisers to investigate the mechanisms involved in CPDs formation.<sup>53,57,77,84-87</sup>

Benzophenone photophysical properties have been intensively studied and are well established. This paradigmatic photosensitiser absorbs UV light, up to 360 nm and displays phosphorescence emission with the typical shape corresponding to molecules with a lowest  $n\pi^*$  triplet. The energy of  $^3\text{BP}^*$  is 289 kJ mol<sup>-1</sup>, slightly inferior to that of thymine. Accordingly, the TTET between

$^3\text{BP}^*$  and thymine is a somewhat disfavoured process, although still observed in solution, traditionally suggested to occur due to thermal population of upper vibrational states of  $^3\text{BP}^*$ .<sup>61,76,88,89</sup> Recently, it has been demonstrated that in this particular case, delocalised triplet excited states may predominate over locally excited triplet states, accounting for most of the experimental observations on the BP-photosensitised pyrimidine dimerisation.<sup>90</sup>

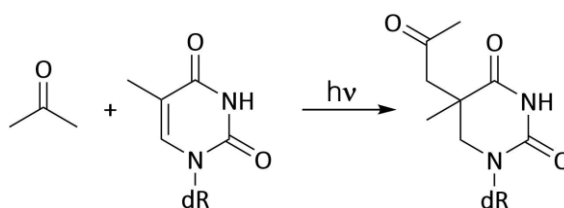
However, the prevailing photoreaction between BP and Thy is a Paternò-Büchi derived from the  $n\pi^*$  nature of  $^3\text{BP}$ , prone to react with an alkene generating a biradical which finally gives rise to oxetanes. Oxetanes are favoured for  $n\pi^*$  triplets when the  $E_T$  of the alkene is comparable to or higher than that of the carbonyl compound, as is the case in benzophenone, which contradicts the requirement previously addressed that a photosensitiser must remain inert.<sup>53,88,91-93</sup> This obviously limits the use of BP as Phs in mechanistic studies on CPDs formation.



Scheme 1.12 Oxetane formation upon irradiation of a mixture of benzophenone and thymidine.

Acetone presents a  $\Phi_{\text{ISC}}$  nearly to the unit and a high triplet energy  $E_T$  ca  $330 \text{ kJ mol}^{-1}$ . This makes it particularly advantageous over other photosensitisers as  $^3\text{Ac}^*$  is of  $\pi\pi^*$  nature and energetic enough to populate both  $^3\text{Thy}^*$  and  $^3\text{Cyt}^*$  ( $334 \text{ kJ mol}^{-1}$ ). In fact, compared to benzophenone and

acetophenone, it is the only one able to photosensitise cytosine cyclobutane dimers (Cyt<->Cyt) in solution.<sup>94</sup> Moreover, the triplet-triplet absorption band of acetone does not interfere with observation of the growth of Pyr triplet excited states at 400 nm and does not overlap with their whole absorption spectra which facilitates kinetic studies.<sup>53,94-96</sup> However, as with benzophenone, by-products of photosensitiser interaction with thymine, such as the acetylonyl derivative shown in Scheme 1.13, have been isolated in a low yield.<sup>24,97,98</sup>



*Scheme 1.13 Acetylonyl byproduct obtained after thymidine photosensitisation with acetone.*

Finally, acetophenone, which has also been used to photosensitise pyrimidine dimerisation, presents a triplet excited state with  $E_T$  close to 310 kJ mol<sup>-1</sup>. Furthermore, its interaction with the DNA duplex has been intensively studied, and no oxetanes have been reported to be formed, being more inert than the other ketones analysed. Variations in the aromatic substitution have a marked influence on the relative energy of the  $n\pi^*/\pi\pi^*$  triplet states and hence on the photophysical properties of this molecule derivatives as shown in Table 1.1.

Table 1.1 Photophysical parameters for acetophenone (AP) and para- and meta-methoxy substituted acetophenones.<sup>99</sup>

	$E_T$ (kJ/mol)	$\tau_{\text{Phos}}$ (s)	$\Phi_{\text{Phos}}$	$\Phi_{\Delta}^{100}$
Acetophenone	310.0	0.004	0.74	0.52
p-methoxy AP	299.2	0.26	0.68	0.42
m-methoxy AP	302.9	0.25	0.35	---

Precisely, 2'-methoxyacetophenone (2M) has been suggested recently to be well-suited as CPDs photosensitiser for TpT. As a matter of fact, this has been the photosensitiser selected to carry out most of the photosensitisation experiments in this Thesis, and will be fully characterised in Chapter 3.<sup>36,101</sup>

## 1.4. Photophysics

### 1.4.1. Transient Absorption Spectroscopy

Transient absorption spectroscopy (TAS) is a basic tool for the study of transient absorption species generated by means of an excitation short pulse (or pump). This intense light pulse is able to create short lived intermediates (excited states, radicals and ions) in sufficient concentration for chemical and physical interaction to occur and for direct observation of the associated temporarily changing absorption characteristics.<sup>7,102</sup>

When a nanosecond laser pulse is used as excitation source, this technique is known as nanosecond laser flash photolysis (ns-LFP) and the absorption changes are recorded using a UV-Vis source (probe) that

interrogates the sample before and after the laser pulse being focused into the sample and located perpendicularly to the direction of the laser light (Figure 1.10 A). These systems, normally operate in the kinetic mode, thus the transient absorption is monitored at a single wavelength as a function of time. Alternatively, transient absorption spectra, at a given time delay with respect to the laser pulse, can also be obtained using gated microchannel plates as light shutters, and diode-array detectors.<sup>7</sup>

Systems with shorter excitation pulses and subnanosecond time resolution (picosecond/femtosecond) usually operate in the spectrographic mode (pump–probe spectroscopy). In this case, the transient absorption can be probed by an ultrafast broadband white-light continuum probe pulse, delayed  $\tau$  from the pump pulse via an optical delay line. The difference absorption spectrum is obtained by subtracting the absorption spectrum of the sample in the ground state from the absorption spectrum of the sample in the excited state ( $\Delta A$ ). Therefore, changing the time delay ( $\tau$ ) between the pump and the probe, and recording the different  $\Delta A$  spectrum, a  $\Delta A$  profile can be obtained as a function of  $\tau$  and wavelength (Figure 1.10 B). Thus, often ns-LFP and ultrafast pump-probe experiments are complementary as they cover different time scale windows.

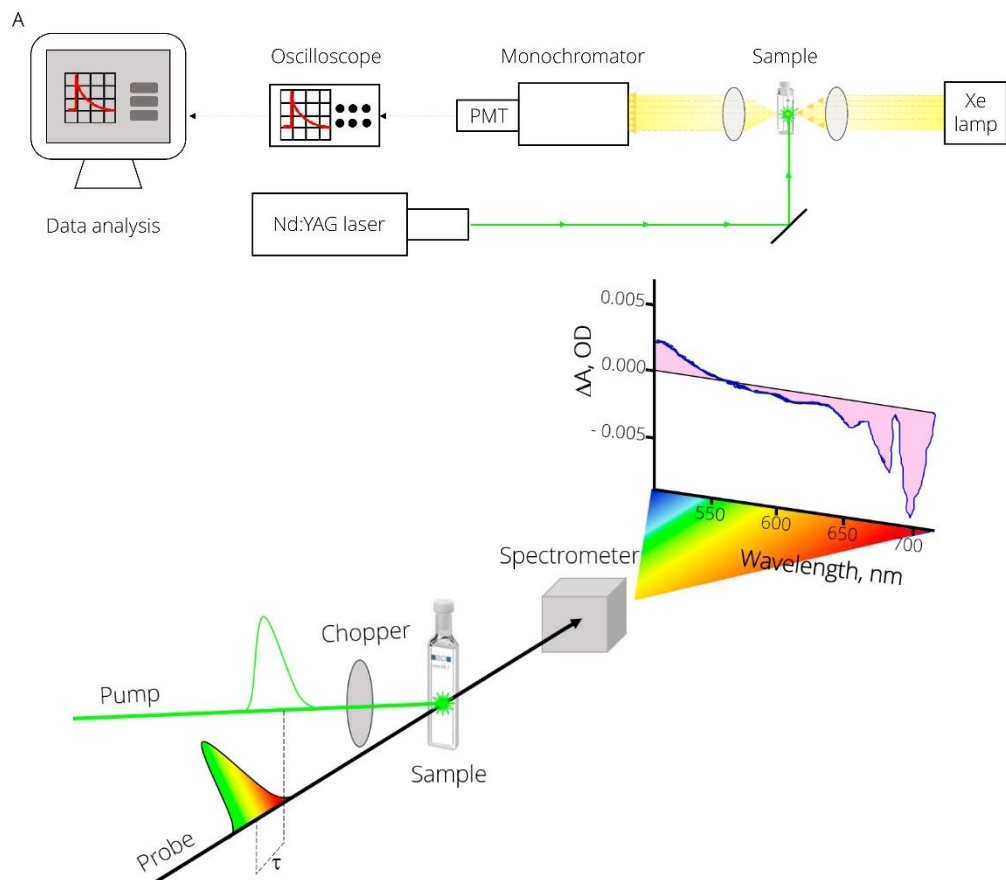


Figure 1.10 A) Nanosecond laser flash photolysis (ns-LFP). B) Ultrafast pump-probe spectroscopy set-up.

A number of studies have been performed to better understand the Pyr excited states, either alone or as substructures of more complex entities (nucleosides, nucleotides, oligonucleotides, etc). Key parameters such as ISC quantum yield, unimolecular decay rate constants, self quenching or quenching by other molecules have been obtained (Table 1.2).<sup>3,7,56,103</sup>

Table 1.2 Photophysical properties of thymine and some thymine derivatives triplet excited states.

	Solvent	$\epsilon_T$ (M <sup>-1</sup> cm <sup>-1</sup> ) at	$\Phi_{ISC}/10^{-2}$	$k_0$ (s <sup>-1</sup> )/10 <sup>5</sup>	$k_s$ (M <sup>-1</sup> s <sup>-1</sup> )/10 <sup>8</sup>
		370 nm <sup>83,104</sup>	83,104	83,96	83,96
Thymine	H <sub>2</sub> O	3500	0.6	0.2	7.9
	ACN	2700	6.0	0.7-2.2	5.3-7.0
Thymidine	H <sub>2</sub> O	3600	1.4	0.4	1.0-1.9
	ACN	3600	6.9	-	-
TMP	H <sub>2</sub> O	3500	0.8-1.5	0.4	0.2
	ETOH	4000	5.5	-	2.0
(T) <sub>20</sub>	H <sub>2</sub> O	2700	2.8	-	100*

\*rate constant in s<sup>-1</sup>.

Furthermore, ns-LFP experiments have been performed to characterise the photosensitiser 2M and also to get a deeper insight into CPDs photosensitisation. Moreover, a short stay in The University of Hong Kong was performed to use their transient absorption spectrometer with IR detection in order investigate several of the compounds synthesised, although they have not been included in the present Thesis.

### 1.4.2. Upper Triplet Excited States: Two Photon Photochemistry

It is commonly assumed that upon reaching the upper excited states ( $S_n$  or  $T_n$ ) the excited molecules relax quickly to their lower excited states ( $S_1$  or  $T_1$ ) from which relaxation to the ground state or a chemical reaction can occur (Figure 1.11). This is because IC from  $S_n$  or  $T_n$  are ultrafast processes, with rate constants in the order of  $10^{14}$ - $10^{11}$  s<sup>-1</sup> making these states ultrashort lived and scarcely populated. Hence, chemical or physical processes from  $S_n$  or  $T_n$  are unlikely. Conversely they usually happen from the  $S_1/T_1$  states, as they are longer lived due the high gap between them and the ground state.

However, there are some exceptions to this rule, since certain molecules present upper excited states with a high energy gap between them and lower lying states of the same multiplicity ( $\Delta E$ , Figure 1.11), as this slows down the IC allowing them to present a lifetime up to hundreds of picoseconds. Consequently, in these systems other processes may compete with IC itself. For example, their  $T_n$  can experience photophysical processes such as TTET or give rise to photochemical reactions (Figure 1.11).<sup>2</sup> This behaviour has been reported for anthracene and its derivatives, anthraquinones or benzyl.<sup>105-112</sup>

This type of chemistry was developed with the employment of lasers to address mechanistic studies; using pulsed light or conventional lamps can give rise to very different results due to the high concentration of transient species that a laser source can generate. These species can compete for the absorption of photons with their precursors in the ground state, thus they can give rise to *multiphotonic chemical processes* different from those observed by direct conventional excitation.<sup>2,109,111</sup>

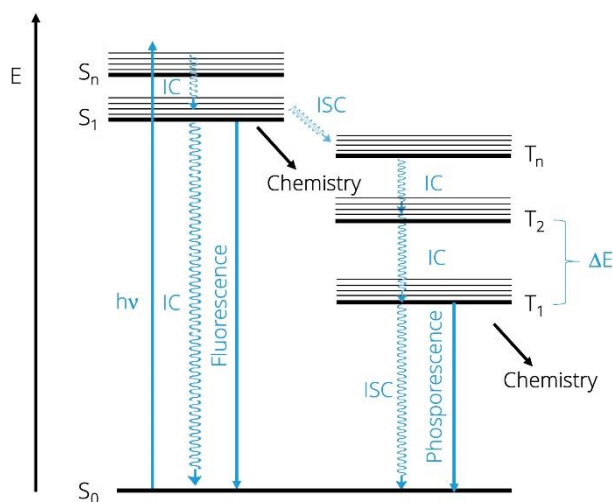


Figure 1.11 Deactivation of upper excited states through radiative and non-radiative processes.

In the case of DNA bases, specifically in Thy, there is a high energy gap between its  $T_1$  and  $T_2$  as seen in Figure 1.12 A. Concretely, the latter is 100 kJ/mol above  $T_1$ , enough for this upper triplet excited state to be populated.<sup>40,41,113</sup>

There are a few studies in the literature which investigate reaction mechanisms involving DNA upper excited states.<sup>114-119</sup> In all cases, high intensity irradiation has been carried out leading to the formation of  $S_1$  or  $T_1$  in high concentration. After the absorption of a second photon, the energy reached exceeds that of the base ionisation, resulting in its loss and DNA fragmentation. For example, in the case of high intensity DNA irradiation at 266 nm performed by Minton and collaborators, a decrease in the production of CPDs and 6-4 PPs was found, but due to the disappearance of their precursors in the irradiation.<sup>119</sup> Analysis of the results presented in these works highlights the limited control in the generation of upper excited states.

For the study of DNA photosensitisation reactions from upper triplet excited states, selective generation of  $T_n$  through TTET processes could provide an elegant design for their controlled generation. This would avoid nucleobase ionisations and also population of singlet excited states, which could deliver secondary reactions making difficult to establish unequivocal conclusions.

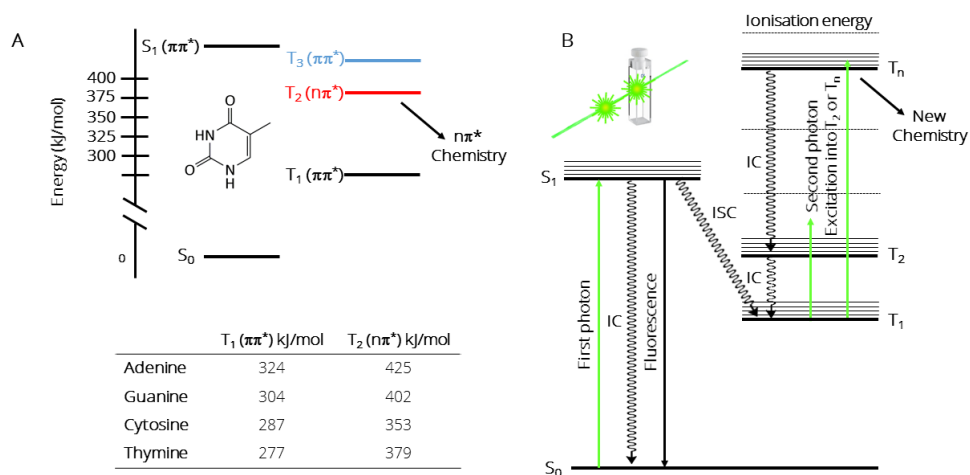


Figure 1.12 A) Energy and nature of DNA bases triplet excited states. B) Two-photon irradiation Jablonski diagram.

However, this represents a challenge from the experimental point of view as  $T_n$  are short-lived, and decay before diffusing through the solution to transfer its energy to the energy acceptor (Figure 1.12 B).

A successful strategy to overcome this drawback and make feasible the TTET from an energy donor in its  $T_n$  has consisted of designing an intramolecular system in which the photosensitiser is covalently bonded to the acceptor to avoid the diffusion step in the TTET. Excitation of the photosensitiser populates efficiently its  $T_1$ . Then, a second photon is

absorbed by this  $T_1$  which leads to  $T_n$ . Finally, a TTET from the latter to the ground state pyrimidine generates the nucleobase  $T_n$ .

This concept was proven, in our group, by the Norrish-Yang photoreaction of a tert-butyluracil (tBU), which is a modified Pyr base susceptible to  $\gamma$  hydrogen abstraction.<sup>41</sup>In Chapter 5 a new intermolecular approach has been proposed to test the feasibility through a more versatile approach to this problem.

## 1.5. References

(1) Turro, N. J.; Ramamurthy, V.; Scaiano, J. C.: *Principles of Molecular Photochemistry: an Introduction*; University Science Books, 2009.

(2) Turro, N. J.; Ramamurthy, V.; Scaiano, J. C.: *Modern Molecular Photochemistry of Organic Molecules*; University Science Books: Herndon, VA, 2010.

(3) Murov, S. L.: *Handbook of Photochemistry*; Marcel Dekker Inc.: New York, 1973.

(4) Coyle, J. D.: *Introduction to Organic Photochemistry*; John Wiley & Sons Can. Ltd.: Canada, 1986.

(5) Jabłoński, A. Über den Mechanismus der Photolumineszenz von Farbstoffphosphoren. *Zeitschrift für Physik* **1935**, *94*, 38-46.

(6) Griesbeck, A.; Oelgemöller, M.; Ghetti, F.: *CRC Handbook of Organic Photochemistry and Photobiology*; Taylor & Francis Group, LLC, 2012.

(7) Klán, P.; Wirz, J.: *Photochemistry of Organic Compounds: From Concepts to Practice*; John Wiley & Sons Ltd, 2009.

(8) Jornet, D.; Tormos, R.; Miranda, M. A. Photobehavior of Mixed  $n\pi^*/\pi\pi^*$  Triplets: Simultaneous Detection of the Two Transients, Solvent-Dependent Hydrogen Abstraction, and Reequilibration upon Protein Binding. *J. Phys. Chem. B* **2011**, *115*, 10768-10774.

(9) Horspool, M.; Lenci, F.: In *Handbook of Organic Photochemistry and Photobiology*; CRC Press: USA, 2003.

(10) Bach, T. Stereoselective Intermolecular [2+2]-Photocycloaddition Reactions and Their Application in Synthesis. *Synthesis* **1998**, 1998, 683-703.

(11) Schuster, D. I.; Lem, G.; Kaprinidis, N. A. New Insights into an Old Mechanism: [2+2] Photocycloaddition of Enones to Alkenes. *Chem. Rev.* **1993**, 93, 3-22.

(12) Downes, A.; Blunt, T. P. Researches on the Effect of Light upon Bacteria and other Organisms. *Proc R Soc Lond* **1877**, 26:488.

(13) Unna, P. G.: *The Histopathology of the Diseases of the Skin*; W. F. Clay: Edinburgh, 1896.

(14) Barbatti, M.; Borin, A. C.; Ullrich, S.: *Photoinduced Phenomena in Nucleic Acids I: Nucleobases in the Gas Phase and in solvents*; Springer, 2015.

(15) Seebode, C.; Lehmann, J.; Emmert, S. Photocarcinogenesis and Skin Cancer Prevention Strategies. *Anticancer Res.* **2016**, 36, 1371-1378.

(16) Douki, T.: Formation and Repair of UV-Induced DNA Damage. In *CRC Handbook of Organic Photochemistry and Photobiology*; 3rd ed.; Griesbeck, A., Oelgemöller, M., Ghetti, F., Eds.; CRC Press: Boca Raton, FL, 2012; Vol. 1; pp 1349-1392.

(17) Ravanat, J. L.; Douki, T.; Cadet, J. Direct and Indirect Effects of UV Radiation on DNA and its Components. *J. Photochem. Photobiol. B: Biol.* **2001**, 63, 88-103.

(18) Cadet, J.; Berger, M.; Douki, T.; Morin, B.; Raoul, S.; Ravanat, J. L.; Spinelli, S. Effects of UV and Visible Radiation on DNA-Final Base Damage. *J. Biol. Chem.* **1997**, 378, 1275-1286.

(19) Schuch, A. P.; Machado Garcia, C. C.; Makita, K.; Martins Menck, C. F. DNA Damage as a Biological Sensor for Environmental Sunlight. *Photochem. Photobiol. Sci.* **2013**, 12, 1259-1272.

(20) Lucas, R.; Norval, M.; Neale, R. E.; Young, A.; de Gruijl, F.; Takizawa, Y.; Leun, J. C. The Consequences for Human Health of Stratospheric Ozone Depletion in Association with other Environmental Factors. *Photochem. Photobiol. Sci.* **2014**, *14*.

(21) Douki, T.; Sage, E. Dewar Valence Isomers, the Third Type of Environmentally Relevant DNA Photoproducts Induced by Solar Radiation. *Photochem. Photobiol. Sci.* **2016**, *15*, 24-30.

(22) Schreier, W. J.; Schrader, T. E.; Koller, F. O.; Gilch, P.; Crespo-Hernández, C. E.; Swaminathan, V. N.; Carell, T.; Zinth, W.; Kohler, B. Thymine Dimerization in DNA is an Ultrafast Process. *Science* **2007**, *315*, 625-629.

(23) Garcés, F.; Dávila, C. A. Alterations in DNA Irradiated with Ultraviolet Radiation - I. The Formation Process of Cyclobutylpyrimidine Dimers: Cross Sections, Action Spectra and Quantum Yields. *Photochem. Photobiol.* **1982**, *35*, 9-16.

(24) Cadet, J.; Voituriez, L.; Hruska, F. E.; Kan, L.-S.; de Leeuw, F. A. A.; Altona, C. Characterization of Thymidine Ultraviolet Photoproducts. Cyclobutane Dimers and 5,6-Dihydrothymidines. *Can. J. Chem.* **1985**, *63*, 2861-2868.

(25) Douki, T.; Cadet, J. Individual Determination of the Yield of the Main UV-Induced Dimeric Pyrimidine Photoproducts in DNA Suggests a High Mutagenicity of CC Photolesions. *Biochemistry* **2001**, *40*, 2495-2501.

(26) Ravanat, J.-L.; Douki, T. UV and Ionizing Radiations Induced DNA Damage, Differences and Similarities. *Radiat. Phys. Chem.* **2016**, *128*, 92-102.

(27) Peng, W.; Shaw, B. R. Accelerated Deamination of Cytosine Residues in UV-Induced Cyclobutane Pyrimidine Dimers Leads to CC-->TT Transitions. *Biochemistry* **1996**, *35*, 10172-10181.

(28) Schreier, W. J.; Gilch, P.; Zinth, W. Early Events of DNA Photodamage. *Annu. Rev. Phys. Chem.* **2015**, *66*, 497-519.

(29) Gontcharov, J.; Liu, L. Z.; Pilles, B. M.; Carell, T.; Schreier, W. J.; Zinth, W. Triplet-Induced Lesion Formation at CpT and TpC Sites in DNA. *Chem. Eur. J.* **2019**, *25*, 15164-15172.

(30) Cadet, J.; Mouret, S.; Ravanat, J.-L.; Douki, T. Photoinduced Damage to Cellular DNA: Direct and Photosensitized Reactions. *Photochem. Photobiol.* **2012**, *88*, 1048-1065.

(31) Kielbassa, C.; Roza, L.; Epe, B. Wavelength Dependence of Oxidative DNA Damage Induced by UV and Visible Light. *Carcinogenesis* **1997**, *18*, 811-816.

(32) Cadet, J.; Douki, T. Formation of UV-Induced DNA Damage Contributing to Skin Cancer Development. *Photochem. Photobiol. Sci.* **2018**, *17*, 1816-1841.

(33) Mouret, S.; Phillippe, C.; Gracia-Chantegrel, J.; Banyasz, A.; Karpati, S.; Markovitsi, D.; Douki, T. UVA-Induced Cyclobutane Pyrimidine Dimers in DNA: a Direct Photochemical Mechanism *Org. Biomol. Chem.* **2010**, *8*, 1706-1711.

(34) Banyasz, A.; Vayá, I.; Changenet-Barret, P.; Gustavsson, T.; Douki, T.; Markovitsi, D. Base Pairing Enhances Fluorescence and Favors Cyclobutane Dimer Formation Induced upon Absorption of UVA Radiation by DNA. *J. Am. Chem. Soc.* **2011**, *133*, 5163-5165.

(35) Pilles, B. M.; Bucher, D. B.; Liu, L.; Clivio, P.; Gilch, P.; Zinth, W.; Schreier, W. J. Mechanism of the Decay of Thymine Triplets in DNA Single Strands. *J. Phys. Chem. Lett.* **2014**, *5*, 1616-1622.

(36) Liu, L.; Pilles, B. M.; Gontcharov, J.; Bucher, D. B.; Zinth, W. Quantum Yield of Cyclobutane Pyrimidine Dimer Formation Via the Triplet Channel Determined by Photosensitization. *J. Phys. Chem. B* **2016**, *120*, 292-298.

(37) Mitchell, D. L.; Allison, J. P.; Nairn, R. S. Immunoprecipitation of Pyrimidine(6-4)pyrimidone Photoproducts and Cyclobutane Pyrimidine Dimers in UV-Irradiated DNA. *Radiat. Res.* **1990**, *123*, 299-303.

(38) Perdiz, D.; Gróf, P.; Mezzina, M.; Nikaido, O.; Moustacchi, E.; Sage, E. Distribution and Repair of Bipyrimidine Photoproducts in Solar UV-Irradiated Mammalian Cells. *J. Biol. Chem.* **2000**, *275*, 26732-26742.

(39) Vendrell-Criado, V.; Rodríguez-Muñiz, G. M.; Lhiaubet-Vallet, V.; Cuquerella, M. C.; Miranda, M. A. The (6-4) Dimeric Lesion as a DNA Photosensitizer. *ChemPhysChem* **2016**, *17*, 1979-1982.

(40) González-Luque, R.; Climent, T.; González-Ramírez, I.; Merchán, M.; Serrano-Andrés, L. Singlet-Triplet States Interaction Regions in DNA/RNA Nucleobase Hypersurfaces. *Journal of Chemical Theory and Computation* **2010**, *6*, 2103-2114.

(41) Vendrell-Criado, V.; Rodríguez-Muñiz, G. M.; Yamaji, M.; Lhiaubet-Vallet, V.; Cuquerella, M. C.; Miranda, M. A. Two-Photon Chemistry from Upper Triplet States of Thymine. *J. Am. Chem. Soc.* **2013**, *135*, 16714-16719.

(42) Melnikova, V. O.; Ananthaswamy, H. N. Cellular and Molecular Events Leading to the Development of Skin Cancer. *Mutat. Res-Fund Mol. M.* **2005**, *571*, 91-106.

(43) Pfeifer, G. P. Formation and Processing of UV Photoproducts: Effects of DNA Sequence and Chromatin Environment. *Photochem. Photobiol.* **1997**, *65*, 270-283.

(44) Boorstein, R. J.; Hilbert, T. P.; Cunningham, R. P.; Teebor, G. W. Formation and Stability of Repairable Pyrimidine Photohydrates in DNA. *Biochemistry* **1990**, *29*, 10455-10460.

(45) Kumar, S.; Sharma, N. D.; Davies, R. J.; Phillipson, D. W.; McCloskey, J. A. The Isolation and Characterisation of a New Type of Dimeric Adenine Photoproduct in UV-Irradiated Deoxyadenylates. *Nucleic Acids Res.* **1987**, *15*, 1199-1216.

(46) Koning, T. M.; Davies, R. J.; Kaptein, R. The Solution Structure of the Intramolecular Photoproduct of d(TpA) Derived with the Use of NMR and

a Combination of Distance Geometry and Molecular Dynamics. *Nucleic Acids Res.* **1990**, *18*, 277-284.

(47) Zhao, X.; Nadji, S.; Kao, J. L.; Taylor, J. S. The Structure of d(TpA), The Major Photoproduct of Thymidyl-(3'5')-deoxyadenosine. *Nucleic Acids Res.* **1996**, *24*, 1554-1560.

(48) Foote, C. S. Definition of Type I and Type II Photosensitized oxidation. *Photochem. Photobiol.* **1991**, *54*, 659-659.

(49) Steenken, S.; Jovanovic, S. V. How Easily Oxidizable Is DNA? One-Electron Reduction Potentials of Adenosine and Guanosine Radicals in Aqueous Solution. *J. Am. Chem. Soc.* **1997**, *119*, 617-618.

(50) Cadet, J.; Delatour, T.; Douki, T.; Gasparutto, D.; Pouget, J.-P.; Ravanat, J.-L.; Sauvaigo, S. Hydroxyl Radicals and DNA Base Damage. *Mutat. Res-Fund Mol. M.* **1999**, *424*, 9-21.

(51) Hubaud, J.-C.; Bombarda, I.; Decome, L.; Wallet, J.-C.; Gaydou, E. M. Synthesis and Spectroscopic Examination of Various Substituted 1,3-Dibenzoylmethane, Active Agents for UVA/UVB Photoprotection. *J. Photochem. Photobiol. B: Biol.* **2008**, *92*, 103-109.

(52) Skovsen, E.; Snyder, J. W.; Lambert, J. D. C.; Ogilby, P. R. Lifetime and Diffusion of Singlet Oxygen in a Cell. *J. Phys. Chem. B* **2005**, *109*, 8570-8573.

(53) Cuquerella, M. C.; Lhiaubet-Vallet, V.; Bosca, F.; Miranda, M. A. Photosensitized Pyrimidine Dimerisation in DNA. *Chem. Sci.* **2011**, *2*, 1219-1232.

(54) Mouret, S.; Baudouin, C.; Charveron, M.; Favier, A.; Cadet, J.; Douki, T. Cyclobutane Pyrimidine Dimers Are Predominant DNA Lesions in Whole Human Skin Exposed to UVA Radiation. *Proc. Natl. Acad. Sci. USA* **2006**, *103*, 13765-13770.

(55) Douki, T.; Reynaud-Angelin, A.; Cadet, J.; Sage, E. Bipyrimidine Photoproducts rather than Oxidative Lesions Are the Main Type of DNA

Damage Involved in the Genotoxic Effect of Solar UVA Radiation. *Biochemistry* **2003**, *42*, 9221-9226.

(56) Barbatti, M.; Borin, A. C.; Ullrich, S.: *Photoinduced Phenomena in Nucleic Acids II: DNA Fragments and Phenomenological Aspects*; Springer, 2015.

(57) Morrison, H.; Kleopfer, R. Organic Photochemistry. VIII. Solvent Effects on Liquid-Phase Photodimerization of Dimethylthymine. *J. Am. Chem. Soc.* **1968**, *90*, 5037-5038.

(58) Kleopfer, R.; Morrison, H. Organic Photochemistry. XVII. Solution-Phase Photodimerization of Dimethylthymine. *J. Am. Chem. Soc.* **1972**, *94*, 255-264.

(59) Rahn, R. O.; Landry, L. C. Pyrimidine Dimer Formation in Poly (d-dT) and Apurinic Acid. *Biochim. Biophys. Acta* **1971**, *247*, 197-206.

(60) Cuquerella, M. C.; Lhiaubet-Vallet, V.; Miranda, M. A.; Bosca, F. Drug-DNA Complexation as the Key Factor in Photosensitized Thymine Dimerization. *Phys. Chem. Chem. Phys.* **2017**, *19*, 4951-4955.

(61) Boscá, F.; Miranda, M. A. New Trends in Photobiology. Photosensitizing Drugs Containing the Benzophenone Chromophore. *J. Photochem. Photobiol. B: Biol.* **1998**, *43*, 1-26.

(62) Klecak, G.; Urbach, F.; Urwyler, H. Fluoroquinolone Antibacterials Enhance UVA-Induced Skin Tumors. *J. Photochem. Photobiol. B: Biol.* **1997**, *37*, 174-181.

(63) Lhiaubet-Vallet, V.; Bosca, F.; Miranda, M. A. Photosensitized DNA Damage: The Case of Fluoroquinolones. *Photochem. Photobiol.* **2009**, *85*, 861-868.

(64) Soldevila, S.; Cuquerella, M. C.; Bosca, F. Understanding of the Photoallergic Properties of Fluoroquinolones: Photoreactivity of Lomefloxacin with Amino Acids and Albumin. *Chem. Res. Toxicol.* **2014**, *27*, 514-523.

(65) Traynor, N. J.; Kratzer, B.; Miranda, M. A.; Gibbs, N. K. Fluoroquinolones Photogenotoxicity in Human Keratinocytes: Involvement of Photoproducts and H<sub>2</sub>O<sub>2</sub>. *Br. J. Dermatol.* **1999**, *140*, 784.

(66) Costalat, R.; Blais, J.; Ballini, J. P.; Moysan, A.; Cadet, J.; Chalvet, O.; Vigny, P. Formation of Cyclobutane Thymine Dimers Photosensitized by Pyridopsoralens- A Triplet-Triplet Energy-Transfer Mechanism. *Photochem. Photobiol.* **1990**, *51*, 255-262.

(67) Moysan, A.; Viari, A.; Vigny, P.; Voituriez, L.; Cadet, J.; Moustacchi, E.; Sage, E. Formation of Cyclobutane Thymine Dimers Photosensitized by Pyridopsoralens - Quantitative and Qualitative Distribution within DNA. *Biochemistry* **1991**, *30*, 7080-7088.

(68) Stern, R. S.; J., L. E.; Väkevä, L. Oral Psoralen and Ultraviolet-A Light (PUVA) Treatment of Psoriasis and Persistent Risk of Nonmelanoma Skin Cancer. *J. Natl. Cancer Inst.* **1998**, *90*, 1278-1284.

(69) Young, A. R. Photocarcinogenicity of Psolarens Used in PUVA Treatment - Present Status in Mouse and Man. *Photochem. Photobiol. B: Biol.* **1990**, *6*, 237-247.

(70) Bosca, F.; Lhiaubet-Vallet, V.; Cuquerella, M. C.; Castell, J. V.; Miranda, M. A. The Triplet Energy of Thymine in DNA. *J. Am. Chem. Soc.* **2006**, *128*, 6318-6319.

(71) Lamola, A. A.; Gueron, M.; Yamane, T.; Eisinger, J.; Shulman, R. G. Triplet State of DNA. *J. Chem. Phys.* **1967**, *47*, 2210-2217.

(72) Wood, P. D.; Redmond, R. W. Triplet State Interactions between Nucleic Acid Bases in Solution at Room Temperature: Intermolecular Energy and Electron Transfer. *J. Am. Chem. Soc.* **1996**, *118*, 4256.

(73) Gut, I. G.; Wood, P. D.; Redmond, R. W. Interaction of Triplet Photosensitizers with Nucleotides and DNA in Aqueous Solution at Room Temperature. *J. Am. Chem. Soc.* **1996**, *118*, 2366-2373.

(74) Abouaf, R.; Pommier, J.; Dunet, H.; Quan, P.; Nam, P. C.; Nguyen, M. T. The Triplet State of Cytosine and its Derivatives: Electron Impact and Quantum Chemical Study. *J. Chem. Phys.* **2004**, *121*, 11668-11674.

(75) Nguyen, M. T.; Zhang, R.; Nam, P.-C.; Ceulemans, A. J. Singlet-Triplet Energy Gaps of Gas-Phase RNA and DNA Bases. A Quantum Chemical Study. *J. Phys. Chem. A* **2004**, *108*, 6554-6561.

(76) Encinas, S.; Belmadoui, N.; Climent, M. J.; Gil, S.; Miranda, M. A. Photosensitization of Thymine Nucleobase by Benzophenone Derivatives as Models for Photoinduced DNA Damage: Paterno-Büchi vs Energy and Electron Transfer Processes. *Chem. Res. Toxicol.* **2004**, *17*, 857-862.

(77) Delatour, T.; Douki, T.; D'Ham, C.; Cadet, J. Photosensitization of Thymine Nucleobase by Benzophenone through Energy Transfer, Hydrogen Abstraction and One-Electron Oxidation. *J. Photochem. Photobiol. B: Biol.* **1998**, *44*, 191-198.

(78) Lhiaubet, V.; Paillous, N.; Chouini-Lalanne, N. Comparison of DNA Damage Photoinduced by Ketoprofen, Fenofibric Acid and Benzophenone via Electron and Energy Transfer. *Photochem. Photobiol.* **2001**, *74*, 670-678.

(79) Lhiaubet-Vallet, V.; Trzcionka, J.; Encinas, S.; Miranda, M. A.; Chouini-Lalanne, N. The Triplet State of a N-phenylphthalimidine with High Intersystem Crossing Efficiency: Characterization by Transient Absorption Spectroscopy and DNA Sensitization Properties. *J. Phys. Chem. B* **2004**, *108*, 14148-14153.

(80) Sauvaigo, S.; Douki, T.; Odin, F.; Caillat, S.; Ravanat, J. L.; Cadet, J. Analysis of Fluoroquinolone-Mediated Photosensitization of 2'-Deoxyguanosine, Calf Thymus and Cellular DNA: Determination of Type-I, Type-II and Triplet-Triplet Energy Transfer Mechanism Contribution. *Photochem. Photobiol.* **2001**, *73*, 230-237.

(81) Lhiaubet-Vallet, V.; Cuquerella, M. C.; Castell, J. V.; Bosca, F.; Miranda, M. A. Triplet Excited Fluoroquinolones as Mediators for Thymine Cyclobutane Dimer Formation in DNA. *J. Phys. Chem. B* **2007**, *111*, 7409-7414.

(82) Sandros, K. Transfer of Triplet State Energy in Fluid Solutions III. Reversible Energy Transfer. *Acta Chem. Scand.* **1964**, *18*, 2355-2374.

(83) Bensasson, R. V.; Land, E. J.; Truscott, T. G.: *Laser Photolysis and Pulse Radiolysis*; 1st ed.: Oxford, 1983.

(84) Greenstock, C. L.; Johns, H. E. Photosensitized Dimerization of Pyrimidines. *Biochem. Biophys. Res. Commun.* **1968**, *30*, 21-27.

(85) Ben-Hur, E.; Elad, D.; Ben-Ishai, R. The Photosensitized Dimerization of Thymidine in Solution. *Biochim. Biophys. Acta* **1967**, *149*, 355-360.

(86) Jennings, B. H.; Pastra, S.-C.; Wellington, J. L. Photosensitized Dimerization of Thymine. *Photochem. Photobiol.* **1970**, *11*, 215-226.

(87) Elad, D.; Krüger, C.; Schmidt, G. M. J. The Photosensitized Solution Dimerization of Dimethyluracil and Dimethylthymine. Four Photodimers of Dimethyluracil. *Photochem. Photobiol.* **1967**, *6*, 495-496.

(88) Cuquerella, M. C.; Lhiaubet-Vallet, V.; Cadet, J.; Miranda, M. A. Benzophenone Photosensitized DNA Damage. *Acc. Chem. Res.* **2012**, *45*, 1558-1570.

(89) Belmadoui, N.; Encinas, S.; Climent, M. J.; Gil, S.; Miranda, M. A. Intramolecular Interactions in the Triplet Excited States of Benzophenone-Thymine Dyads. *Chem. Eur. J.* **2006**, *12*, 553-561.

(90) Miro, P.; Lhiaubet-Vallet, V.; Marin, M. L.; Miranda, M. A. Photosensitized Thymine Dimerization via Delocalized Triplet Excited States. *Chem. Eur. J.* **2015**, *21*, 17051-17056.

(91) Nakatani, K.; Yoshida, T.; Saito, I. Photochemistry of Benzophenone Immobilized in a Major Groove of DNA: Formation of

Thermally Reversible Interstrand Cross-link. *J. Am. Chem. Soc.* **2002**, *124*, 2118-2119.

(92) Charlier, M.; Helene, C. Photochemical Reactions of Aromatic Ketones with Nucleic Acids and their Components. I. Purine and Pyrimidine Bases and Nucleosides. *Photochem Photobiol* **1972**, *15*, 71-87.

(93) Prakash, G.; Falvey, D. E. Model Studies of the (6-4) Photoproduct DNA Photolyase: Synthesis and Photosensitized Splitting of a Thymine-5,6-oxetane. *J. Am. Chem. Soc.* **1995**, *117*, 11375-11376.

(94) Varghese, A. J. Acetone-Sensitized Dimerization of Cytosine Derivatives. *Photochem. Photobiol.* **1972**, *15*, 113-118.

(95) Zuo, Z.-h.; Yao, S.-d.; Luo, J.; Wang, W.-f.; Zhang, J.-s.; Lin, N.-y. Laser Photolysis of Cytosine, Cytidine and dCMP in Aqueous Solution. *J. Photochem. Photobiol. B: Biol.* **1992**, *15*, 215-222.

(96) Song, Q. H.; Lin, W. Z.; Yao, S. D.; Lin, N. Y. Comparative Studies of Triplet States of Thymine Components by Acetone Sensitization and Direct Excitation in Aqueous Solution at Room Temperature. *J. Photochem. Photobiol. A: Chem.* **1998**, *114*, 181-184.

(97) Varghese, A. J. Photocycloaddition of Acetone to Uracil and Cytosine *Photochem. Photobiol.* **1975**, *21*, 147-151.

(98) Vendrell-Criado, V.; Lhiaubet-Vallet, V.; Yamaji, M.; Cuquerella, M. C.; Miranda, M. A. Blocking Cyclobutane Pyrimidine Dimer Formation by Steric Hindrance. *Org. Biomol. Chem.* **2016**, *14*, 4110-4115.

(99) Yang, N.-C.; McClure, D. S.; Murov, S.; Houser, J. J.; Dusenbery, R. Photoreduction of Acetophenone and Substituted Acetophenones. *J. Am. Chem. Soc.* **1967**, *89*, 5466-5468.

(100) Chattopadhyay, S. K.; Kumar, C. V.; Das, P. K. Substituent Effects in the Quenching of Acetophenone and Benzophenone Triplets by Oxygen and the Di-tert-butylnitroxy Radical, and the Efficiency of Singlet Oxygen Photogeneration. *J. Photochem.* **1985**, *30*, 81-91.

(101) Liu, L.; Pilles, B. M.; Reiner, A. M.; Gontcharov, J.; Zinth, W. 2'-Methoxyacetophenone: an Efficient Photosensitizer for Cyclobutane Pyrimidine Dimer Formation. *ChemPhysChem* **2015**, *16*, 3483-3487.

(102) Albini, A.: *Photochemistry: Past, Present and Future*; Springer, 2016.

(103) Marguet, S.; Markovitsi, D. Time-Resolved Study of Thymine Dimer Formation. *J. Am. Chem. Soc.* **2005**, *127*, 5780-5781.

(104) Kwok, W. M.; Ma, C.; Phillips, D. L. A Doorway State Leads to Photostability or Triplet Photodamage in Thymine DNA. *J. Am. Chem. Soc.* **2008**, *130*, 5131-5139.

(105) Wang, Z.; Weininger, S. J.; McGimpsey, W. G. Photochemistry of the Triplet T<sub>2</sub> State of Anthracene. *J. Phys. Chem.* **1993**, *97*, 374-378.

(106) McGimpsey, W. G.; Scaiano, J. C. Photochemistry and Photophysics from Upper Triplet Levels of 9,10-Dibromoanthracene. *J. Am. Chem. Soc.* **1989**, *111*, 335-340.

(107) Cai, X.; Hara, M.; Kawai, K.; Tojo, S.; Fujitsuka, M.; Majima, T. Some Triplet Energy-Transfer Reactions Initiated by Photoexcitation of Triplet Excited State of Dibenz[a,h]anthracene to the Higher Triplet Excited States. *Tetrahedron Lett.* **2003**, *44*, 6117-6120.

(108) McGimpsey, W. G.; Scaiano, J. C. A Two-Photon Study of the "Reluctant" Norrish Type I Reaction of Benzil. *J. Am. Chem. Soc.* **1987**, *109*, 2179-2181.

(109) Thomas, J. K. Higher Excited States in Multiphoton Photochemical Reactions "Hint" Toward Rapid Chemistry. *J. Phys. Chem. Lett.* **2014**, *5*, 2586-2587.

(110) Liu, R. S. H.; Edman, J. R. Role of Second Triplet States in Solution Photochemistry. IV. Triplet-Triplet Energy Transfer from the Second Triplet States of Anthracenes. Chemical Studies. *J. Am. Chem. Soc.* **1969**, *91*, 1492-1497.

(111) Scaiano, J. C.; Johnston, L. J.; McGimpsey, W. G.; Weir, D. Photochemistry of Organic Reaction Intermediates: Novel Reaction Paths Induced by Two-Photon Laser Excitation. *Acc. Chem. Res.* **1988**, *21*, 22-29.

(112) McGimpsey, W. G.: Chemical and Photophysical Processes of Transients Derived from Multiphoton Excitation: Upper Excited States and Excited Radicals. In *Organic and Inorganic Photochemistry*; Ramamurthy, V., Schanze, K. S., Eds.; Marcel Dekker, 1998; Vol. 2; pp 249-306.

(113) Harada, Y.; Okabe, C.; Kobayashi, T.; Suzuki, T.; Ichimura, T.; Nishi, N.; Xu, Y.-Z. Ultrafast Intersystem Crossing of 4-Thiothymidine in Aqueous Solution. *J. Phys. Chem. Lett.* **2010**, *1*, 480-484.

(114) Leupold, D.; Kochevar, I. E. Multiphoton Photochemistry in Biological Systems Introduction. *Photochem. Photobiol.* **1997**, *66*, 562-565.

(115) Gut, I. G.; Farmer, R.; Huang, R. C.; Kochevar, I. E. Upper Excited State Photochemistry of DNA. *Photochem. Photobiol.* **1993**, *58*, 313-317.

(116) Brocklehurst, B. Radiation Damage in DNA: Possible Role of Higher Triplet States. *Radiat. Res.* **2001**, *155*, 637-640.

(117) Rubin, L. B.; Menshonkova, T. N.; Simukova, N. A.; Budowsky, E. I. The Effects of High-Intensity UV-Radiation on Nucleic Acids and their Components - I. Thymine. *Photochem. Photobiol.* **1981**, *34*, 339-344.

(118) Gurzadyan, G. G.; Görner, H. Depopulation of Highly Excited Singlet States of DNA Model Compounds: Quantum Yields of 193 and 245 nm Photoproducts of Pyrimidine Monomers and Dinucleoside Monophosphates. *Photochem. Photobiol.* **1996**, *63*, 143-153.

(119) Masnyk, T. W.; Nguyen, H. T.; Minton, K. W. Reduced Formation of Bipyrimidine Photoproducts in DNA UV Irradiated at High Intensity. *J. Biol. Chem.* **1989**, *264*, 2482-2488.



# CHAPTER 2

## Chapter 2. General Objectives

---



This Doctoral Thesis focuses on photosensitised DNA damage, related with UVA light that is not directly absorbed by the biomolecule, but by endogenous or exogenous chromophores present in drugs, cosmetic agents, metabolites, etc. The general objective is to gain a deeper understanding of the molecular processes involved in the formation of pyrimidine dimers in the triplet excited state. With this goal, 2'-methoxyacetophenone has been chosen as photosensitiser to investigate the photochemistry of different DNA models of increasing complexity from their triplet excited states.

Accordingly, this has been approached through the following specific objectives, which correspond to the different chapters of this Doctoral Thesis:

- 1) To undertake a more complete characterisation of the photosensitiser 2'-methoxyacetophenone using UV-VIS transient absorption spectroscopy, making a special emphasis on its triplet excited state and the rate constant of its quenching by a dimeric thymine model, in connection with CPDs formation.
- 2) To determine the nature of the rate controlling step in the 2'-methoxyacetophenone photosensitised cyclisation of polymethylene-linked homo- and heterobipyrimidine models, making use of C5 substitution in combination with entropic factors related to the length of the linking bridge.
- 3) To develop a methodology to generate the  $T_2(n\pi^*)$  of thymine through excitation of its  $T_1$ , populated in turn by energy transfer from the  $T_1$  of the photosensitiser, 2'-methoxyacetophenone. For demonstrating the feasibility of the concept two model reactions have been chosen:

the Norrish-Yang photocyclisation of a *tert*-butyluracil and the photohydration of its parent uracil analogue.

# CHAPTER 3

## Chapter 3. Transient UV-Vis Absorption Spectroscopic Characterisation of 2'-Methoxyacetophenone as a DNA Photosensitiser

---

---



### 3.1. Introduction

As mentioned previously in the introduction, the behaviour of aromatic ketones upon light absorption has been intensively investigated due to their particular features, such as relatively long absorption wavelengths and high intersystem crossing quantum yields.<sup>1</sup> The photoreactivity of these compounds depends on the nature ( $n\pi^*$  vs  $\pi\pi^*$ ) of the lowest triplet state; thus, Norrish I/II, hydrogen abstraction or Paternò-Büchi are typical  $n\pi^*$  photoreactions. In this context, variations in the aromatic substituents or the solvents have a marked influence on the relative energy of the  $n\pi^*/\pi\pi^*$  triplet states and hence on the photoreactivity pattern.<sup>2</sup> Aromatic ketones such as benzophenones and acetophenones have been often used as triplet photosensitisers;<sup>1</sup> in particular, they have turned out to be very useful tools to investigate the photosensitisation mechanism responsible for the formation of DNA lesions like oxidative damage or cyclobutane pyrimidine dimers (CPDs).<sup>3-9</sup>

2'-Methoxyacetophenone (**2M**) presents enhanced UVA absorption as compared with other acetophenone derivatives.<sup>10</sup> This allows selective excitation of **2M** in the presence of pyrimidines, which is mandatory for an appropriate CPDs photosensitiser.<sup>11</sup> Previous transient spectroscopic studies have made use of pico- and nanosecond IR detection to show formation of thymine dimers through a **2M**-photosensitised pathway.<sup>10</sup> Although valuable photophysical information was provided like the time constant of triplet formation (in the sub-ns region) and the intersystem crossing quantum yield ( $\Phi_{ISC}$ , close to unity) a more detailed investigation on **2M** properties would be necessary to fully characterise this ketone as a potential DNA photosensitiser, not only for CPDs formation, but also for oxidative DNA damage.

With this background, this chapter aims to undertake a complete UV-Vis transient absorption spectroscopy characterisation of this compound, including triplet-triplet spectra, triplet lifetimes and rate constants for quenching of **2M** by a dimeric thymine derivative. Furthermore, the capability of **2M** to produce  $^1\text{O}_2$ , as a key parameter related to oxidative DNA damage is also studied by means of time-resolved near IR phosphorescence measurements at 1270 nm.

### 3.2. Results and Discussion

The ultraviolet (UV) spectrum of **2M** was registered, displaying two maxima centred *ca* 250 and 310 nm and a tail extending up to 360 nm (Figure 3.1 A). Accordingly, transient absorption spectra were recorded upon excitation at 355 nm in deaerated  $\text{H}_2\text{O}$ , ACN and EtOH, with a Nd: YAG laser (Figure 3.1B). A band with a broad maximum between 400 and 450 nm was found in every solvent immediately after excitation, being more intense and 10 nm red-shifted in aqueous solution.

The temporal evolution of the observed transient species was monitored at 430 nm, and the lifetime was determined from the decay traces. In buffered aqueous solution the lifetime was 3.8  $\mu\text{s}$  (Figure 3.1 C, Inset). Based on the high ISC of **2M** (*ca.* 1),<sup>10</sup> this transient was tentatively assigned as the triplet excited state. Indeed, this is consistent with the quenching observed under air and  $\text{O}_2$  atmospheres.

However, an unambiguous spectroscopic evidence for the nature of this transient species was needed. To confirm the assignment, a triplet-triplet energy transfer (TTET) experiment was carried out, in which the energy of the triplet excited state of **2M** was transferred to *S*-flurbiprofen (*S*-FB), to form unequivocally its triplet excited state.

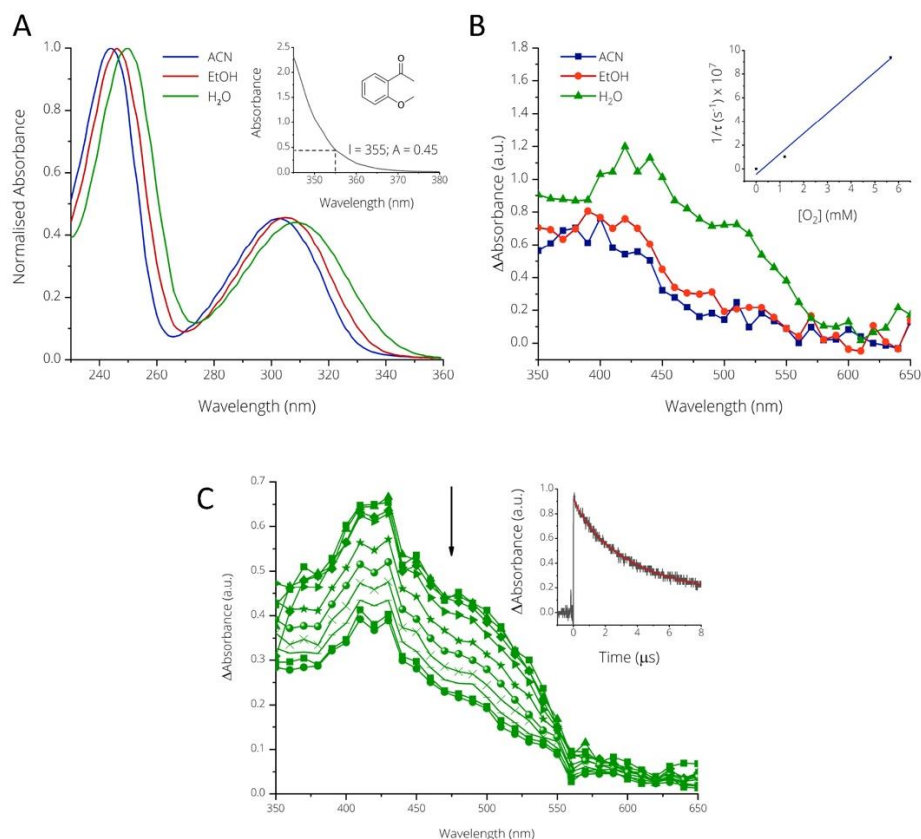


Figure 3.1 A) **2M** UV-Vis spectra in acetonitrile, ethanol and water. Inset) Magnification of the long-wavelength absorption region of **2M** (6.5 mM) in buffered aqueous solution, used in the transient absorption experiments. B) **2M** transient absorption spectra in anaerobic ACN, EtOH and H<sub>2</sub>O immediately after laser excitation. Inset) Reciprocal of  $^3\text{2M}^*$  lifetime in ACN at 430 nm under N<sub>2</sub>, air and O<sub>2</sub> against O<sub>2</sub> concentration (Stern-Volmer plot). C) Transient absorption spectra of **2M** in neutral PB under deaerated conditions at different times after 355 nm laser excitation. Inset) Kinetic decay of **2M** at 430 nm in PB under deaerated conditions.

In the present case, *S*-FB does not absorb light beyond 300 nm,<sup>12</sup> allowing for selective excitation of **2M** at 355 nm. As a matter of fact, when a 1.2 mM *S*-FB solution was submitted to the LFP at  $\lambda_{\text{exc}} = 355$  nm no signal was observed. Moreover, although the triplet absorption spectrum of *S*-FB shows some overlap with that of **2M**, it is possible to discriminate between the two species based on their differences in molar absorption coefficients and lifetimes.<sup>12</sup>

Thus, it is possible to monitor the increase of the signal corresponding to  $^3\text{S-FB}^*$  at the expense of  $^3\text{2M}^*$ . As shown in Figure 3.2, the  $^3\text{2M}^*$  spectrum displayed immediately upon laser excitation disappeared with time; concomitantly, a new spectrum built up presenting an intense band centred at 370 nm. Two microseconds after laser excitation, the observed spectrum was coincident with that of  $^3\text{S-FB}^*$ ,<sup>12</sup> indicating that the TTET was complete.

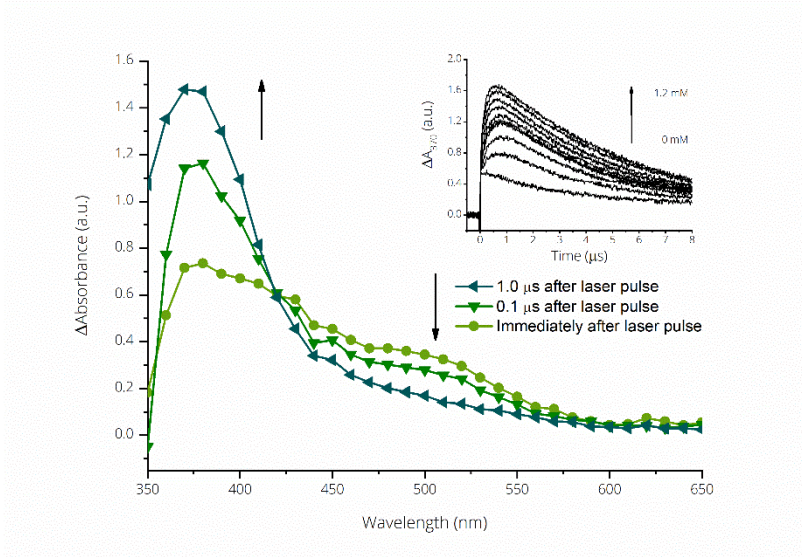


Figure 3.2 Transient absorption spectra of **2M** in the presence of *S*-flurbiprofen (1.2mM) immediately after the laser pulse, 0.1 and 1  $\mu\text{s}$  after laser excitation (355 nm). Inset) Kinetic trace for the *S*-FB band at 370 nm.

Furthermore, the transient absorption at 370 nm increased with increasing concentration of S-FB (Figure 3.2, Inset). When  ${}^3\mathbf{2M}^*$  was monitored at 500 nm in the presence of S-FB (Figure 3.3), a faster decay was progressively observed. Plotting the reciprocal of  ${}^3\mathbf{2M}^*$  lifetime against S-FB concentration, a  $k_q$  of  $3.3 \times 10^9 \text{ M}^{-1} \text{ s}^{-1}$  was obtained (Figure 3.3, Inset).

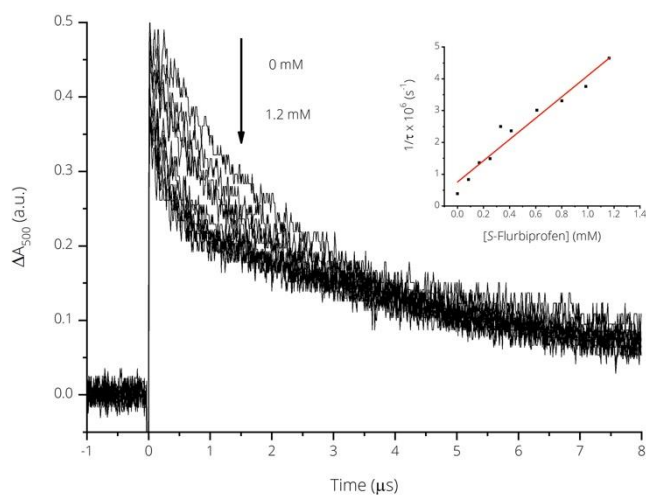


Figure 3.3 Kinetic decay of  $\mathbf{2M}$  at 500 nm after increasing amounts of S-flurbiprofen (from 0 to 1.2 mM) were added. Inset) Stern-Volmer quenching of  $\mathbf{2M}$  triplet by S-flurbiprofen.

To further characterise  $\mathbf{2M}$  as a DNA photosensitiser, its capability to induce oxidative photodamage through a Type II mechanism was evaluated by measuring  ${}^1\text{O}_2$  production. Thus, time-resolved phosphorescence emission at 1270 nm upon 355 nm laser excitation of a  $\mathbf{2M}$  solution was monitored using acetonitrile as solvent and the parent acetophenone as a reference (Figure 3.4).

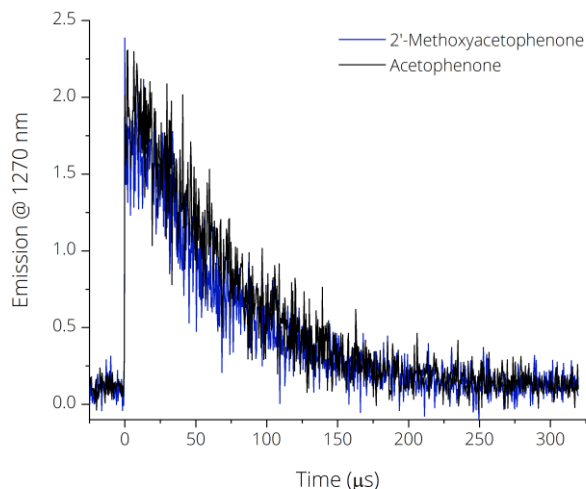


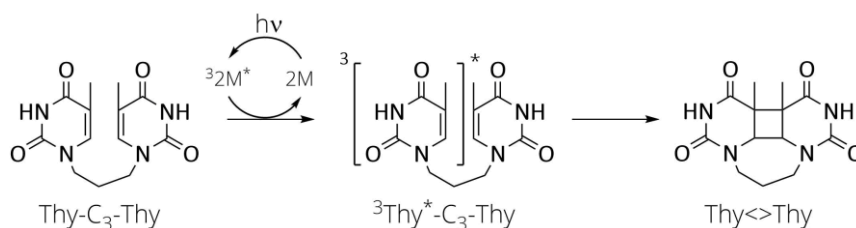
Figure 3.4 Time-resolved detection of singlet oxygen emission at 1270 nm for acetonitrile solutions of **2M** and acetophenone.

The decay traces were nearly superimposable, which indicates that the singlet oxygen quantum yield ( $\Phi_{\Delta}$ ) of **2M** equals that of acetophenone ( $\Phi_{\Delta} = 0.52$ ).<sup>13</sup> This indicates that **2M** can indeed promote DNA oxidation via a Type II photosensitisation.

At this point, a more complete picture of **2M** as a potential DNA photosensitiser was available. Since the singlet oxygen reactivity towards DNA is well known, attention was focused on triplet photosensitisation. In this pathway, thymine (Thy) should be involved in the process as it is the canonical DNA base with the lowest triplet energy.

Irradiation of **2M** in the presence of the dimeric thymine derivative **Thy-C<sub>3</sub>-Thy** was performed and monitored through UV-Vis spectroscopy in order to test the disappearance of the enone chromophore associated with CPDs formation.

The key steps involved in the overall process following irradiation of **2M** are energy transfer from  $^3\mathbf{2M}^*$  to a thymine unit leading to  $^3\text{Thy}^*$  and the subsequent reaction of the excited base with another Thy in its ground state giving rise to the final CPD through a formal [2+2] photocycloaddition (Scheme 3.1).



*Scheme 3.1 CPDs formation process through 2M photosensitisation.*

Under the employed conditions **2M** was found to be photostable, as demonstrated by the fact that its absorption band with maximum at 310 nm remained unaltered along the irradiation. Conversely, a progressive decrease corresponding to the unaltered Thy unit was observed. It is noteworthy that as the photoreaction proceeds, the absorption displayed by the reaction mixture resembles that of **2M** as the CPDs formed do not absorb significantly above 240 nm (the absorption spectrum of the isolated CPD is shown in Figure 3.5 A, blue line). It is also noticeable that, in this experiment, **2M** did not give rise to oxetane by-products as a result of a Paternò-Büchi reaction, as it happens with benzophenone, widely used in pyrimidine photosensitisation experiments.<sup>5</sup>

After 60 min under the employed irradiation conditions **Thy-C<sub>3</sub>-Thy** practically disappeared, (Figure 3.5 A and inset). To confirm that an excited state reaction was actually taking place, quenching of  $^3\mathbf{2M}^*$  by **Thy-C<sub>3</sub>-Thy** was examined. Indeed, addition of increasing concentrations of **Thy-C<sub>3</sub>-Thy** (Figure 3.5 B) resulted in a consistent shortening of the **2M** triplet lifetime.

From the slope of the Stern-Volmer linear plot (Figure 3.5 B, inset) a  $k_q$  value of  $2.1 \times 10^9 \text{ M}^{-1} \text{ s}^{-1}$  was obtained.

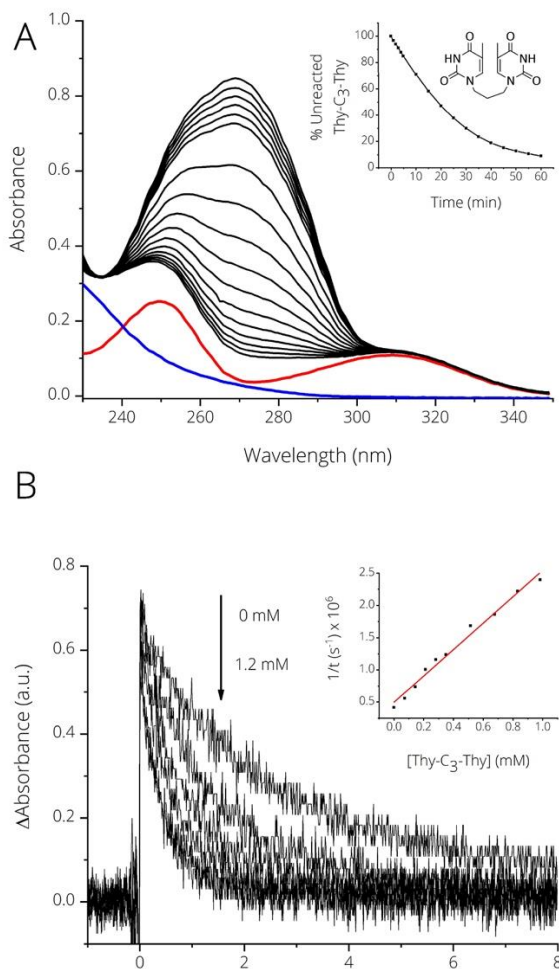


Figure 3.5 A) 2-Methoxyacetophenone photosensitised irradiation of Thy-C<sub>3</sub>-Thy in PB, under deaerated conditions. Spectra of 2M (red) and Thy-C<sub>3</sub>-Thy CPDs (blue) at the same concentration are shown for better comparison. Inset) Unreacted Thy-C<sub>3</sub>-Thy (%) monitored at 270 nm. B) Kinetic decays of 2M in deaerated PB at 500 nm upon addition of increasing amounts of Thy-C<sub>3</sub>-Thy (from 0 M to  $9.8 \times 10^{-4}$  M). Inset) Stern-Volmer quenching of 2M triplet by Thy-C<sub>3</sub>-Thy.

In summary, the photophysical parameters determined for **2M** as a potential DNA photosensitiser are given in Table 3.1

*Table 3.1 Triplet characterisation of 2'-methoxyacetophenone by transient UV-Vis transient absorption spectroscopy.*

$k_{O_2}$	$1.7 \times 10^9 \text{ M}^{-1} \text{ s}^{-1}$
$\tau_T$	$3.8 \mu\text{s}$
$\Phi_\Delta$	0.5
$k_q(\text{S-FB})$	$3.3 \times 10^9 \text{ M}^{-1} \text{ s}^{-1}$
$k_q(\text{Thy-C}_3\text{-Thy})$	$2.1 \times 10^9 \text{ M}^{-1} \text{ s}^{-1}$

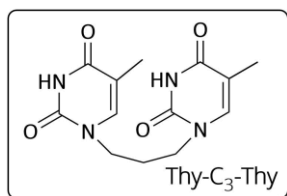
### 3.3. Conclusions

Overall, a complete UV-Vis transient spectroscopic characterisation of 2'-methoxyacetophenone has been performed. The triplet state reactivity of this photosensitiser towards a Thy model has been determined based on the obtained photophysical parameters and on the rate of CPDs formation revealed by UV-Vis monitoring of the steady-state irradiation. These results confirm the potential of **2M** as a convenient DNA photosensitiser for mechanistic studies.

### 3.4. Experimental Section

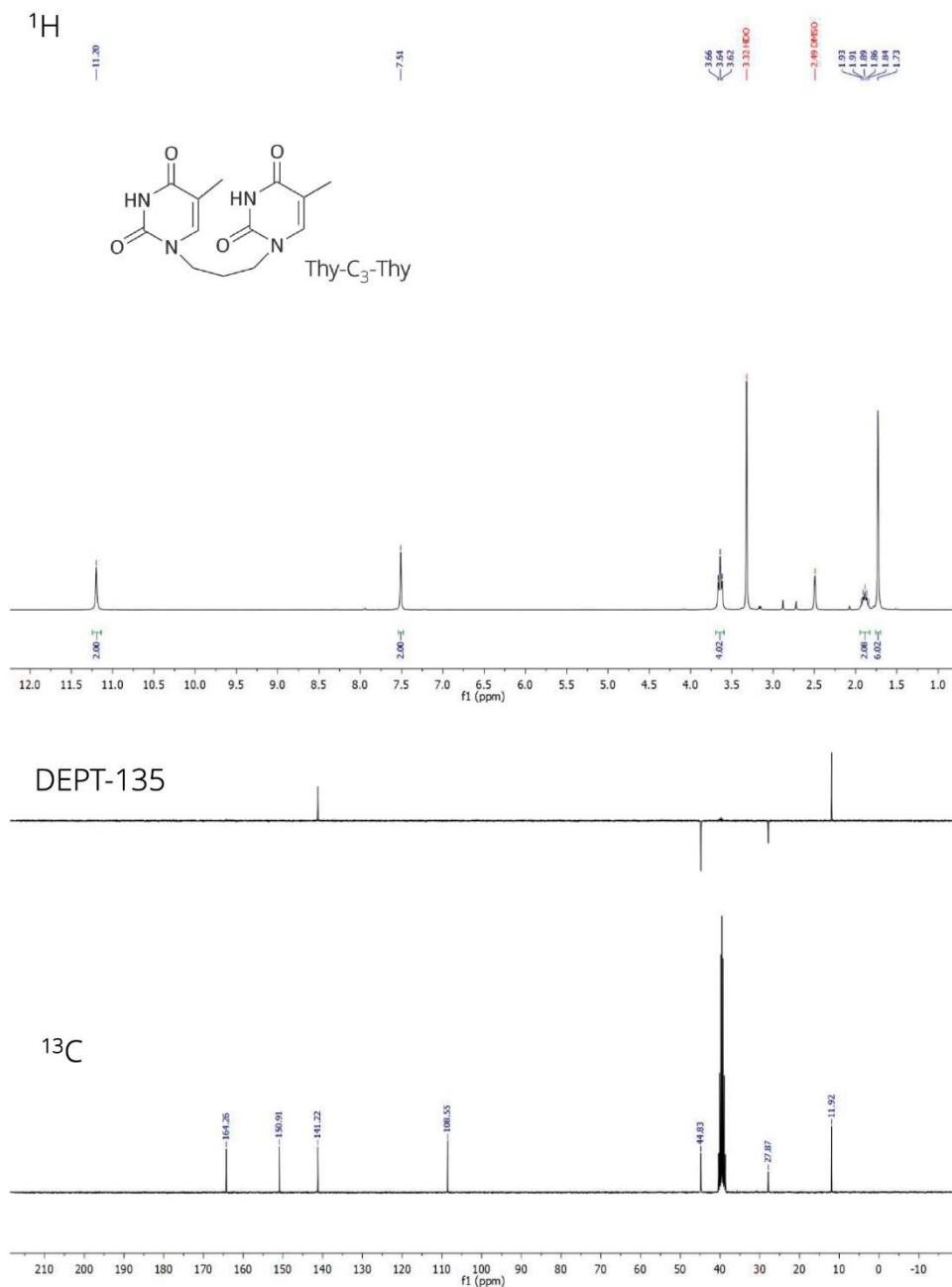
#### 3.4.1. Synthesis and Characterisation

**1,1'-(propane-1,3-diyl)bis(5-methylpyrimidine-2,4(1H,3H)-dione) (Thy-C<sub>3</sub>-Thy):** The dimeric model was synthesised heating 2,4-bis(trimethylsilyloxy)thymine with 1,3-dibromopropane, following the established procedure in the literature.<sup>14-16</sup>

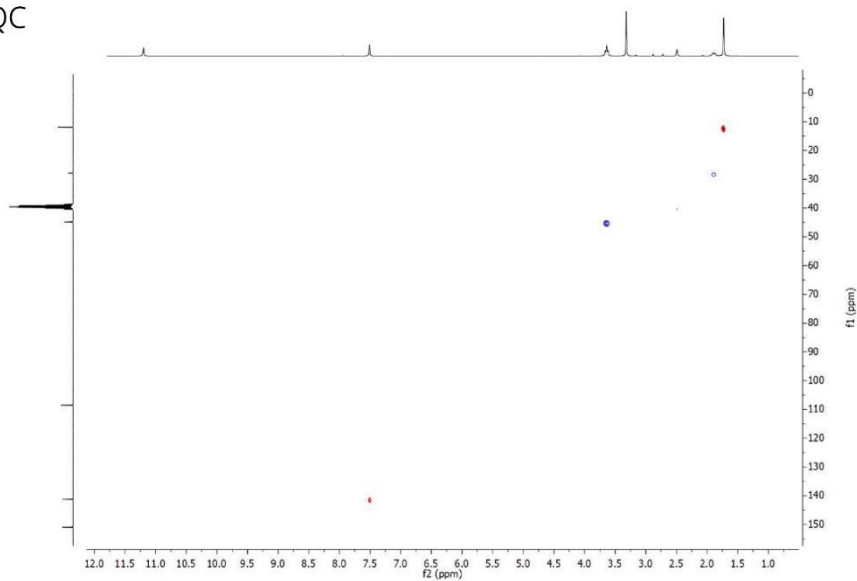


To a solution of O,O'-bis(trimethylsilyl)thymine (1 g, 3.7 mmol) in 8 mL of anhydrous DMF, 1,3-dibromopropane (0.16 mL, 1.6 mmol) was added and the stirred mixture

heated to 170°C overnight. The reaction was cooled to 0°C and 10 mL of water was added to precipitate the product. The white solid was collected by filtration, washed with a CHCl<sub>3</sub>: MeOH 1:1 mixture and dried under reduced pressure to yield 378.6 mg (81%) of Thy-C<sub>3</sub>-Thy. **<sup>1</sup>H NMR** (300 MHz, DMSO-d<sub>6</sub>) δ<sub>H</sub>: 11.20 (s, 2H), 7.51 (s, 2H), 3.64 (t, *J* = 7.1 Hz, 4H), 1.95 – 1.83 (m, 2H), 1.73 (s, 6H). **<sup>13</sup>C NMR** (75 MHz, DMSO-d<sub>6</sub>): 164.3 (2CO), 150.9 (2CO), 141.2 (2CH), 108.6 (2C), 44.8 (2CH<sub>2</sub>), 27.9 (CH<sub>2</sub>), 11.9 (2CH<sub>3</sub>). **HRMS (ESI-TOF) m/z:** [M + H]<sup>+</sup> calcd for C<sub>13</sub>H<sub>17</sub>N<sub>4</sub>O<sub>4</sub> 293.1238; found 293.1250.



HSQC



### 3.4.2. Irradiation Procedures

2M-Photosensitised irradiation of **Thy-C<sub>3</sub>-Thy** was performed by preparing a 0.043 mM solution of **2M** in PB 10 mM. To 172 mL of this solution, **Thy-C<sub>3</sub>-Thy** (2.2 mg) was added in order to have the same concentration as **2M**. The irradiation was performed in quartz cuvettes with lamps emitting in the 310–390 nm range (with a maximum at 350 nm), using a multilamp photoreactor (see Section 6.2.2). UV-Vis absorption spectra were registered with a simple beam spectrophotometer (see Section 6.2.1).

### 3.4.3. Laser Flash Photolysis

A pulsed Nd: YAG SL404G-10 Spectron Laser Systems, (see Section 6.2.3), was employed to carry out the laser flash photolysis experiments. Transient absorption spectra were obtained from a deaerated solution of **2M** in ACN, EtOH and aqueous medium (absorbance between 0.3 and 0.4 at  $\lambda_{\text{exc}} = 355$  nm).

For quenching experiments *S*-FB (from 0 to 1.2 mM) and **Thy-C<sub>3</sub>-Thy** (from 0 to 1 mM) were added to a solution of **2M** in PB 10 mM with an absorbance of 0.4 at 355 nm. Kinetic decays were monitored at 370 and 500 nm for the *S*-FB quenching and at 500 nm for **Thy-C<sub>3</sub>-Thy**.

Lifetime of singlet oxygen in ACN was recorded at 1270 nm with a Hamamatsu NIR detector upon excitation with a 355 nm Nd: YAG laser (see Section 6.2.4).

### 3.5. References

(1) Turro, N. J.; Ramamurthy, V.; Scaiano, J. C.: *Modern Molecular Photochemistry of Organic Molecules*; University Science Books: Herndon, VA, 2010.

(2) Jornet, D.; Tormos, R.; Miranda, M. A. Photobehavior of Mixed  $n\pi^*/\pi\pi^*$  Triplets: Simultaneous Detection of the Two Transients, Solvent-Dependent Hydrogen Abstraction, and Reequilibration upon Protein Binding. *J. Phys. Chem. B* **2011**, *115*, 10768-10774.

(3) Antusch, L.; Gaß, N.; Wagenknecht, H.-A. Elucidation of the Dexter-Type Energy Transfer in DNA by Thymine–Thymine Dimer Formation Using Photosensitizers as Artificial Nucleosides. *Angew. Chem. Int. Ed.* **2017**, *56*, 1385-1389.

(4) Liu, X.-L.; Wang, J.-B.; Tong, Y.; Song, Q.-H. Regioselectivity and Competition of the Paternò–Büchi Reaction and Triplet–Triplet Energy Transfer Between Triplet Benzophenones and Pyrimidines: Control by Triplet Energy Levels. *Chem. Eur. J.* **2013**, *19*, 13216-13223.

(5) Cuquerella, M. C.; Lhiaubet-Vallet, V.; Cadet, J.; Miranda, M. A. Benzophenone Photosensitized DNA Damage. *Acc. Chem. Res.* **2012**, *45*, 1558-1570.

(6) Belmadoui, N.; Encinas, S.; Climent, M. J.; Gil, S.; Miranda, M. A. Intramolecular Interactions in the Triplet Excited States of Benzophenone–Thymine Dyads. *Chem. Eur. J.* **2006**, *12*, 553-561.

(7) Encinas, S.; Belmadoui, N.; Climent, M. J.; Gil, S.; Miranda, M. A. Photosensitization of Thymine Nucleobase by Benzophenone Derivatives as Models for Photoinduced DNA Damage: Paterno–Büchi vs Energy and Electron Transfer Processes. *Chem. Res. Toxicol.* **2004**, *17*, 857-862.

(8) Delatour, T.; Douki, T.; D'Ham, C.; Cadet, J. Photosensitization of Thymine Nucleobase by Benzophenone through Energy Transfer,

---

Hydrogen Abstraction and One-Electron Oxidation. *J. Photochem. Photobiol. B: Biol.* **1998**, *44*, 191-198.

(9) Murai, H.; Obi, K. Photochemistry of Higher Excited Triplet States of Benzaldehyde, Acetophenone, and Benzophenone at 77K. *J. Phys. Chem.* **1975**, *79*, 2446-2450.

(10) Liu, L.; Pilles, B. M.; Reiner, A. M.; Gontcharov, J.; Zinth, W. 2'-Methoxyacetophenone: an Efficient Photosensitizer for Cyclobutane Pyrimidine Dimer Formation. *ChemPhysChem* **2015**, *16*, 3483-3487.

(11) Cuquerella, M. C.; Lhiaubet-Vallet, V.; Bosca, F.; Miranda, M. A. Photosensitised Pyrimidine Dimerisation in DNA. *Chem. Sci.* **2011**, *2*, 1219-1232.

(12) Jiménez, M. C.; Miranda, M. A.; Tormos, R.; Vayá, I. Characterisation of the Lowest Singlet and Triplet Excited States of S-Flurbiprofen. *Photochem. Photobiol. Sci.* **2004**, *3*, 1038-1041.

(13) Yang, N.-C.; McClure, D. S.; Murov, S.; Houser, J. J.; Dusenbery, R. Photoreduction of Acetophenone and Substituted Acetophenones. *J. Am. Chem. Soc.* **1967**, *89*, 5466-5468.

(14) Vince, R.; Raza, A.; Dreis, C. Agents that Prevent or Repair Skin Damage US 20140350036, US 9403778, US9403778B2, WO 2013106728.

(15) Fenick, D. J.; Carr, H. S.; Falvey, D. E. Synthesis and Photochemical Cleavage of Cis-Syn Pyrimidine Cyclobutane Dimer Analogs. *J. Org. Chem.* **1995**, *60*, 624-631.

(16) Asaftei, S.; Lepadatu, A. M.; Ciobanu, M. Novel Compounds with a Viologen Skeleton and N-Heterocycles on the Peripheries: Electrochemical and Spectroscopic Properties. *Helv. Chim. Acta* **2011**, *94*, 1091-1101.



# CHAPTER 4

## Chapter 4. Triplet Energy Transfer versus Excited State Cyclisation as the Controlling Step in Photosensitised Bipyrimidine Dimerisation

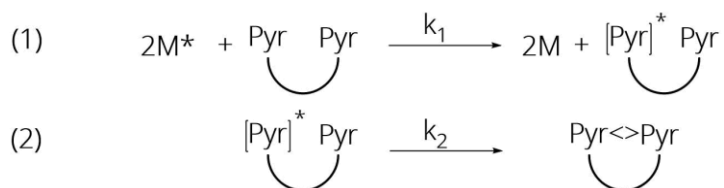
---

---



## 4.1. Introduction

As addressed in the introduction, the chemical stability of organic molecules can be compromised upon exposure to light. This is of special importance for DNA, whose irradiation leads to different types of damage of considerable biological relevance.<sup>1,2</sup> Among them, cyclobutane pyrimidine dimers (CPDs) has been intensively investigated, since they represent 75% of the DNA photolesions produced upon direct sunlight absorption and have been related to the appearance of skin cancer.<sup>2-8</sup> However, it is well documented that these lesions can also be formed through a triplet photosensitisation mechanism.<sup>2,9-14</sup> In this kind of process, a photosensitising compound reaches its triplet excited state upon absorption of UVA light and subsequent intersystem crossing. When interacting with DNA, the excited photosensitiser may transfer its energy to a pyrimidine (Pyr) unit (Scheme 4.1, step 1). The resulting  $\text{Pyr}^*$ , can react with a neighboring ground state Pyr leading to CPDs through a photocyclisation involving 1,4-biradical intermediates (Scheme 4.1, step 2).<sup>13</sup> Photosensitisation is a convenient tool to investigate triplet  $\text{Pyr}^*$ -mediated chemistry as formation of the Pyr-singlet excited states is circumvented, thus reducing the mechanistic complexity.<sup>9</sup>

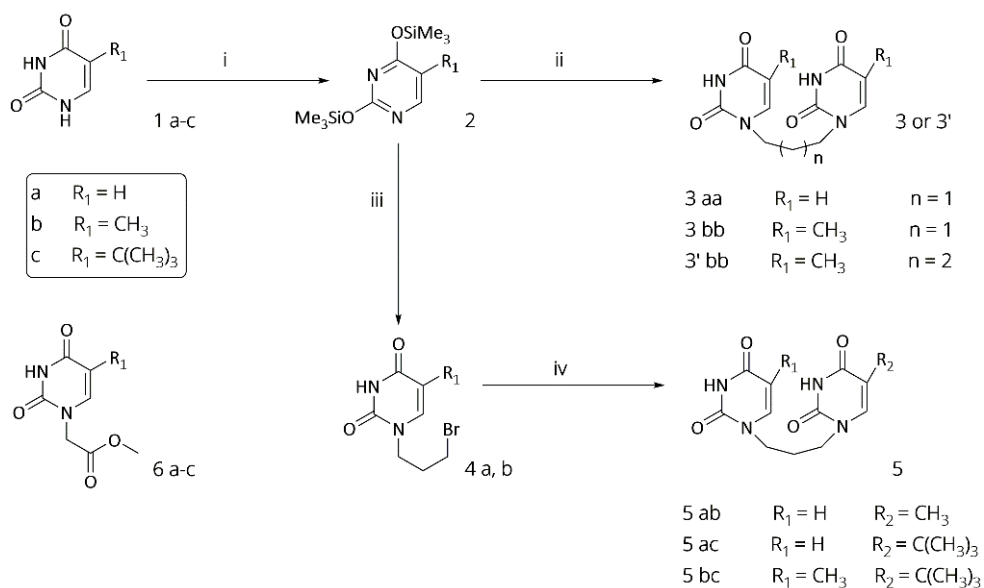


*Scheme 4.1 Steps involved in the photosensitised pyrimidine dimerisation to form cyclobutane pyrimidine dimers (CPDs).*

In this context, the aim of the present Chapter is to determine the nature of the rate controlling step in the photosensitised cyclisation of

bipyrimidines, making use of C5 substitution in combination with entropic factors related to the length of the linking bridge.

To our knowledge this issue has not been previously addressed, in spite of the expected influence of the relative rates of energy transfer versus intrinsic triplet Pyr dimerisation on the overall efficiency of the process. To achieve this goal, polymethylene linked homo- and hetero- bipyrimidine models have been designed with a variety of C5 substitution (Scheme 4.2, series **3** and **5**) and, in one case, different bridge length (compounds **3bb** and **3'bb**). The monomeric uracil, thymine and *tert*-butyluracil derivatives **6** have also been included for comparison.



Scheme 4.2 Synthetic strategy to prepare homo- bipyrimidine models (route i + ii) and hetero- bipyrimidine models (route i + iii + iv). Reagents and conditions (i) hexamethyldisilazane, chlorotrimethylsilane, 130°C, 2h; (ii) 1,3-dibromopropane or 1,4-dibromobutane, DMF, 170°C, 18h; (iii) 1,3-dibromopropane, DMF, 80°C, 18h; (iv) 2,4-bis(trimethylsilyloxy)pyrimidine (2a-c), DMF, 80°C, 18h.

Instead of benzophenone, 2'-methoxyacetophenone (**2M**) has been chosen as photosensitiser because, as confirmed in the first work of this Thesis i) it is an efficient CPDs photosensitiser<sup>15-17</sup> and ii) unlike benzophenone, **2M** does not yield any unwanted side process, such as the Paternò-Büchi photoreaction.<sup>15,16</sup> Actually, **2M** has been previously used as photosensitiser of a thymine dinucleotide; the results are consistent with formation of the **2M** triplet state, followed by triplet-triplet energy transfer leading to a biradical and ultimately to CPDs formation in the submicrosecond timescale.<sup>13</sup> Furthermore, a similar result was obtained shown in Chapter 3 of this Thesis with the **Thy-C<sub>3</sub>-Thy** model.

## 4.2. Results and Discussion

As expected, all the UV spectra of the bipyrimidine models displayed a band with its maximum centred at *ca.* 260-270 nm and a tail extending up to *ca.* 300 nm, redshifted by 4-7 nm with respect to the monomeric pyrimidines (Figure 4.1).<sup>18</sup>

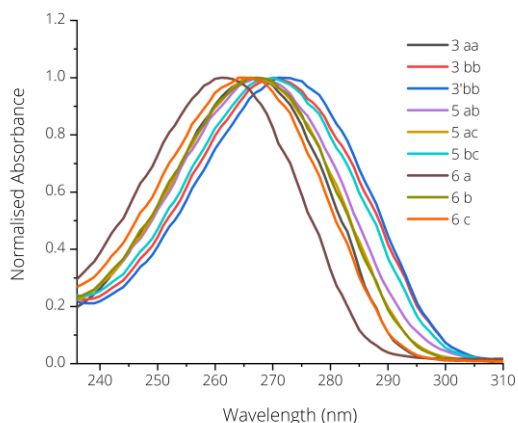
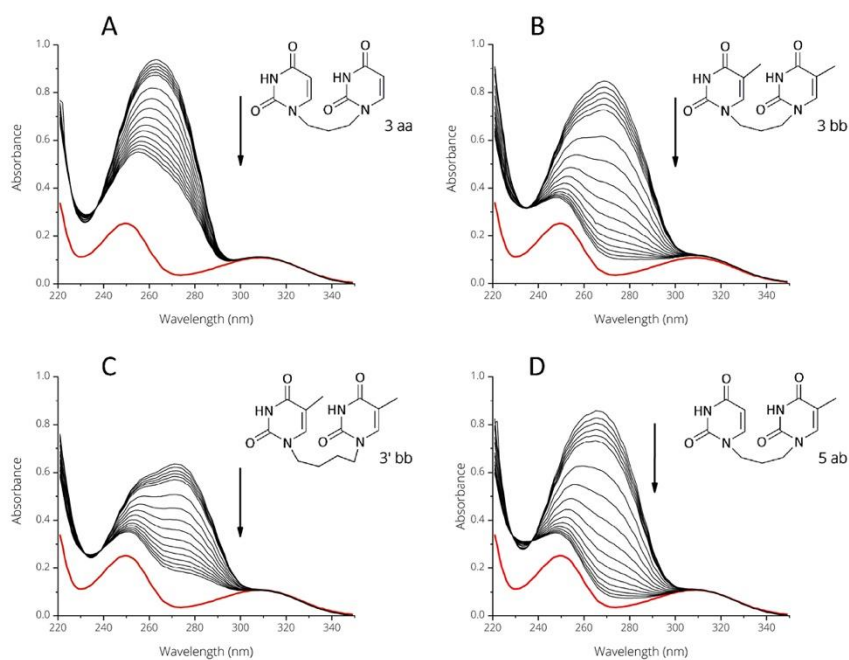


Figure 4.1 A) UV spectra of bipyrimidine models (**3** and **5**) and monomeric methyl pyrimidineacetates (**6**).

Irradiation of solutions containing equimolar mixtures of the models and **2M** with lamps emitting in the 310-390 nm range allowed for selective excitation of **2M**, ensuring photosensitisation (Figure 4.2 A-I). Also, a control experiment was run in which irradiation of **3bb** was performed with the 350 nm centred lamps but in the absence of **2M**. As expected, no changes were observed, which allowed us to rule out CPDs formation upon direct irradiation under the employed conditions (Figure 4.2 J). The **2M** photosensitised reaction was monitored by UV spectroscopy, and in all cases a progressive decrease of the absorption in the 240-290 nm region along with a blue shift in the absolute UV maxima of the mixtures was clearly observed. Conversely, the spectra remained unaltered in the region above 300 nm, where the photosensitiser is the only light-absorbing species (Figure 4.2 A-I). This is fully consistent with the disappearance of the enone chromophore of the Pyr bases that occurs when CPDs are formed. As the reactions proceeded the final UV spectrum resembled progressively that of **2M**, which as expected for a photosensitiser remained unaltered.



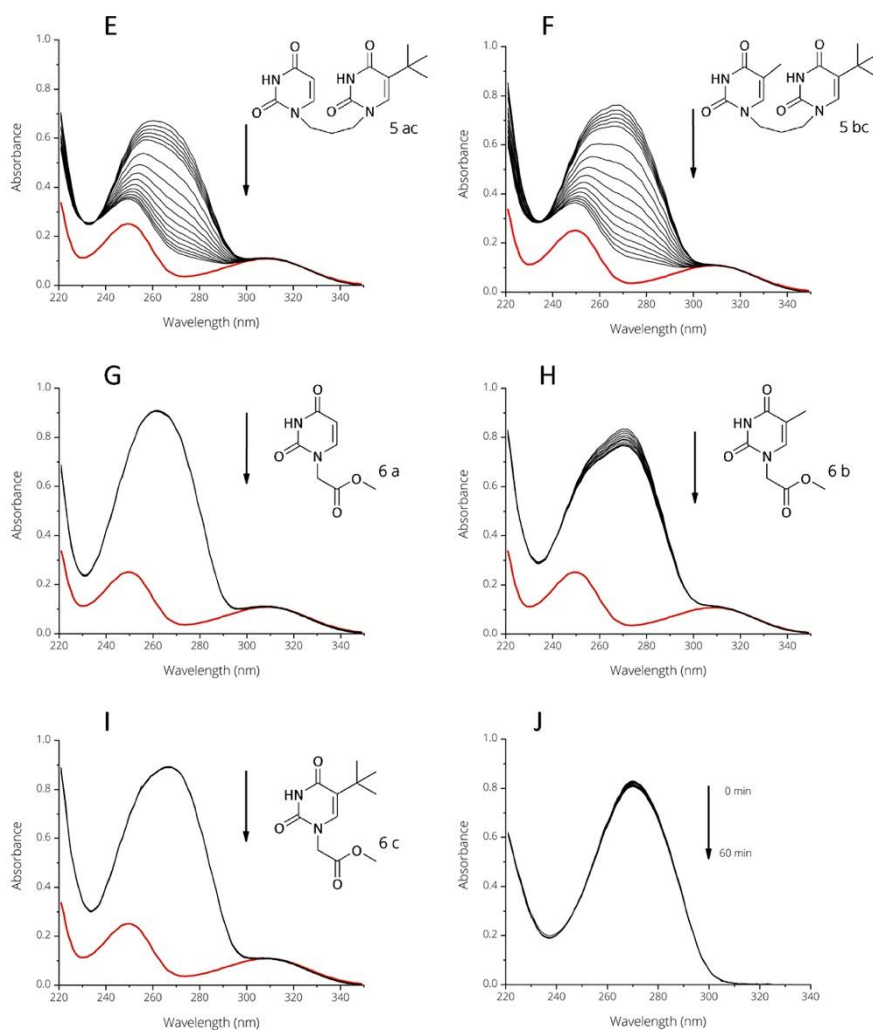


Figure 4.2 2'-Methoxyacetophenone photosensitised irradiation of A) **3aa** B) **3bb** C) **3'bb** D) **5ab** E) **5ac** F) **5bc** G) **6a** H) **6b** and I) **6c** in PB under deaerated conditions (the spectrum of **2M** in red is included for reference). J) UV-Vis spectra of control experiment in which irradiation of **3bb** was performed with the 350 nm centered lamps but in the absence of **2M**.

To secure that *cis-syn* CPDs were actually the photoproducts, parallel irradiations were run at a larger scale, using either **2M** or acetone as photosensitisers.<sup>19</sup> The photoproducts were isolated and fully identified by a thorough NMR spectroscopic analysis. Their structures are shown in Figure 4.3.

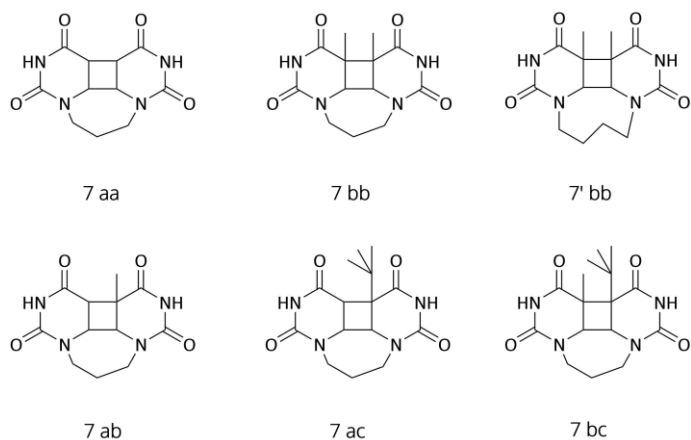


Figure 4.3 Structure of the homo- and hetero- cyclobutane pyrimidine dimers (CPDs).

Parallel experiments were run with the monomers (in the form of pyrimidineacetates **6**, Scheme 4.2) although changing the molar ratio to 2:1 in order to maintain the number of chromophores in solution. The kinetics obtained for all the compounds evaluated are presented as percentages of unreacted substrates alongside with the corresponding semilogarithmic plots in Figure 4.4.

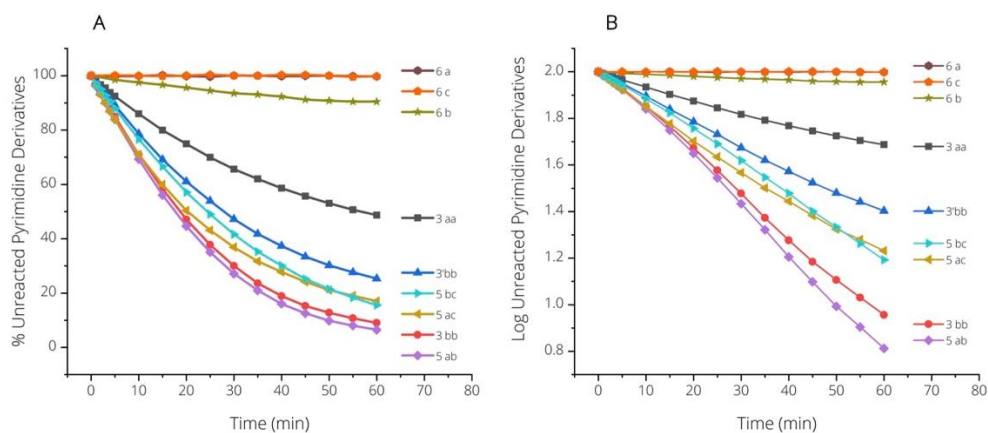


Figure 4.4 A) Percentage (%) of unreacted Pyr models **3**, **3'**, **5**, and **6**. Monitoring was performed by UV-Vis spectrophotometry at their maximum wavelength. B) Semilogarithmic plots of % of these unreacted Pyr models vs reaction.

The outcome of these experiments revealed that the intermolecular photoreaction is practically non-existent, while the intramolecular counterpart in the model compounds is efficient (Figure 4.4). In addition, the observed reactivity order (**5ab** > **3bb** > **5ac** > **5bc** > **3'bb** > **3aa**) revealed the intriguing case of **3aa**, whose kinetics is much slower than that of the other analogues, in spite of the expectedly lower steric hindrance associated with the lack of a bulky C5 alkyl substituent. As a general trend, the process is faster when the bipyrimidine contains a thymine unit (**3bb**, **5ab** and **5bc**), but if the polymethylene bridge between the two bases is elongated (**3'bb**) a decrease in the photoreaction rate is observed. The latter effect was previously observed for the direct and acetone-photosensitised photoreaction and was explained by means of base stacking. In addition, increasing the number of methylene groups from 3 to 4 should be associated with the probability for the model molecule to populate a reactive folded conformation.<sup>18,19</sup>

As stated above, **2M** photosensitisation of the model compounds **3**, **3'**, **5** and **6** led to CPDs formation with substantial variations in their reaction kinetics. In order to explain the observed behavior, a photophysical study was undertaken. Substitution at C5 was expected to affect both the relative triplet energies ( $E_{T(\text{rel})}$ ) of the Pyr derivatives and the steric hindrance towards energy transfer and triplet  $\text{Pyr}^*$  quenching ultimately affording the photocyclisation products (Scheme 4.1, steps 1 and 2). Based on these considerations, phosphorescence and transient absorption spectroscopic studies were performed to identify the rate determining step. Thus, phosphorescence emission spectra were registered (Figure 4.5) in ethanol matrix at 77 K, and the relative triplet energies were arbitrarily determined from the wavelength at which the emission raised 20% of its maximum (Figure 4.5).

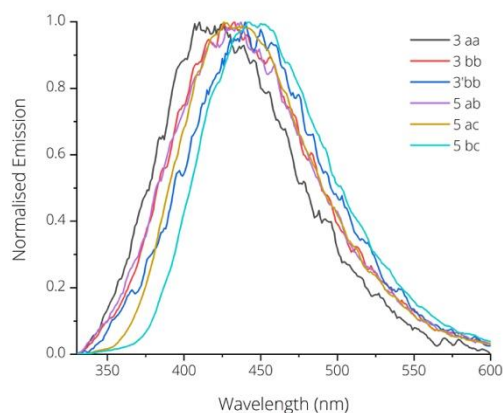
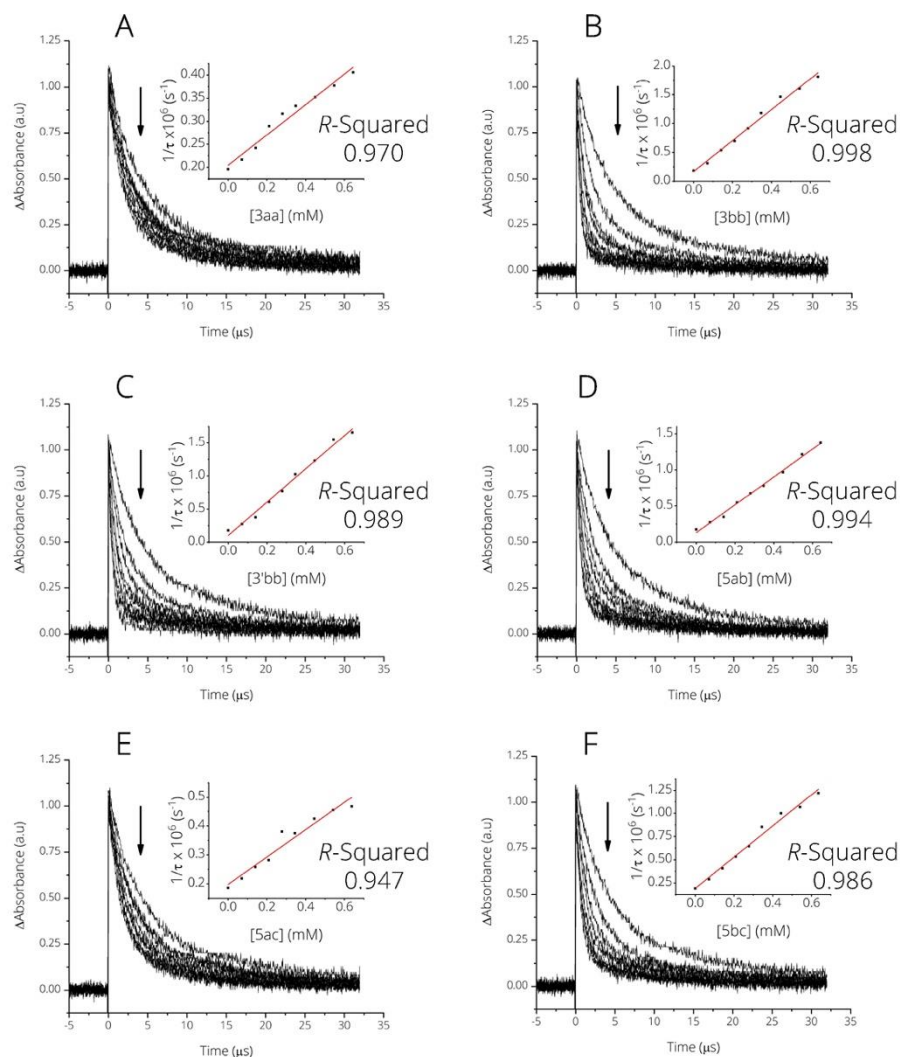


Figure 4.5 Phosphorescence of the prepared bipyrimidine models.

Clearly, alkyl substitution at C5 resulted in a significant decrease of the  $E_{T(\text{rel})}$  value, which was especially remarkable in the case of the *tert*-butyl containing compounds. The energy transfer process was investigated in solution, at room temperature, by means of laser flash photolysis upon excitation at 355 nm. The triplet excited state of **2M** was detected as a

transient species with maximum at 420 nm,<sup>16</sup> whose decay was followed in the presence of increasing amounts of the selected Pyr derivatives. In all cases, the triplet lifetime of  $2M^*$  was progressively shortened, in agreement with the expected quenching process (Figure 4.6).



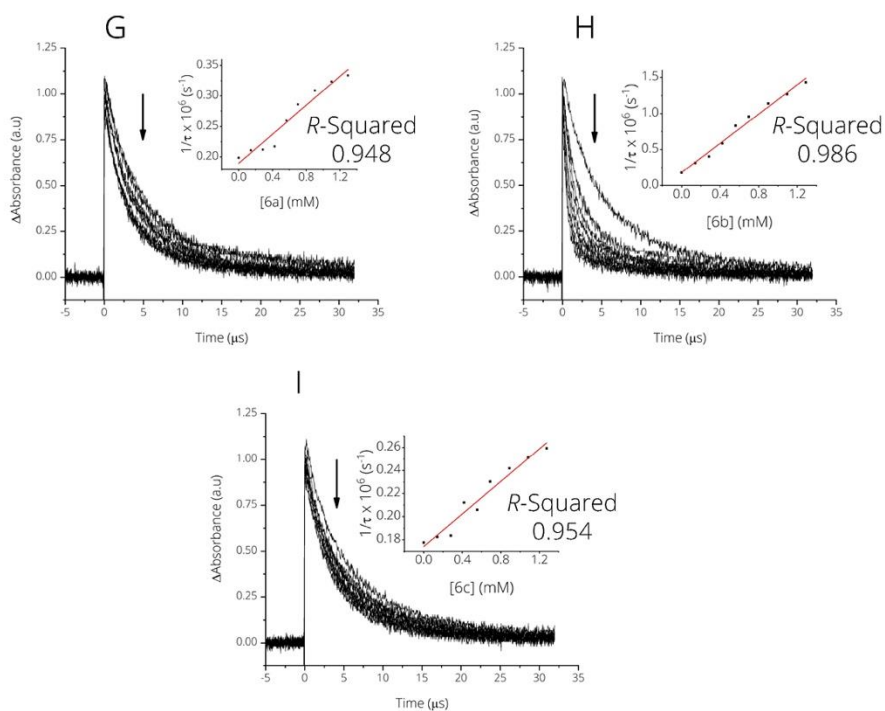


Figure 4.6 Kinetic decay of  $2M^*$  at 420 nm in PB under deaerated conditions after A) **3aa**, B) **3bb** C) **3'bb** D) **5ab** E) **5ac** F) **5bc** G) **6a** H) **6b** and I) **6c** were added (from 0 to 1.3 mM). Inset) Stern-Volmer quenching of  $2M^*$  by A) **3aa**, B) **3bb** C) **3'bb** D) **5ab** E) **5ac** F) **5bc** G) **6a** H) **6b** and I) **6c**.

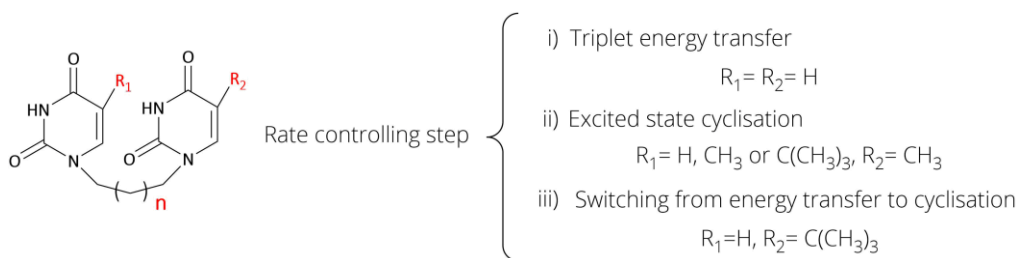
Fitting the  $2M^*$  decays to a monoexponential law, the corresponding lifetimes were determined which allowed us to obtain the  $k_q$  through the Stern-Volmer plot, in which the reciprocal of the lifetimes are represented against quencher concentration (Figure 4.6, insets).

Table 4.1 Relative triplet energies (in kcal/mol, estimated error  $\pm 0.1$ ) and quenching rate constants (in  $M^{-1}s^{-1}$ ) for compounds **3**, **5** and **6**.

Compound	$E_{T(\text{rel})}$	$10^{-8} \times k_q$
<i>6a</i>	80.3	$1.2 \pm 0.1$
<i>6b</i>	78.8	$10.2 \pm 0.5$
<i>6c</i>	76.5	$0.7 \pm 0.1$
<i>3aa</i>	80.3	$3.3 \pm 0.2$
<i>3bb</i>	78.6	$26.8 \pm 1.0$
<i>3'bb</i>	76.9	$25.2 \pm 1.0$
<i>5ab</i>	79.2	$19.3 \pm 0.5$
<i>5ac</i>	76.3	$4.7 \pm 0.4$
<i>5bc</i>	73.9	$16.8 \pm 0.7$

As a general trend, all the thymine-containing compounds showed  $k_q$  values higher than  $10^9 \text{ M}^{-1} \text{ s}^{-1}$ . The rate constants determined for the uracil and *tert*-butyluracil analogues were one order of magnitude lower. This can be attributed to the higher  $E_{T(\text{rel})}$  of the former, according to Sandros' theory,<sup>20</sup> and to the steric hindrance of the latter. Finally, the process was apparently faster in bipyrimidines than in their corresponding monomeric analogues, but this mainly reflects the different number of nucleobase units at the same molar concentration.

At first sight, it seems difficult to establish a satisfactory correlation between the photoreaction rates observed for the steady state photolysis and the photophysical parameters determined by emission measurements and transient absorption spectroscopy. However, all the obtained data can be explained by taking into account that the rate controlling step (1 vs 2 in Scheme 4.1) switches along the selected series of model compounds. Thus, three different scenarios (Scheme 4.3) can be considered, as detailed below.



Scheme 4.3 Dependence of the rate controlling step on the structures of bipyrimidines.

---

*Triplet energy transfer is the rate controlling step.* This is the case for **3aa**, whose  $k_q$  is relatively low (ca.  $3 \times 10^8 \text{ M}^{-1} \text{ s}^{-1}$ ) and therefore the intermolecular quenching of **2M\*** by Pyr becomes the bottleneck for the whole process. As a consequence, the differences that could be expected in the reaction of  $\text{Pyr}^*$  with ground state Pyr associated with steric hindrance play little if any role.

*Excited state cyclisation is the rate controlling process.* This is the case of thymine derivatives **5ab**, **3bb** and **5bc**, which display  $k_q$  values higher than  $10^9 \text{ M}^{-1} \text{ s}^{-1}$ . As a result, the relatively slower intramolecular reaction of  $\text{Pyr}^*$  with the other Pyr unit takes over. It has to be mentioned that this is in turn a complex process, which involves formation of a 1,4-biradical and its subsequent coupling to give the cyclobutane ring. Moreover, at high concentrations of related bipyrimidines (ca.  $2 \times 10^{-2} \text{ M}$ ) biradical coupling has been found to be the slowest step.<sup>13</sup> In our series of compounds, steric hindrance has a considerable impact on the photoreaction rates, which follow the order **5ab**>**3bb**>**5bc**. Here, one thymine is maintained while the C5 substituent of the other base changes from hydrogen to methyl or *tert*-butyl along the series. The differences found between **3bb** and **3'bb** can also be rationalised assuming that excited state cyclisation is the rate determining step. However, in this case, the kinetic control is achieved by elongating the linking bridge, which results in a lower probability for the molecule to populate a reactive folded conformation.

*The rate controlling step switches along the reaction.* Given that triplet energy transfer is an intermolecular process, by contrast with the intramolecular excited state cyclisation, the former must be favoured at higher concentrations of the bipyrimidine derivative. Thus, it is conceivable that the rate controlling step switches along the reaction, due to the progressively decreasing concentration of unreacted starting material. This is illustrated by the comparison between **5ac** and **5bc**. In both cases, the

second step is slower at the beginning of the reaction, and hence the photocyclodimerisation of **5ac** is faster due to a lower steric hindrance. Conversely, at a later stage the concentration of unreacted material drops considerably, and consequently intermolecular energy transfer becomes the rate controlling step. As a result, **5bc** progresses faster as reflected in Figure 4.4 B in the crossing of the kinetic plots.

### 4.3. Conclusions

The present work has allowed establishing the nature of the rate controlling step in the photosensitised dimerisation of bipyrimidine models. By introducing variations in the substitution at C5, the length of the linking bridge or the substrate concentration it is possible to switch from a reaction governed by the intrinsic dimerisation process (intramolecular reaction of  $\text{Pyr}^*$  with ground state Pyr, followed by ring closure of the resulting 1,4-biradical intermediate) to an energy transfer controlled process.

The presence of a bulky alkyl substituent at C5 results in a decrease of the triplet level, but at the same time increases the steric hindrance. The former effect has a positive impact on the rate of triplet energy transfer, whereas the latter tends to retard both, the energy transfer and the excited state cyclisation steps.

## 4.4. Experimental Section

### 4.4.1. Synthesis and Characterisation

To obtain both homo- and hetero- bipyrimidine models the corresponding 2,4-bis(trimethylsilyloxy)pyrimidine derivatives (**2a-c**) were synthesised in a first stage. Subsequent addition of 0.4 equivalents of 1,3-dibromopropane/1,4-dibromobutane at 170°C led to formation of **3** or **3'** (Scheme 4.2, paths i + ii). When milder reaction conditions (80°C) were employed, the N<sub>1</sub> bromo alkylated Pyr derivatives (**4a,b**, Scheme 4.2, paths i + iii) were isolated. Compounds **5** were obtained as a result of dropwise addition of **4** to the conveniently functionalised Pyr **2** (Scheme 4.2, path iv). In addition, monomeric methyl pyrimidineacetates were synthesised and purified following the established procedure in bibliography, to be used as reference compounds (**6**, Scheme 4.2).<sup>21,22</sup> Compound 5-*tert-butyl uracil* was prepared according to literature procedures<sup>23</sup> (see Annex 4.5 for its characterisation).

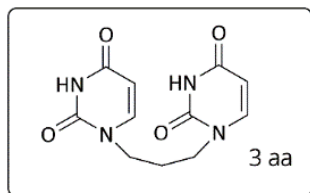
#### 4.4.1.1. Compounds 2 a-c

Hexamethyldisilazane (5.8 mL, 27.3 mmol) and chlorotrimethylsilane (0.5 mL, 4.2 mmol) were added to a dry deaerated reaction flask containing uracil (1 g, 8.9 mmol). The mixture was stirred for 2h at reflux (130°C), until it turned transparent (**2a**). Compound **2c** was prepared from 5-*tert-butyl uracil*,<sup>23</sup> following the same procedure. All the obtained compounds were used as intermediates for the synthesis of homo- bipyrimidine models (**3** and **3'**), bromo alkylated pyrimidine derivatives (**4a,b**) and hetero- bipyrimidine models (**5**), without isolation as they are air sensitive and hydrolyse readily.

## 4.4.1.2. Compounds 3 and 3'

Compound **3aa** was prepared following the same procedure described for **Thy-C<sub>3</sub>-Thy (3bb)** in Chapter 3. In the case of **3'bb** 1,4-dibromobutane was used instead of 1,3-dibromopropane.

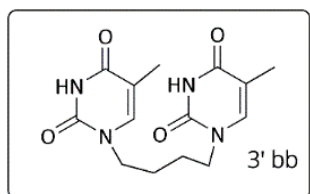
**1,1'-(Propane-1,3-diyl)bis(pyrimidine-2,4(1H,3H)-dione) (3aa)**, white solid



(283.2 mg, 67%). <sup>1</sup>H NMR (300 MHz, DMSO-d<sub>6</sub>) δ<sub>H</sub>: 11.24 (s, 2H), 7.65 (d, *J* = 7.9 Hz, 2H), 5.54 (d, *J* = 7.8, 2.2 Hz, 2H), 3.68 (t, *J* = 7.1 Hz, 4H), 1.89 (m, 2H). <sup>13</sup>C NMR (75 MHz, DMSO-d<sub>6</sub>): 163.7 (2CO), 151.0 (2CO), 145.5 (2CH), 101.0 (2CH), 45.0 (2CH<sub>2</sub>), 28.0 (CH<sub>2</sub>).

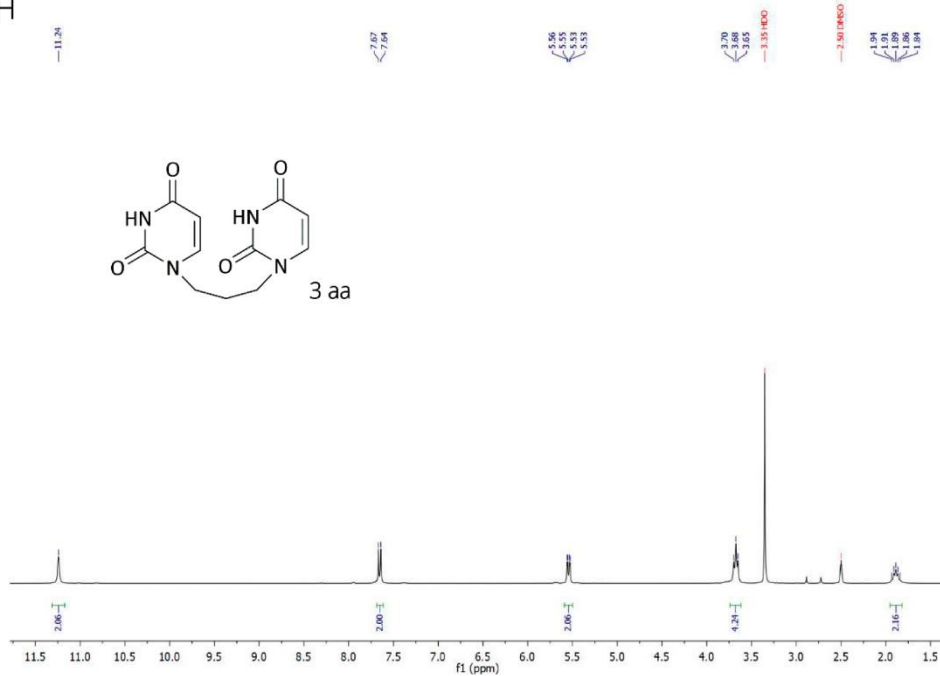
HRMS (ESI-TOF) *m/z*: [M + H]<sup>+</sup> calcd for C<sub>11</sub>H<sub>13</sub>N<sub>4</sub>O<sub>4</sub> 265.0946; found 265.0937.

**1,1'-(Butane-1,4-diyl)bis(5-methylpyrimidine-2,4(1H,3H)-dione) (3'bb)**, pale

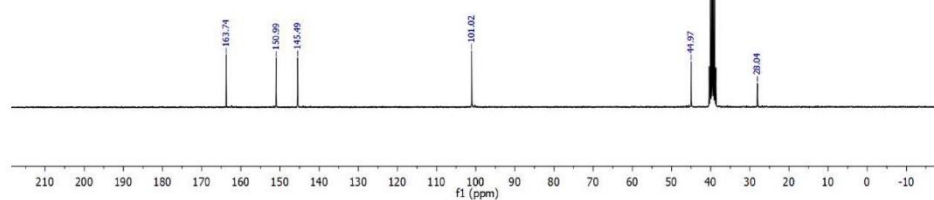


yellow solid (367.4mg, 75%). <sup>1</sup>H NMR (300 MHz, DMSO-d<sub>6</sub>) δ<sub>H</sub>: 11.21 (s, 2H), 7.56 – 7.47 (m, 2H), 3.63 (d, *J* = 6.1 Hz, 4H), 1.73 (s, 6H), 1.54 (d, *J* = 6.2 Hz, 4H). <sup>13</sup>C NMR (75 MHz, DMSO-d<sub>6</sub>): 164.3 (2CO), 151.0 (2CO), 141.4 (2CH), 108.5 (2C), 46.7 (2CH<sub>2</sub>),

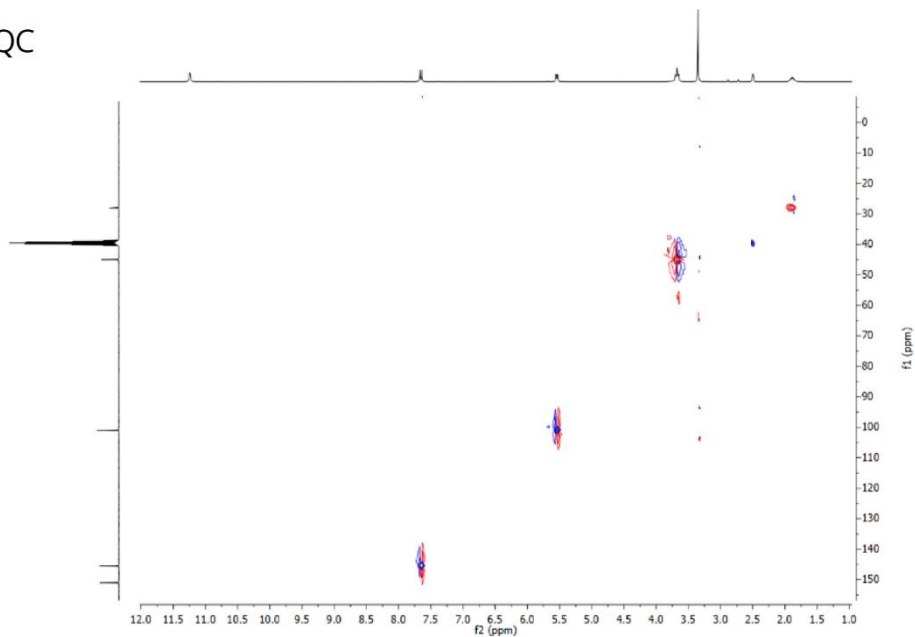
25.4 (2CH<sub>2</sub>), 12.0 (2CH<sub>3</sub>). HRMS (ESI-TOF) *m/z*: [M + H]<sup>+</sup> calcd for C<sub>14</sub>H<sub>19</sub>N<sub>4</sub>O<sub>4</sub> 307.1398; found 307.1406.

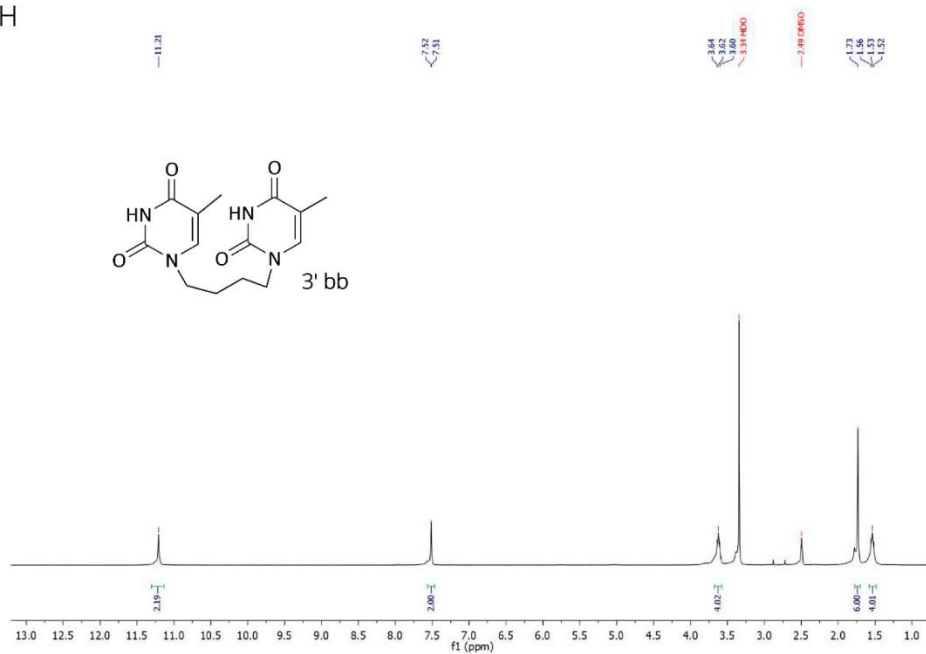
$^1\text{H}$ 

DEPT-135

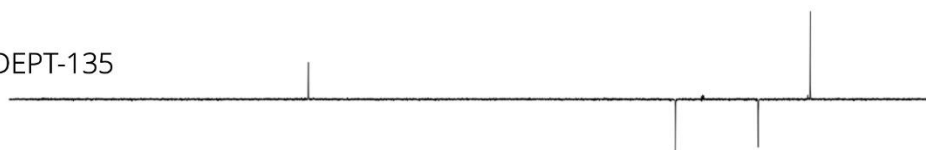
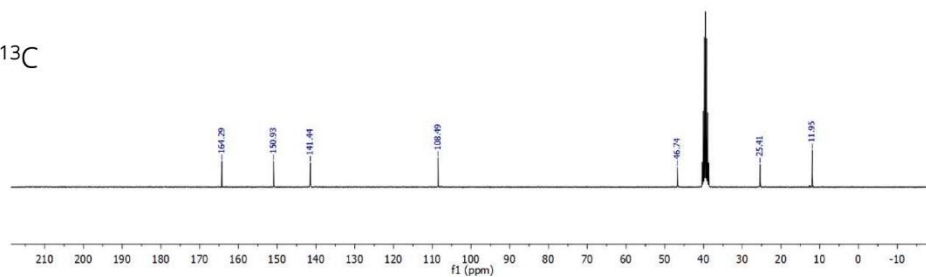
 $^{13}\text{C}$ 

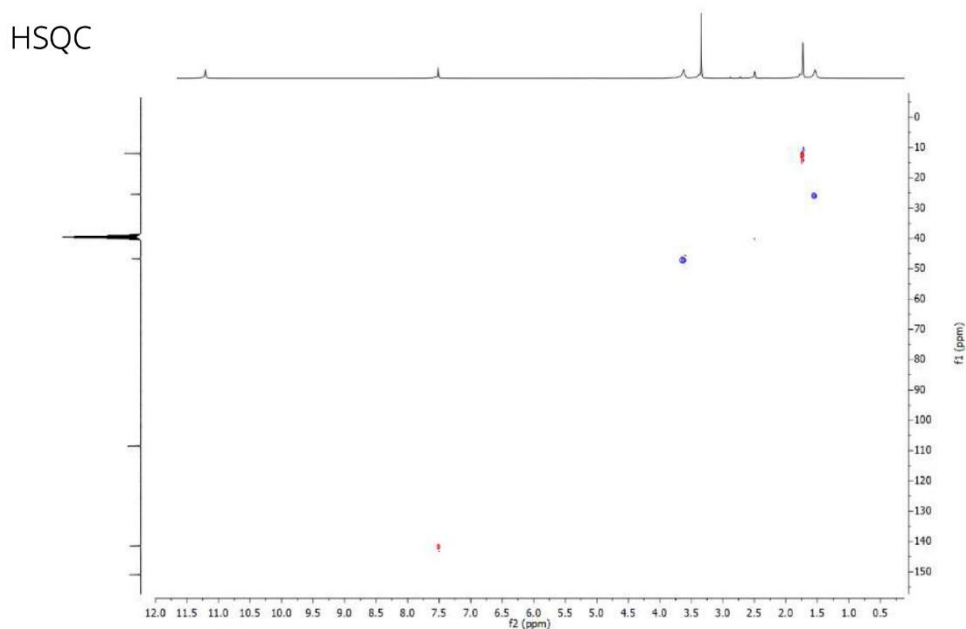
HSQC



$^1\text{H}$ 

DEPT-135

 $^{13}\text{C}$ 

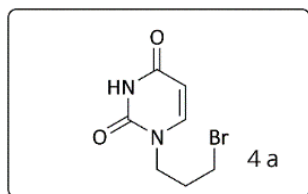


#### 4.4.1.3. Compounds 4 a,b

Compounds **4a** and **4b** were synthesised by 2,4-bis(trimethylsilyloxy)pyrimidines (**2a,b**) alkylation after treatment with an excess of 1,3-dibromopropane in DMF. To a magnetically stirred solution of **2b** (1 g, 3.7 mmol) in anhydrous DMF (2 mL), 1,3-dibromopropane (1,13 mL, 11.1 mmol) was added and the reaction heated at 80°C during 18 h. The reaction was cooled to 0°C and water was added to precipitate undesired unreacted thymine or little amounts of **3bb**. The solid was filtered and the brown solution extracted with dichloromethane. Organic layers were washed with water and brine. After drying with magnesium sulfate the solvent was evaporated and the crude purified by flash chromatography (SiO<sub>2</sub>,

cyclohexane/ ethyl acetate 1:3) to afford compound **4b** as a pale yellow solid (600 mg, 66%).

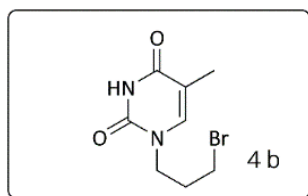
**1-(3-Bromopropyl)-5-methylpyridine-2,4(1H,3H)-dione (4b).**  $^1\text{H NMR}$  (300



MHz, DMSO- $d_6$ )  $\delta_{\text{H}}$ : 11.22 (s, 1H), 7.48 (d,  $J = 1.3$  Hz, 1H), 3.73 (t,  $J = 7.0$  Hz, 2H), 3.51 (t,  $J = 6.6$  Hz, 2H), 2.12 (m, 2H), 1.74 (d,  $J = 1.2$  Hz, 3H).  $^{13}\text{C NMR}$  (75 MHz, DMSO- $d_6$ ) 164.3 (CO), 150.9 (CO), 141.3 (CH), 108.6 (C), 46.2 (CH $_2$ ), 31.5 (CH $_2$ ), 31.3 (CH $_2$ ), 11.9

(CH $_2$ ). HRMS (ESI-TOF)  $m/z$ :  $[\text{M} + \text{H}]^+$  calcd for  $\text{C}_8\text{H}_{13}\text{BrN}_2\text{O}_2$  247.0082; found 247.0081.

**1-(3-Bromopropyl)pyrimidine-2,4(1H,3H)-dione (4a),** pale yellow solid (518



mg, 57%).  $^1\text{H NMR}$  (300 MHz, DMSO- $d_6$ )  $\delta_{\text{H}}$ : 11.25 (s, 1H), 7.60 (d,  $J = 7.8$  Hz, 1H), 5.55 (dd,  $J = 7.8, 2.3$  Hz, 1H), 3.76 (t,  $J = 6.9$  Hz, 2H), 3.51 (t,  $J = 6.6$  Hz, 2H), 2.13 (m, 2H).  $^{13}\text{C NMR}$  (75 MHz, DMSO- $d_6$ ): 163.7 (CO), 150.9 (CO), 145.6 (CH), 101.0 (CH), 46.5 (CH $_2$ ),

31.3 (CH $_2$ ), 31.2 (CH $_2$ ). HRMS (ESI-TOF)  $m/z$ :  $[\text{M} + \text{H}]^+$  calcd for  $\text{C}_7\text{H}_{10}\text{BrN}_2\text{O}_2$  232.9926; found 232.9928.

# Chapter 4

$^1\text{H}$

-11.25

7.62  
7.59

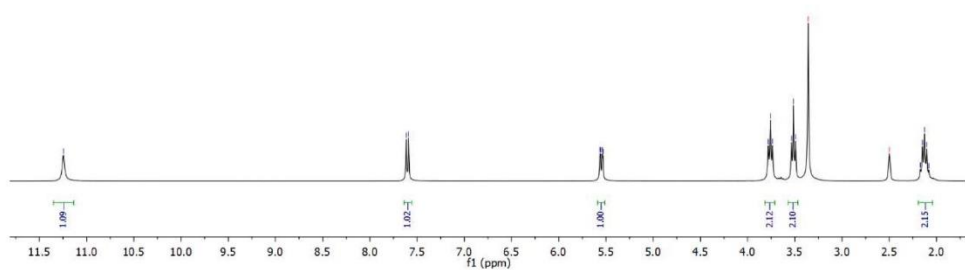
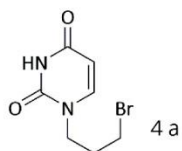
5.56  
5.56  
5.53

3.78  
3.74  
3.74  
3.51  
3.49  
3.49

3.36 H<sub>2</sub>O

-2.90 DMSO

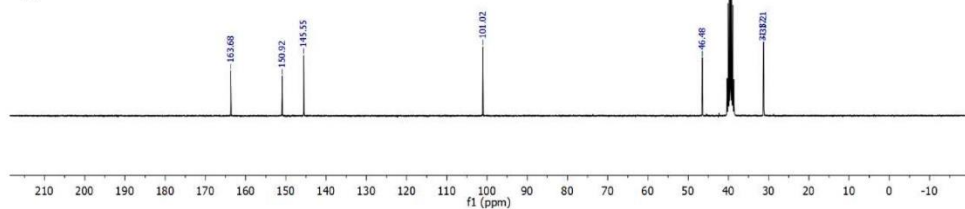
2.17  
2.13  
2.10  
2.08



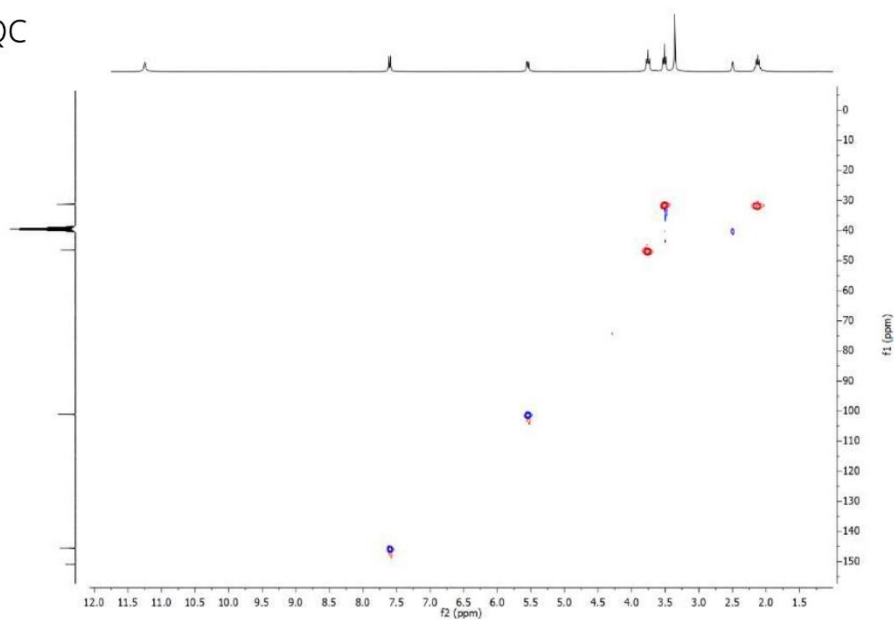
DEPT-135



$^{13}\text{C}$

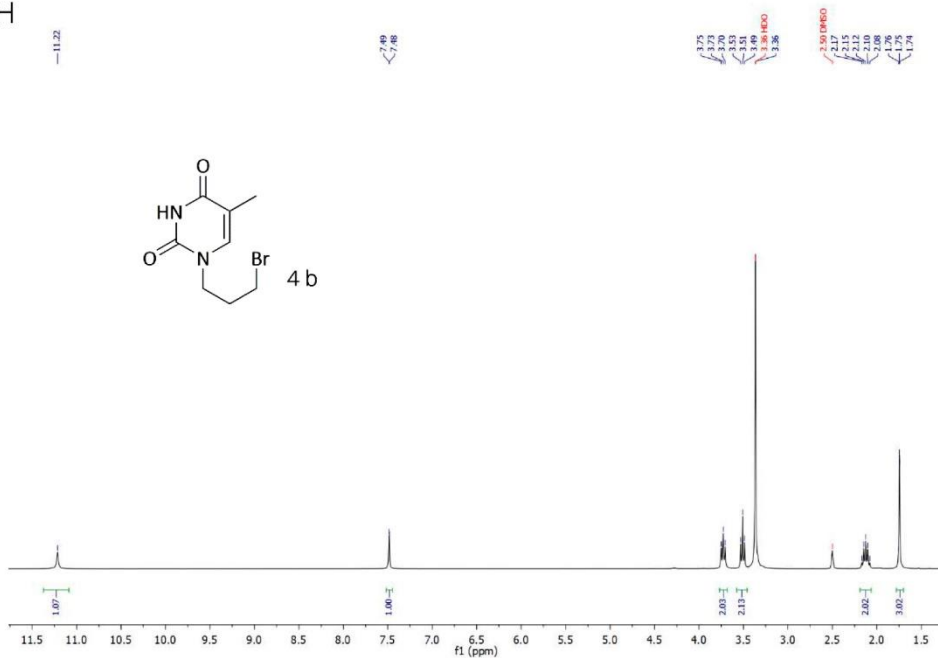


HSQC

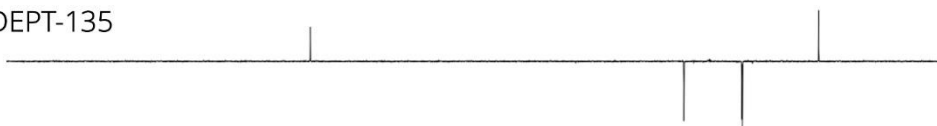


# Chapter 4

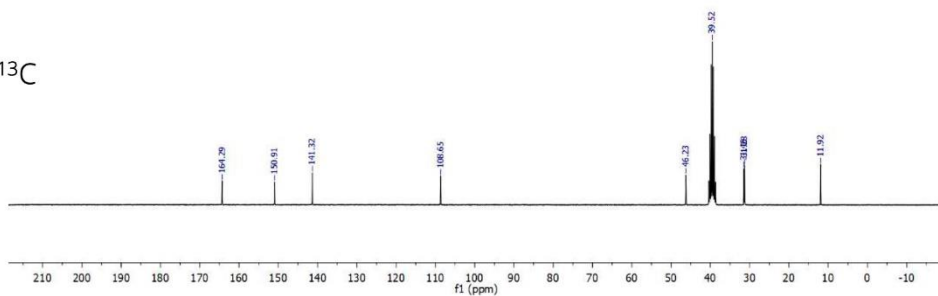
$^1\text{H}$

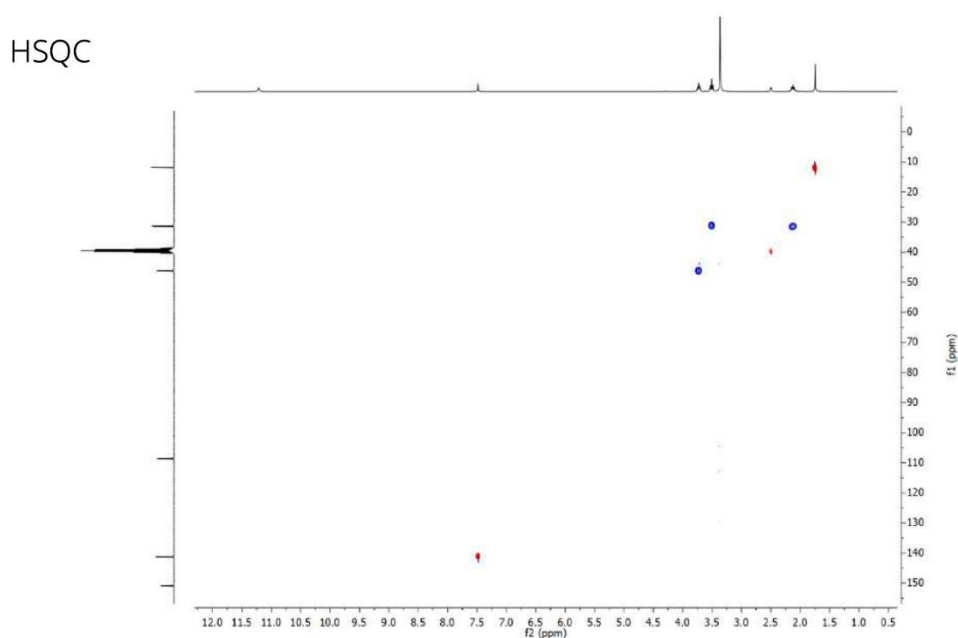


DEPT-135



$^{13}\text{C}$

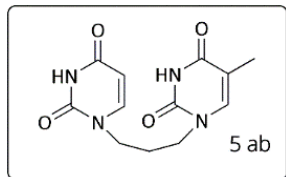




#### 4.4.1.4. Compounds 5

Hetero- bipyrimidine compounds (**5ab**, **5ac** and **5bc**) were prepared by linking the corresponding bromo alkylated pyrimidine derivative (**4a,b**) to a 2,4-bis(trimethylsilyloxy)pyrimidine compound (**2a-c**). To a solution of O,O'-bis(trimethylsilyl)thymine (**2b**, 1 g, 3.7 mmol) in 15 mL of anhydrous DMF, **4a** (0.9 g, 4.1 mmol) was added and the stirred mixture heated at reflux (80°C) overnight. Water was added to the cooled reaction (0°C), precipitating the product **5ab**. The white solid was filtered and washed several times with a chloroform: methanol 1:1 mixture and dried under vacuum to obtain **5ab**.

1-(3-(2,4-dioxo-3,4-dihydropyridin-1(2H)-yl)propyl)-5-methylpyridine-2,4 (1H, 3H)-dione (**5ab**) (431 mg, 43%). <sup>1</sup>H NMR (300 MHz, DMSO-d<sub>6</sub>) δ<sub>H</sub>: 11.23 (s, 2H),

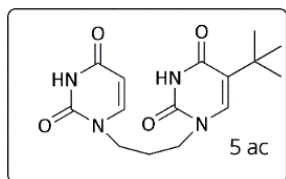


7.65 (d, *J* = 7.8 Hz, 1H), 7.53 (s, 1H), 5.54 (d, *J* = 7.8 Hz, 1H), 3.66 (q, *J* = 7.7 Hz, 4H), 1.88 (m, 2H), 1.73 (s, 3H).

<sup>13</sup>C NMR (75 MHz, DMSO-d<sub>6</sub>): 164.3 (CO), 163.8 (CO), 151.0 (CO), 151.0 (CO), 145.5 (CH), 141.3 (CH), 108.6

(CH), 101.0 (C), 45.1 (CH<sub>2</sub>), 44.7 (CH<sub>2</sub>), 28.0 (CH<sub>2</sub>), 12.0 (CH<sub>3</sub>). HRMS (ESI-TOF) *m/z*: [M + H]<sup>+</sup> calcd for C<sub>12</sub>H<sub>15</sub>N<sub>4</sub>O<sub>4</sub> 279.1094; found 279.1093.

5-(*tert*-Butyl)-1-(3-(2,4-dioxo-3,4-dihydropyrimidin-1(2H)-yl)propyl)pyrimidine-2,4(1H,3H)-dione (**5ac**) (white solid, 272.6 mg, 23%). <sup>1</sup>H

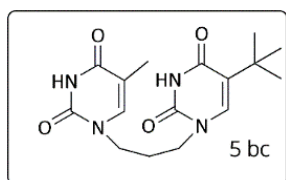


NMR (300 MHz, DMSO-d<sub>6</sub>) δ<sub>H</sub>: 11.15 (d, *J* = 38.4 Hz, 2H), 7.64 (d, *J* = 7.9 Hz, 1H), 7.32 (s, 1H), 5.54 (dd, *J* =

7.8, 1.5 Hz, 1H), 3.69 (td, *J* = 7.0, 4.4 Hz, 4H), 1.90 (m, 2H), 1.20 (s, 9H). <sup>13</sup>C NMR (75 MHz, DMSO-d<sub>6</sub>): 163.7

(CO), 163.0 (CO), 151.0 (CO), 150.7 (CO), 145.5 (CH), 139.9 (CH), 120.3 (2C), 101.0 (CH), 45.0 (2CH<sub>2</sub>), 32.5 (C), 28.6 (3CH<sub>3</sub>), 28.0 (CH<sub>2</sub>). HRMS (ESI-TOF) *m/z*: [M + H]<sup>+</sup> calcd for C<sub>15</sub>H<sub>21</sub>N<sub>4</sub>O<sub>4</sub> 321.1557; found 321.1563.

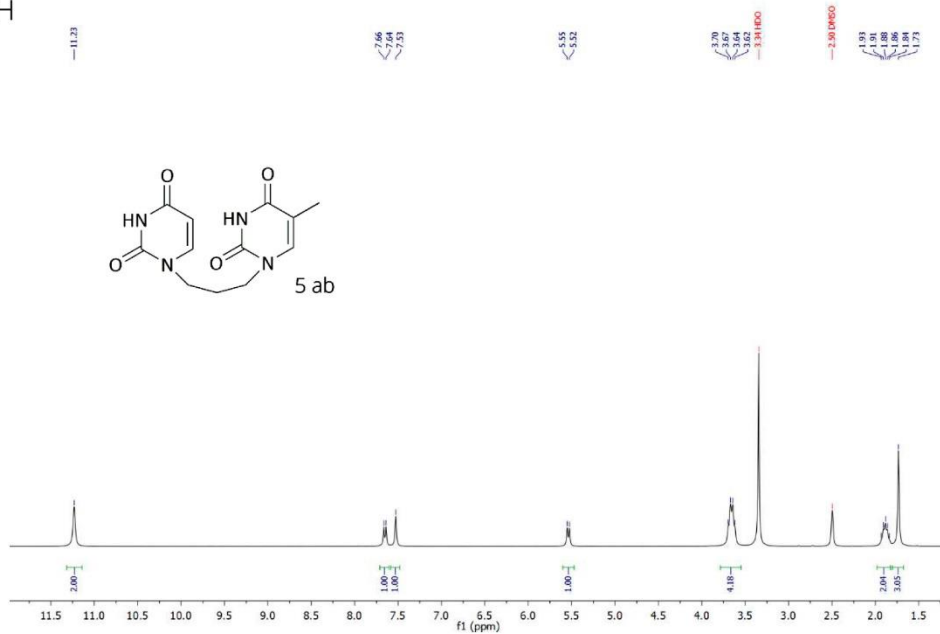
5-(*tert*-Butyl)-1-(3-(5-methyl-2,4-dioxo-3,4-dihydropyridin-1(2H)-yl)propyl)pyrimidine-2,4(1H,3H)-dione (**5bc**) (white solid, 346 mg, 28%). <sup>1</sup>H



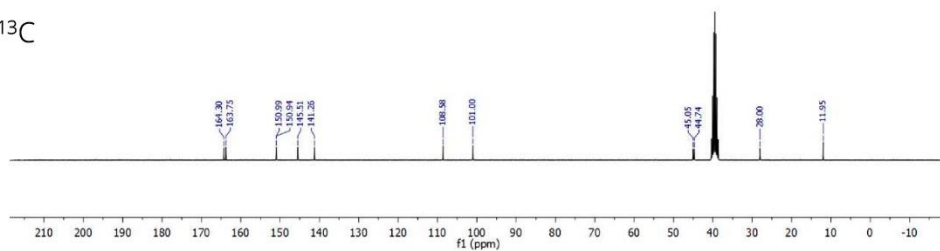
NMR (300 MHz, DMSO-d<sub>6</sub>) δ<sub>H</sub>: 11.17 (d, *J* = 33.1 Hz, 2H), 7.51 (d, *J* = 1.4 Hz, 1H), 7.33 (s, 1H), 3.67 (dt, *J* =

13.8, 6.9 Hz, 4H), 1.90 (m, 2H), 1.74 (d, *J* = 1.1 Hz, 3H), 1.20 (s, 9H). <sup>13</sup>C NMR (75 MHz, DMSO-d<sub>6</sub>) δ 164.3

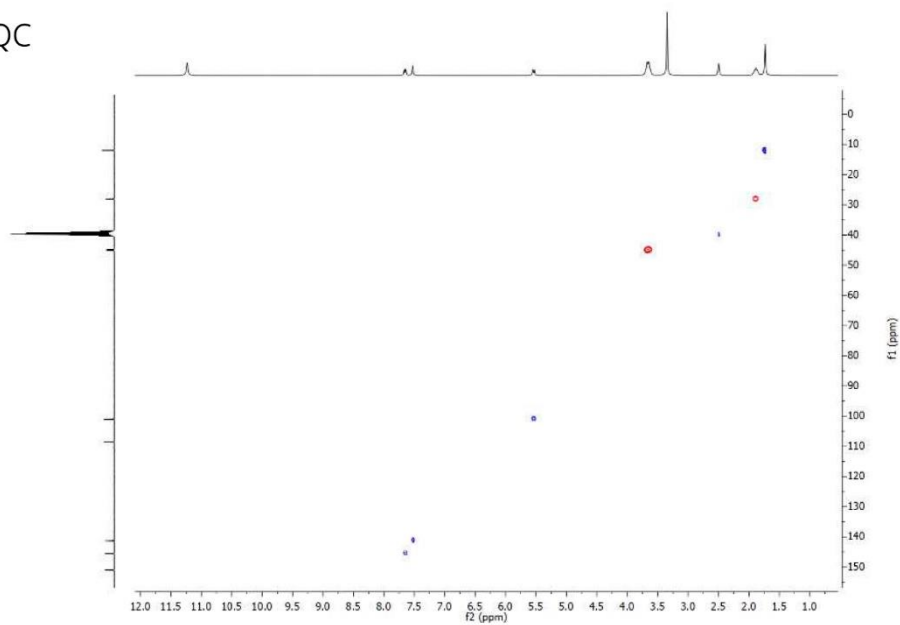
(CO), 163.0 (CO), 151.0 (CO), 150.7 (CO), 141.2 (CH), 139.9 (CH), 120.3 (C), 108.6 (C), 45.1 (CH<sub>2</sub>), 44.8 (2CH<sub>2</sub>), 32.4 (C), 28.6 (3CH<sub>3</sub>), 27.9 (CH<sub>2</sub>), 11.9 (CH<sub>3</sub>). HRMS (ESI-TOF) *m/z*: [M + H]<sup>+</sup> calcd for C<sub>16</sub>H<sub>23</sub>N<sub>4</sub>O<sub>4</sub> 335.1719; found 335.1704.

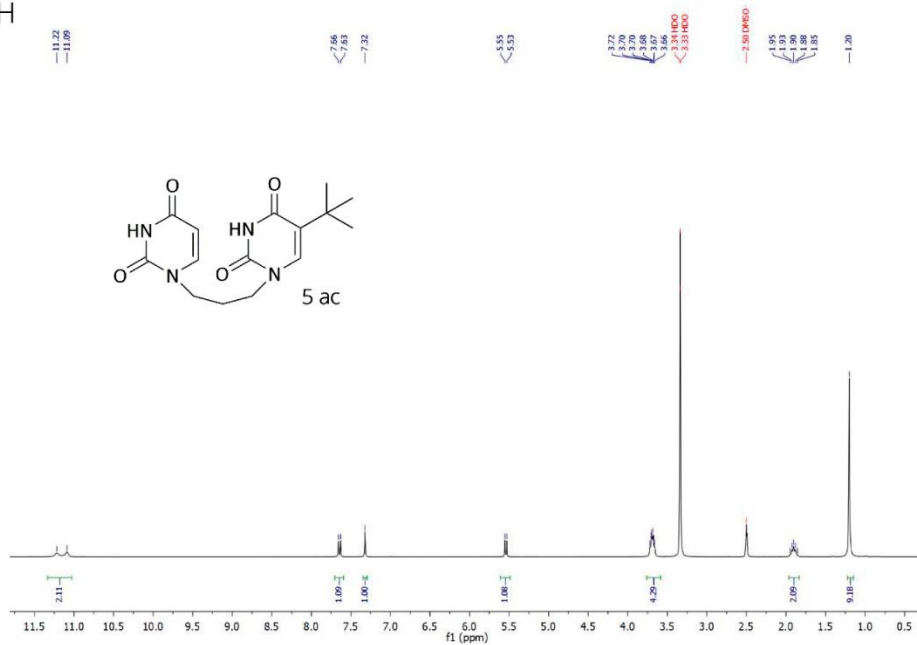
$^1\text{H}$ 

DEPT-135

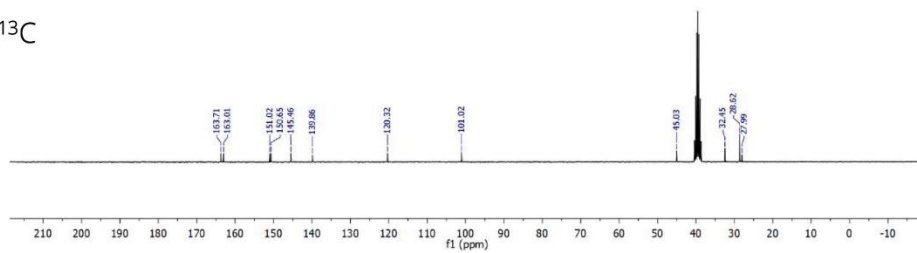
 $^{13}\text{C}$ 

HSQC

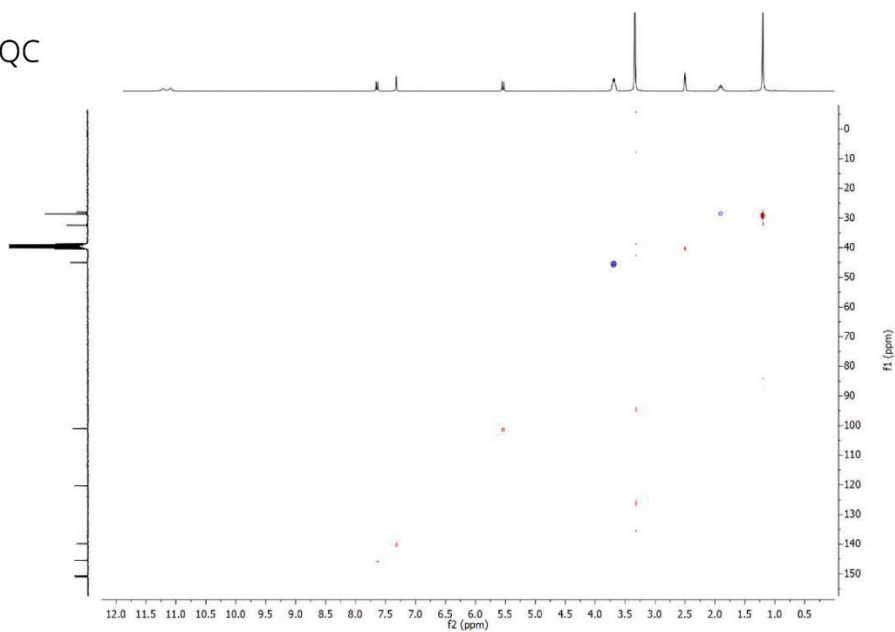


$^1\text{H}$ 

DEPT-135

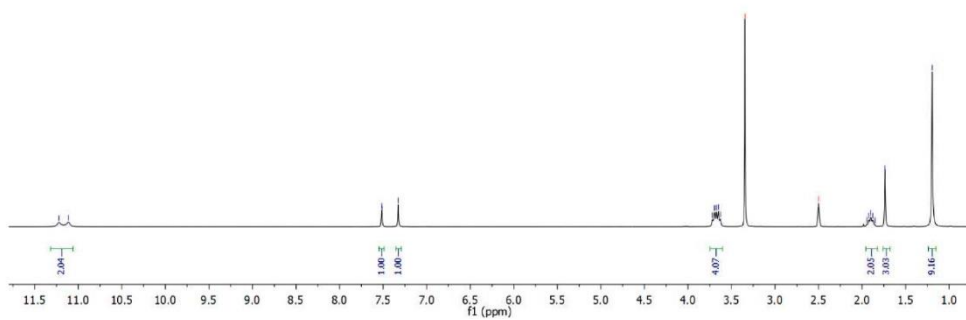
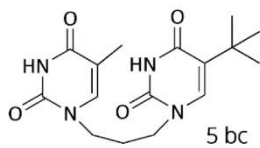
 $^{13}\text{C}$ 

HSQC

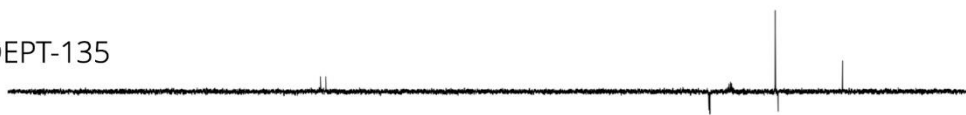
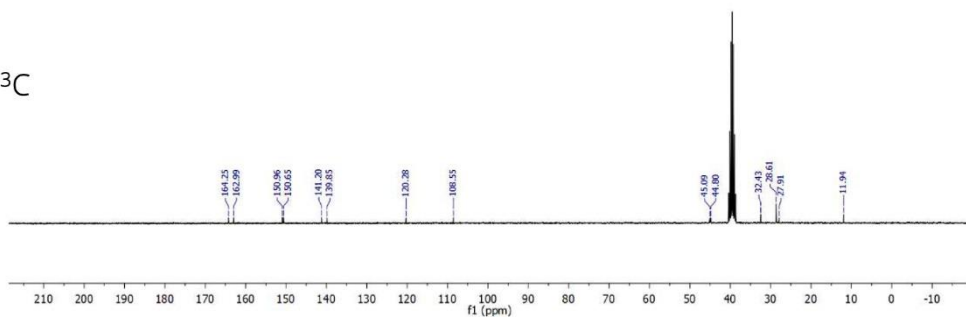


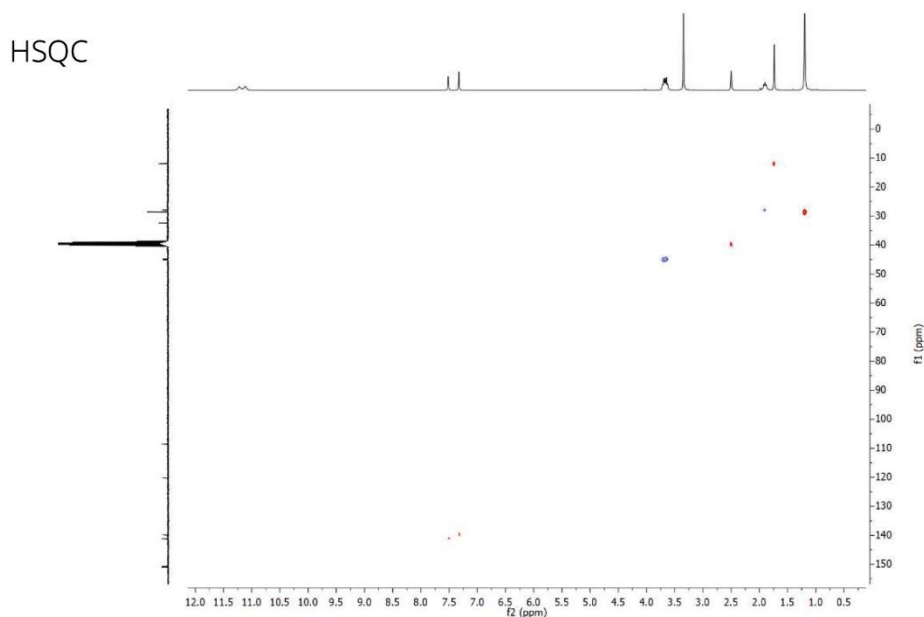
$^1\text{H}$ 11.22  
11.117.52  
7.51  
7.333.75  
3.70  
3.67  
3.65  
3.60  
3.54 H<sub>2</sub>O

2.50 DMSO

1.95  
1.92  
1.88  
1.85  
1.77  
1.20

DEPT-135

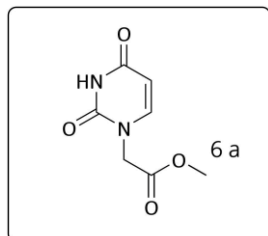
 $^{13}\text{C}$ 



#### 4.4.1.5. Compounds 6

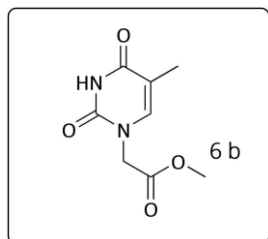
Pyrimidineacetates (**6a**, **6b** and **6c**) were prepared by esterification of their respective carboxylic acids (see Annex 4.5 for characterisation) with MeOH in the presence of H<sub>2</sub>SO<sub>4</sub>. To a solution of uracil (0.2 g, 1.2 mmol), thymine (0.2 g, 1.1 mmol) or *tert*-butyl uracil (0.2 g, 0.9 mmol) carboxylic acids in methanol (5 mL) H<sub>2</sub>SO<sub>4</sub> was added, and the stirred mixture heated at reflux overnight. The solvent was removed under vacuum, and the solid obtained was dissolved in AcOEt and washed three times with a saturated NaCl solution, and then dried over anhydrous MgSO<sub>4</sub>.

Methyl 2-(2,4-dioxo-3,4-dihydropyrimidin-1(2H)-yl) acetate (**6a**), white solid (177 mg, 80 %).  $^1\text{H NMR}$  (300 MHz,  $\text{DMSO-}d_6$ )  $\delta_{\text{H}}$ : 11.40 (s, 1H), 7.61 (d,  $J = 7.9$



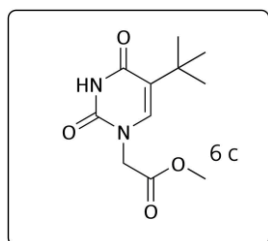
Hz, 1H), 5.61 (d,  $J = 7.8$  Hz, 1H), 4.52 (s, 2H), 3.69 (s, 3H).  $^{13}\text{C NMR}$  (75 MHz,  $\text{DMSO-}d_6$ ): 168.60 (CO), 163.67 (CO), 150.90 (CO), 145.79 (CH), 101.07 (CH), 52.25 ( $\text{CH}_3$ ), 48.47 ( $\text{CH}_2$ ). HRMS (ESI-TOF)  $m/z$ :  $[\text{M} + \text{H}]^+$  calcd for  $\text{C}_7\text{H}_9\text{N}_2\text{O}_4$  185.0562; found 185.0553.

Methyl 2-(5-methyl-2,4-dioxo-3,4-dihydropyrimidin-1(2H)-yl) acetate (**6b**), white solid (195 mg, 90 %).  $^1\text{H NMR}$  (300 MHz,  $\text{DMSO-}d_6$ )  $\delta_{\text{H}}$ : 11.38 (s, 1H), 7.49



(d,  $J = 1.2$  Hz, 1H), 4.48 (s, 2H), 3.68 (s, 3H), 1.75 (d,  $J = 1.2$  Hz, 3H).  $^{13}\text{C NMR}$  (75 MHz,  $\text{DMSO-}d_6$ ): 168.68 (CO), 164.26 (CO), 150.88 (CO), 141.49 (CH), 108.57 (C), 52.21 ( $\text{CH}_3$ ), 48.29 ( $\text{CH}_2$ ), 11.82 ( $\text{CH}_3$ ). HRMS (ESI-TOF)  $m/z$ :  $[\text{M} + \text{H}]^+$  calcd for  $\text{C}_8\text{H}_{11}\text{N}_2\text{O}_4$  199.0719 found 199.0713.

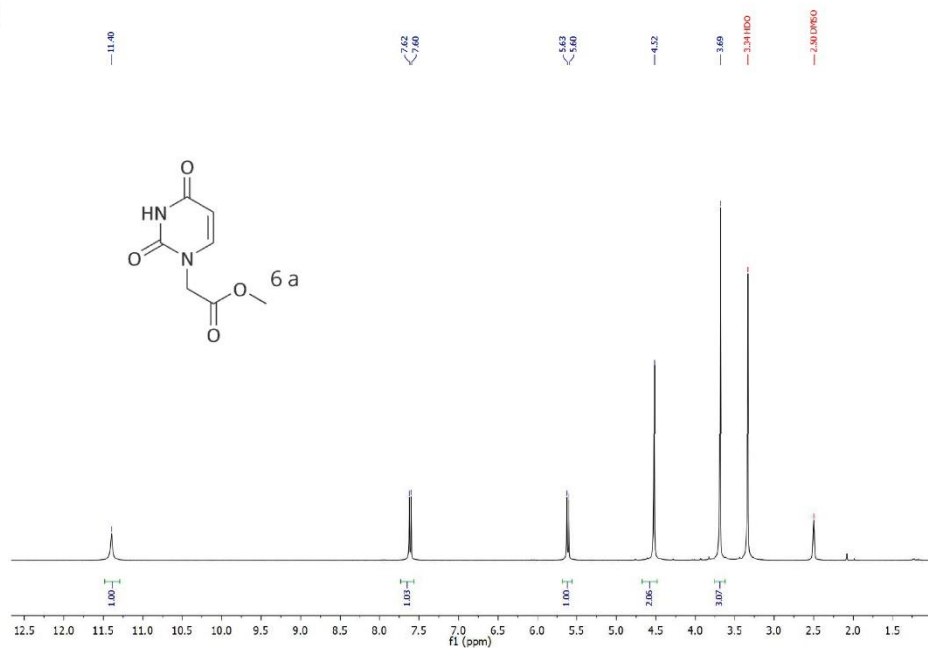
Methyl 2-(5-(tert-butyl)-2,4-dioxo-3,4-dihydropyrimidin-1(2H)-yl) acetate (**6c**), white solid (162 mg, 75 %).  $^1\text{H NMR}$  (300 MHz,  $\text{DMSO-}d_6$ )  $\delta_{\text{H}}$ : 11.25 (s, 1H), 7.39



(s, 1H), 4.53 (s, 2H), 3.69 (s, 3H), 1.20 (s, 9H).  $^{13}\text{C NMR}$  (75 MHz,  $\text{DMSO-}d_6$ )  $\delta$  168.74 (CO), 163.02 (CO), 150.62 (CO), 140.36 (CH), 120.20 (C), 52.15 ( $\text{CH}_3$ ), 48.53 ( $\text{CH}_2$ ), 32.42 (C), 28.55 ( $\text{CH}_3$ ). HRMS (ESI-TOF)  $m/z$ :  $[\text{M} + \text{H}]^+$  calcd for  $\text{C}_{11}\text{H}_{17}\text{N}_2\text{O}_4$  241.1188; found 241.1183.

# Chapter 4

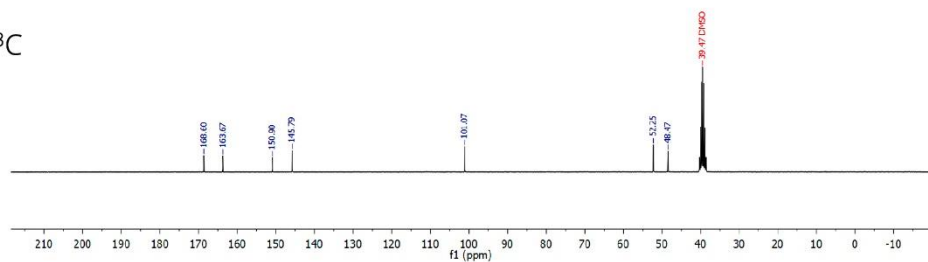
$^1\text{H}$



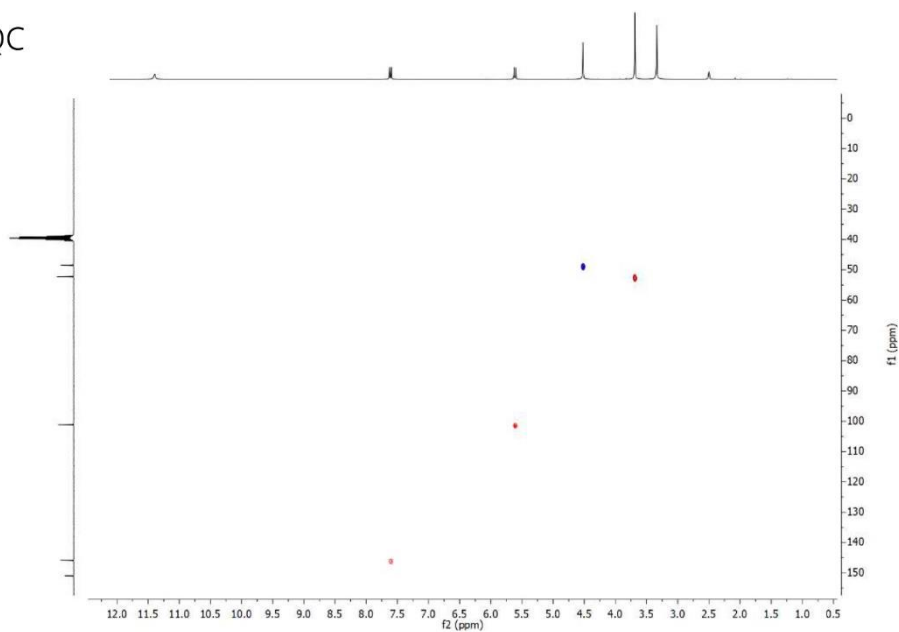
DEPT-135



$^{13}\text{C}$

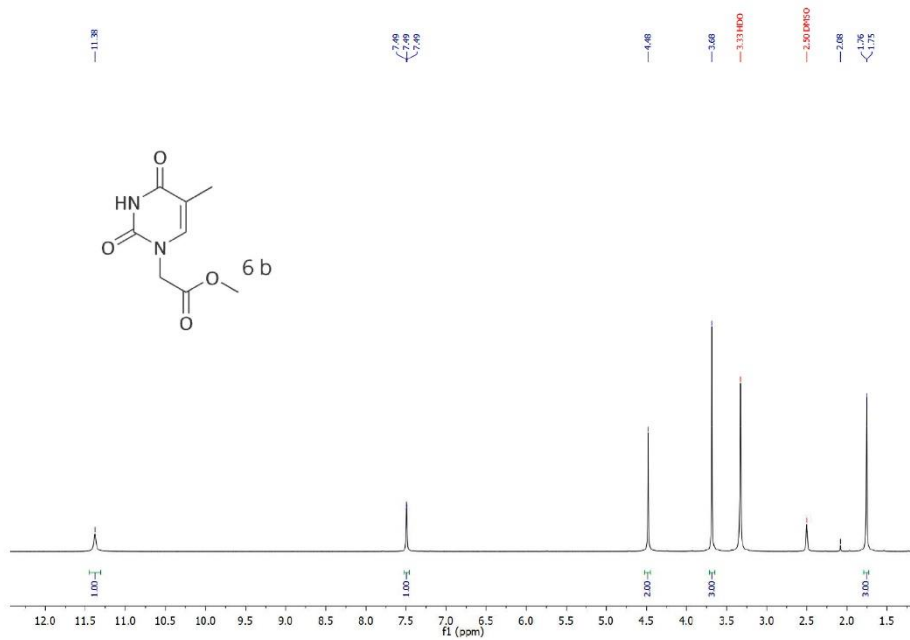


HSQC



# Chapter 4

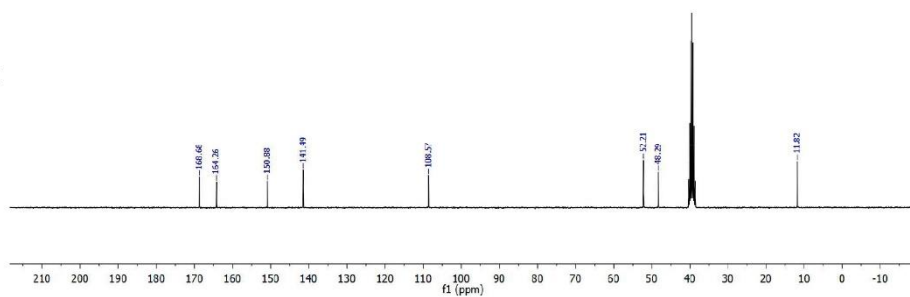
$^1\text{H}$



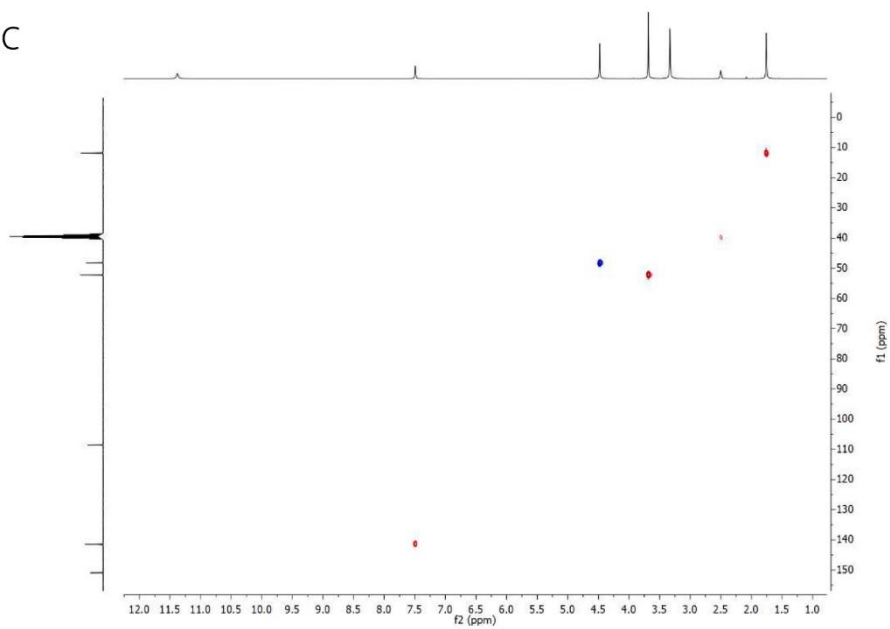
DEPT-135



$^{13}\text{C}$



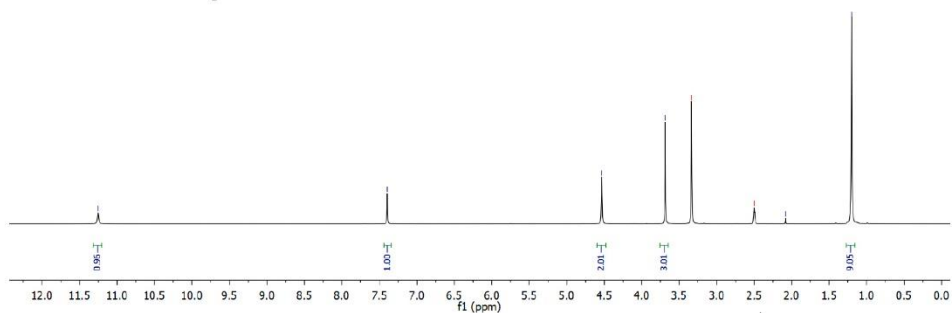
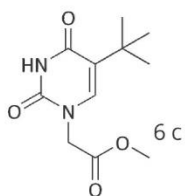
HSQC



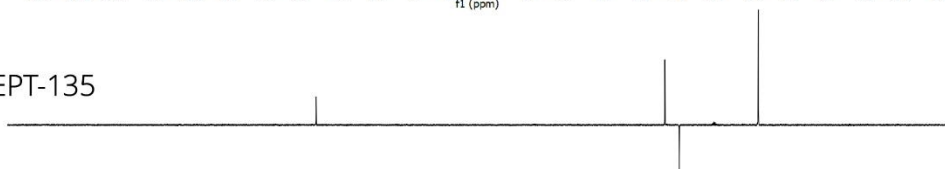
# Chapter 4

$^1\text{H}$

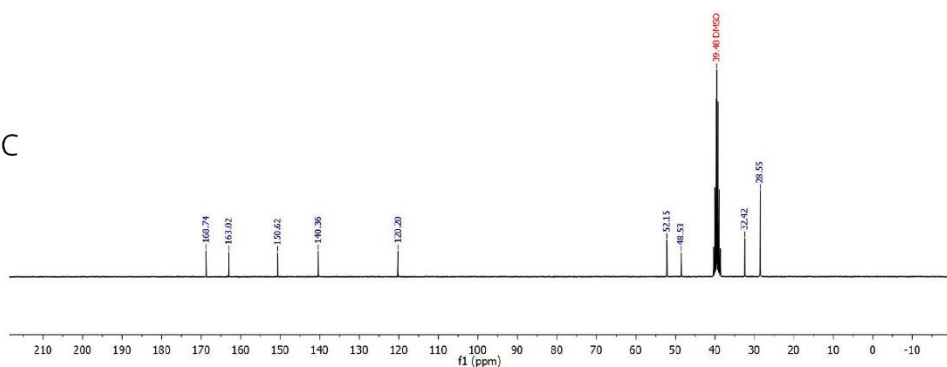
11.25      7.39      4.13      2.69      3.01 H<sub>2</sub>O      2.00 DMSO      2.88      1.20



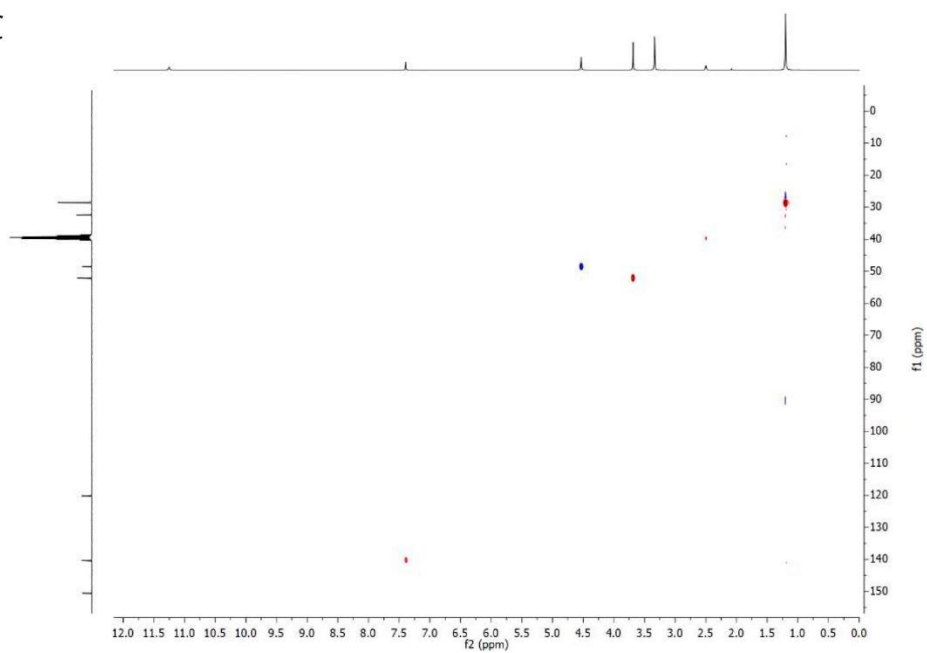
DEPT-135



$^{13}\text{C}$



HSQC



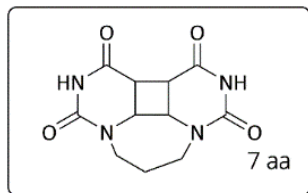
## 4.4.2. Irradiation Procedures

### 4.4.2.1. Photosensitised Irradiation with Acetone in H<sub>2</sub>O

Solutions of compounds **3** and **5** (0.2 mmol) in 180 mL of deionised water were boiled to increase the solubility and then cooled while bubbling N<sub>2</sub> in pyrex erlenmeyer flasks. To the solutions, 20 mL of HPLC grade acetone was added as photosensitiser and irradiated in a multilamp photoreactor with 14 lamps (Luzchem lamps, LZC-UVB centred at approx. 300 nm, with a peak of 313 nm, 8 Watt) during 7.5 h. The progress of the reaction was monitored by using a UV-Vis spectrophotometer following the disappearance of the 260-270 nm band corresponding to unreacted starting material band. Once the reaction was completed the solvent was evaporated under vacuum obtaining the *cis-syn* CPDs, **7**.

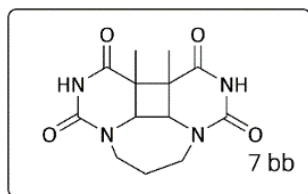
#### Hexahydro-1H-3a,5,8,9a-tetraazacyclohepta[def]biphenylene-

**4,6,7,9(5H,8H)-tetraone (7aa)**, white solid (25 mg, 47 %). <sup>1</sup>H NMR (300 MHz, DMSO-d<sub>6</sub>) δ<sub>H</sub>: 10.28 (s, 2H), 4.23 – 4.04 (m, 4H), 3.83 (dd, *J* = 7.0, 3.4 Hz, 2H), 2.77 (ddd, *J* = 14.6, 12.0, 2.5 Hz, 2H), 1.94 – 1.72 (m, 1H), 1.48 (d, *J* = 14.6 Hz, 1H). <sup>13</sup>C NMR (75 MHz, DMSO-d<sub>6</sub>): 166.2 (2CO), 150.9 (2CO), 54.4 (2CH), 46.8 (2CH<sub>2</sub>), 36.7 (2CH), 24.1 (2CH<sub>2</sub>). HRMS (ESI-TOF) *m/z*: [M + H]<sup>+</sup> calcd for C<sub>11</sub>H<sub>13</sub>N<sub>4</sub>O<sub>4</sub> 265.0937; found 265.0932.



## 6a,6b-Dimethylhexahydro-1H-3a,5,8,9a-

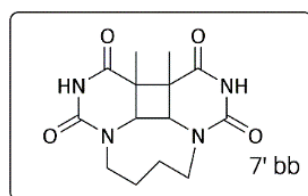
tetraazacyclohepta[def]biphenylene-4,6,7,9 (5H,8H)-tetraone (7bb), white



solid (32 mg, 54 %).  $^1\text{H NMR}$  (300 MHz,  $\text{DMSO-d}_6$ ),  $\delta_{\text{H}}$ : 10.28 (s, 2H), 4.08 (dt,  $J = 14.2, 3.9$  Hz, 2H), 3.91 (s, 2H), 2.81 – 2.66 (m, 2H), 1.95 – 1.80 (m, 1H), 1.56 – 1.44 (m, 1H), 1.38 (s, 6H).  $^{13}\text{C NMR}$  (75 MHz,  $\text{DMSO-d}_6$ ): 169.7 (CO), 150.9 (CO), 59.8 (2CH), 46.6

(2 $\text{CH}_2$ ), 44.7 (2C), 23.5 ( $\text{CH}_2$ ), 20.0 (2 $\text{CH}_3$ ). HRMS (ESI-TOF)  $m/z$ :  $[\text{M} + \text{H}]^+$  calcd for  $\text{C}_{13}\text{H}_{17}\text{N}_4\text{O}_4$  293.1250; found 293.1241.

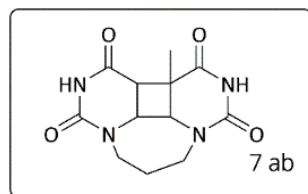
## 7a,7b-Dimethyloctahydro-4a,6,9,10a-tetraazacycloocta[def]biphenylene-

5,7,8,10 (6H,9H)-tetraone (7'bb), white solid (31 mg, 51%).  $^1\text{H NMR}$  (300 MHz,

$\text{DMSO-d}_6$ )  $\delta_{\text{H}}$ : 10.23 (s, 2H), 4.08 (d,  $J = 13.7$  Hz, 2H), 3.87 (s, 2H), 2.63 (d,  $J = 13.8$  Hz, 2H), 1.62 (s, 4H), 1.34 (s, 6H).  $^{13}\text{C NMR}$  (75 MHz,  $\text{DMSO-d}_6$ ): 169.9 (2CO), 152.2 (2CO), 59.8 (2CH), 47.4 (2 $\text{CH}_2$ ), 46.4 (2C), 25.4 (2 $\text{CH}_2$ ), 18.9 (2 $\text{CH}_3$ ). HRMS (ESI-TOF)  $m/z$ :

$[\text{M} + \text{H}]^+$  calcd for  $\text{C}_{14}\text{H}_{19}\text{N}_4\text{O}_4$  307.1406; found 307.1392.

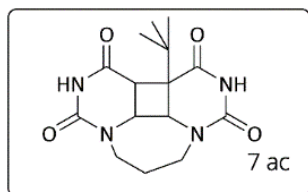
## 6b-Methylhexahydro-1H-3a,5,8,9a-tetraazacyclohepta[def]biphenylene-

4,6,7,9(5H,8H)-tetraone (7ab), white solid (23 mg, 42%).  $^1\text{H NMR}$  (300 MHz,

$\text{DMSO-d}_6$ )  $\delta_{\text{H}}$ : 10.28 (d,  $J = 6.5$  Hz, 2H), 4.26 (dd,  $J = 9.7, 5.8$  Hz, 1H), 4.18 – 3.99 (m, 2H), 3.91 (d,  $J = 5.8$  Hz, 1H), 3.39 (s, 1H), 2.75 (t,  $J = 12.6$  Hz, 2H), 1.84 (dd,  $J = 25.5, 12.1$  Hz, 1H), 1.56 (s, 3H), 1.49 (d,  $J = 17.1$  Hz, 1H).  $^{13}\text{C NMR}$  (75 MHz,  $\text{DMSO-d}_6$ ): 168.6

(CO), 166.1 (CO), 150.9 (CO), 150.8 (CO), 61.0 (CH), 51.8 (CH), 46.7 (2 $\text{CH}_2$ ), 44.3 (CH), 42.9 (C), 25.1 ( $\text{CH}_3$ ), 23.8 ( $\text{CH}_2$ ). HRMS (ESI-TOF)  $m/z$ :  $[\text{M} + \text{H}]^+$  calcd for  $\text{C}_{12}\text{H}_{15}\text{N}_4\text{O}_4$  279.1093; found 279.1081.

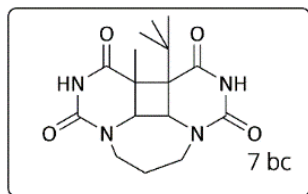
6b-(*tert*-Butyl)hexahydro-1H-3a,5,8,9a-tetraazacyclohepta[def]biphenylene-4,6,7,9(5H,8H)-tetraone (7ac), white solid (25 mg, 39%).



$^1\text{H NMR}$  (300 MHz, DMSO- $d_6$ )  $\delta_{\text{H}}$ : 10.30 (s, 1H), 10.21 (s, 1H), 4.23 (d,  $J$  = 6.2 Hz, 1H), 4.16 – 4.04 (m, 2H), 3.99 (dd,  $J$  = 9.5, 6.2 Hz, 1H), 3.50 (d,  $J$  = 9.5 Hz, 1H), 2.94 – 2.82 (m, 1H), 2.81 – 2.68 (m, 1H), 1.79 (d,  $J$  = 14.1 Hz, 1H), 1.53 (d,  $J$  = 14.4 Hz, 1H), 1.05 (s, 9H).  $^{13}\text{C NMR}$  (75 MHz, DMSO- $d_6$ ): 168.3 (CO), 166.2 (CO), 150.8 (CO), 150.7 (CO), 56.0 (CH), 54.8 (C), 51.8 (CH), 46.8 (CH<sub>2</sub>), 46.0 (CH<sub>2</sub>), 38.0 (CH), 35.8 (C), 25.1 (3CH<sub>3</sub>), 24.3 (CH<sub>2</sub>).

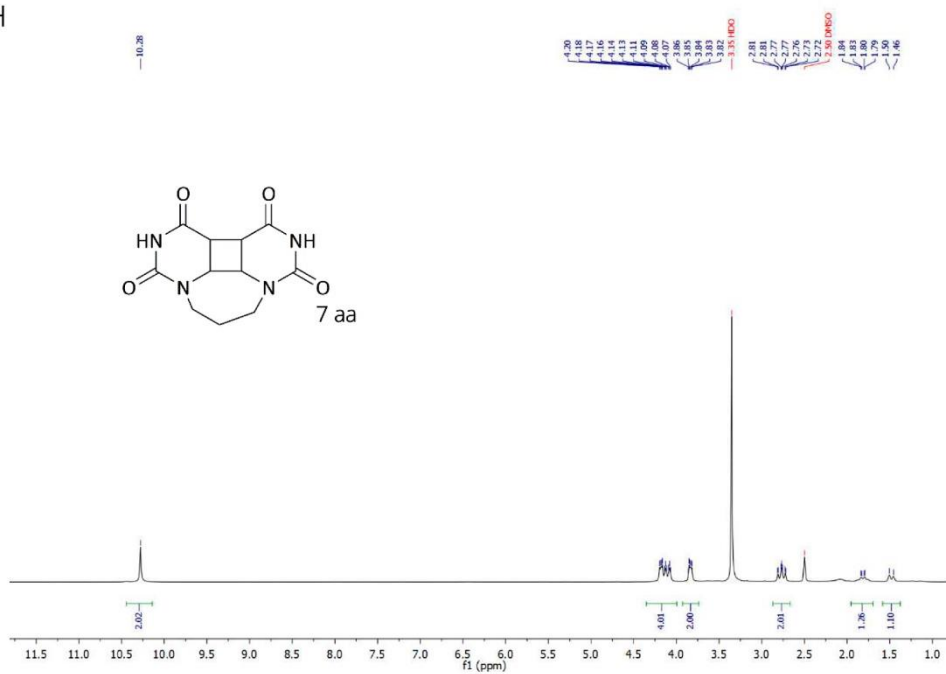
HRMS (ESI-TOF)  $m/z$ :  $[\text{M} + \text{H}]^+$  calcd for C<sub>15</sub>H<sub>21</sub>N<sub>4</sub>O<sub>4</sub> 321.1563; found 321.1556.

6b-(*tert*-Butyl)-6a-methylhexahydro-1H-3a,5,8,9a-tetraazacyclohepta[def]biphenylene-4,6,7,9(5H,8H)-tetraone (7bc), white solid (31 mg, 46%).

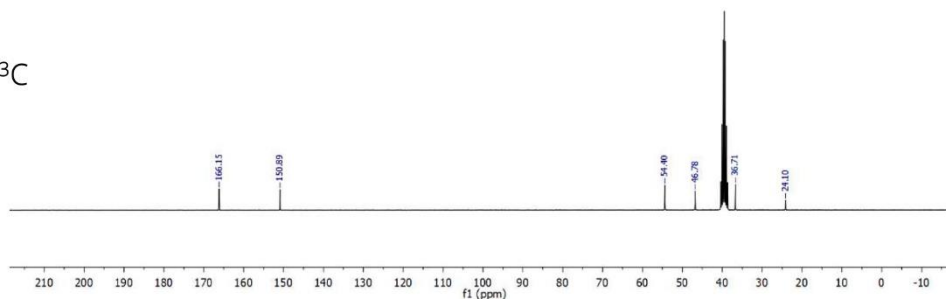


$^1\text{H NMR}$  (300 MHz, DMSO- $d_6$ )  $\delta_{\text{H}}$ : 10.34 (s, 1H), 10.11 (s, 1H), 4.41 (d,  $J$  = 6.7 Hz, 1H), 4.07 (dd,  $J$  = 11.7, 7.2 Hz, 1H), 3.97 (dt,  $J$  = 14.5, 4.4 Hz, 1H), 3.75 (d,  $J$  = 6.7 Hz, 1H), 2.93 (ddd,  $J$  = 13.6, 10.0, 3.3 Hz, 1H), 2.81 (td,  $J$  = 12.0, 11.2, 5.9 Hz, 1H), 1.94 – 1.78 (m, 1H), 1.62 (s, 1H), 1.57 (s, 3H), 1.11 (s, 9H).

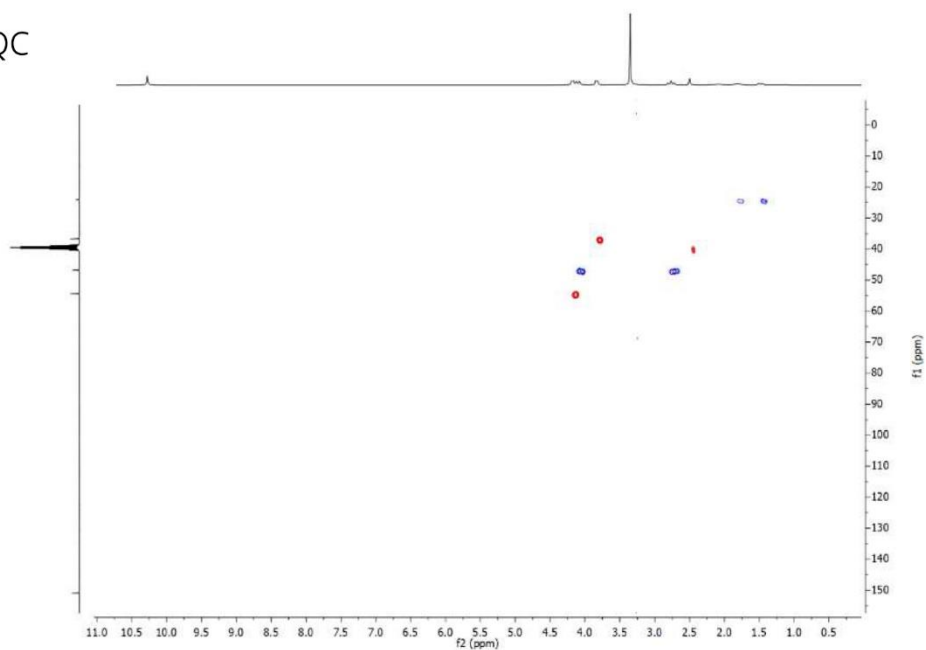
$^{13}\text{C NMR}$  (75 MHz, DMSO- $d_6$ ): 169.5 (CO), 169.3 (CO), 151.5 (CO), 150.8 (CO), 59.9 (CH), 56.5 (2C), 55.1 (CH), 46.3 (CH<sub>2</sub>), 45.8 (CH<sub>2</sub>), 45.8 (CH<sub>2</sub>), 36.7 (C), 27.6 (3CH<sub>3</sub>), 23.5 (CH<sub>2</sub>), 22.3 (CH<sub>3</sub>). HRMS (ESI-TOF)  $m/z$ :  $[\text{M} + \text{H}]^+$  calcd for C<sub>16</sub>H<sub>23</sub>N<sub>4</sub>O<sub>4</sub> 335.1719; found 335.1704.

$^1\text{H}$ 

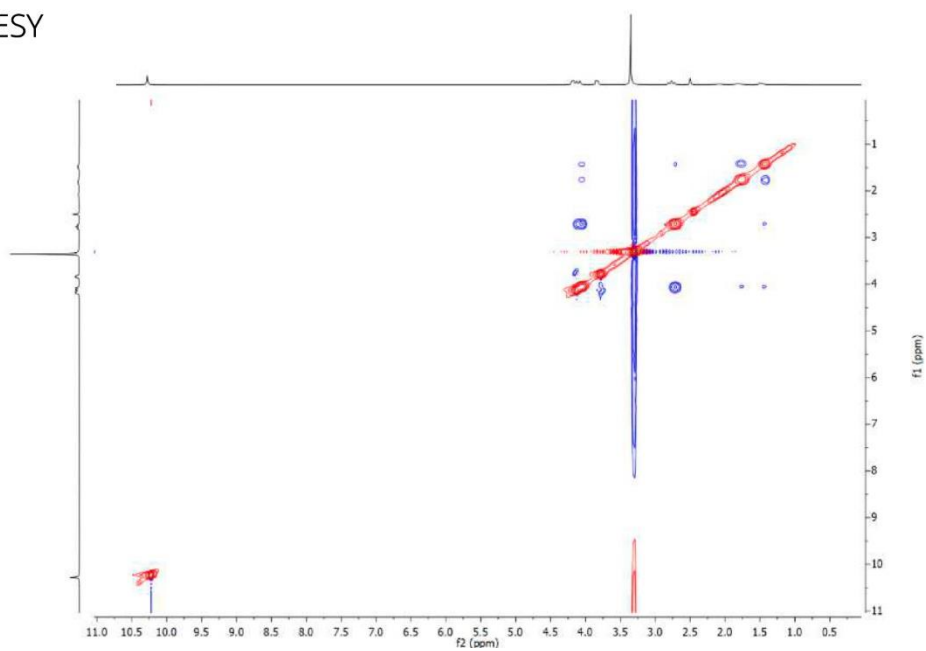
DEPT-135

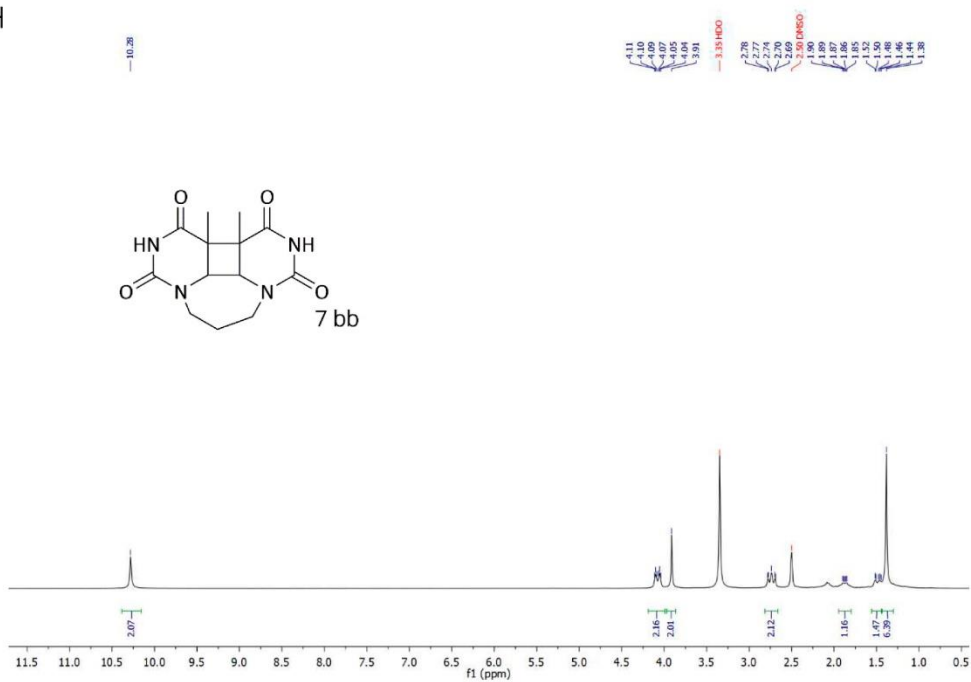
 $^{13}\text{C}$ 

HSQC

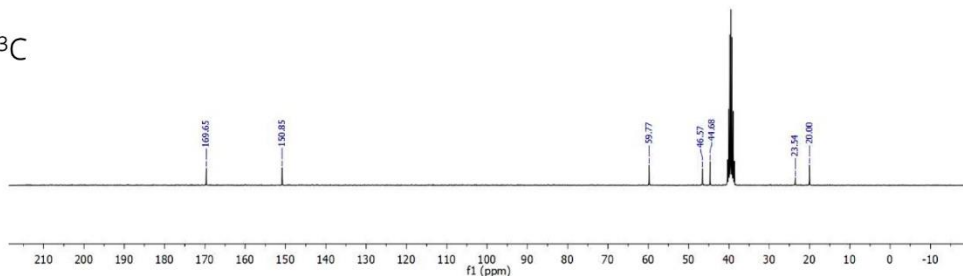


NOESY

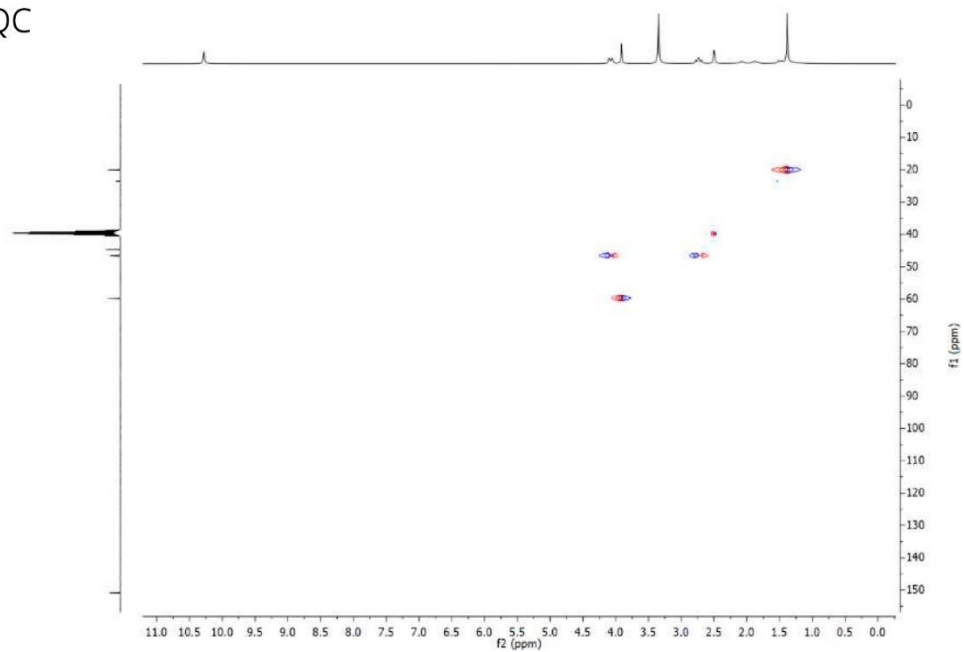


$^1\text{H}$ 

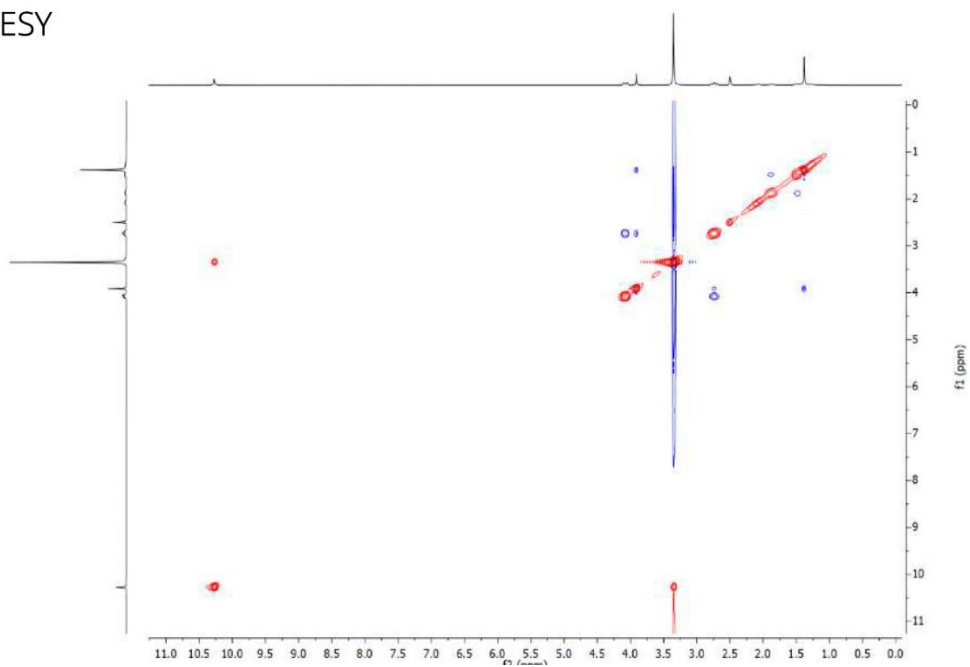
DEPT-135

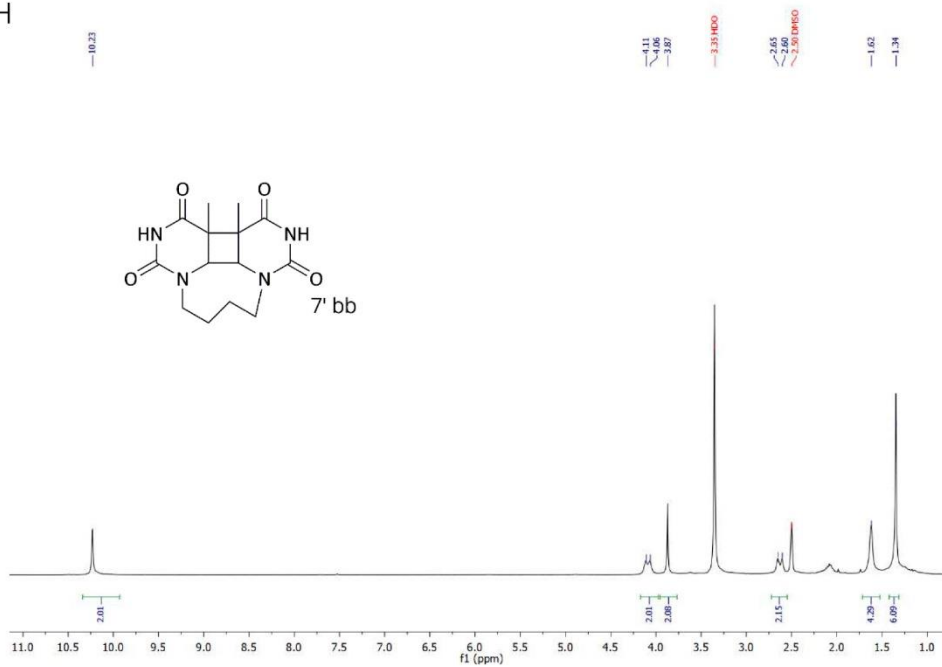
 $^{13}\text{C}$ 

HSQC

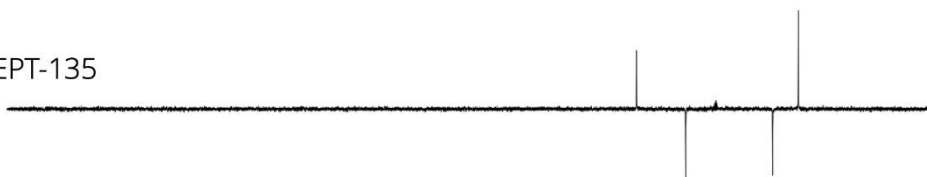
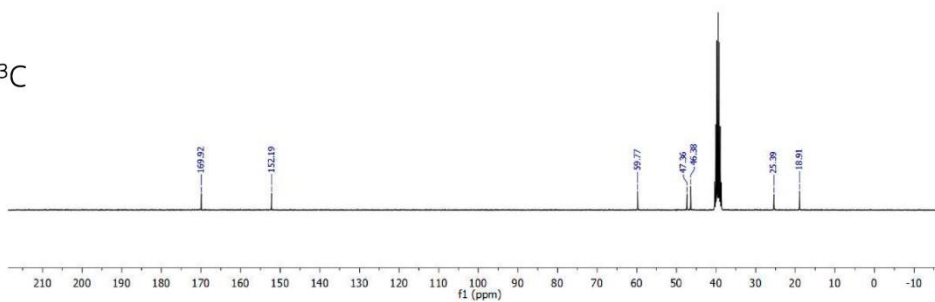


NOESY

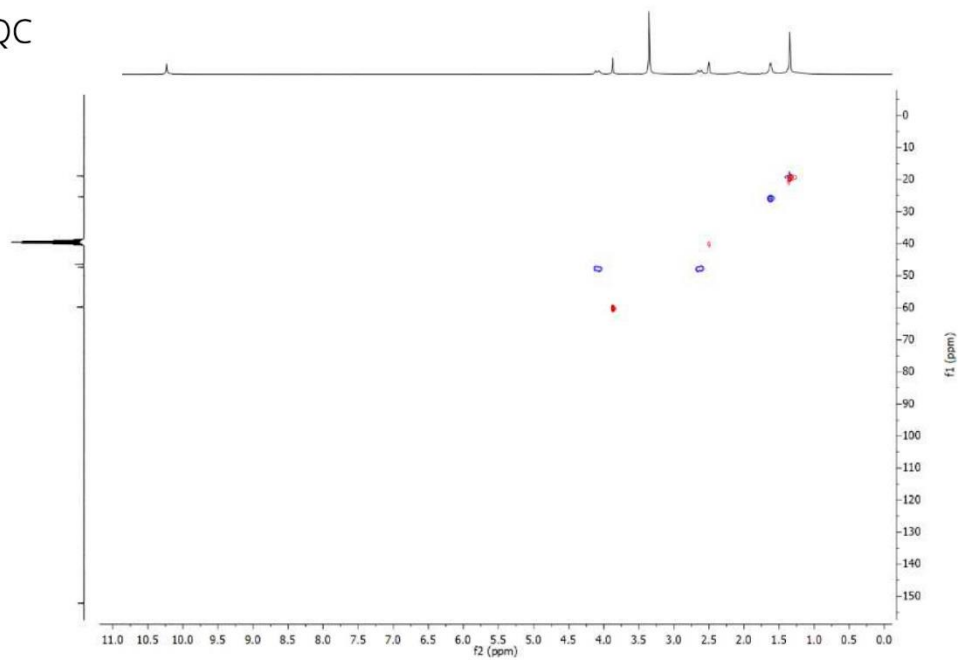


$^1\text{H}$ 

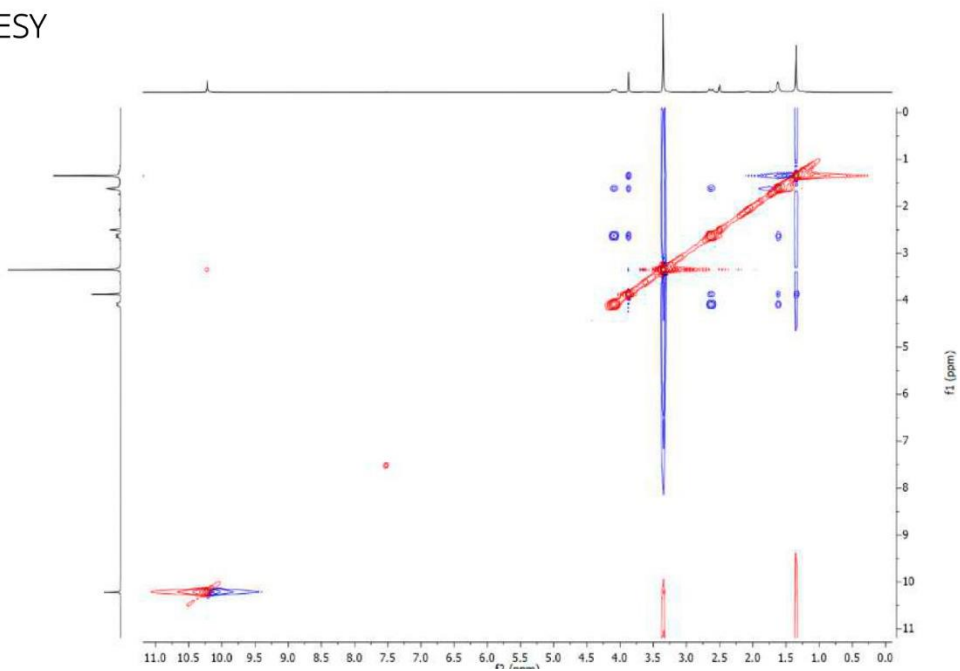
DEPT-135

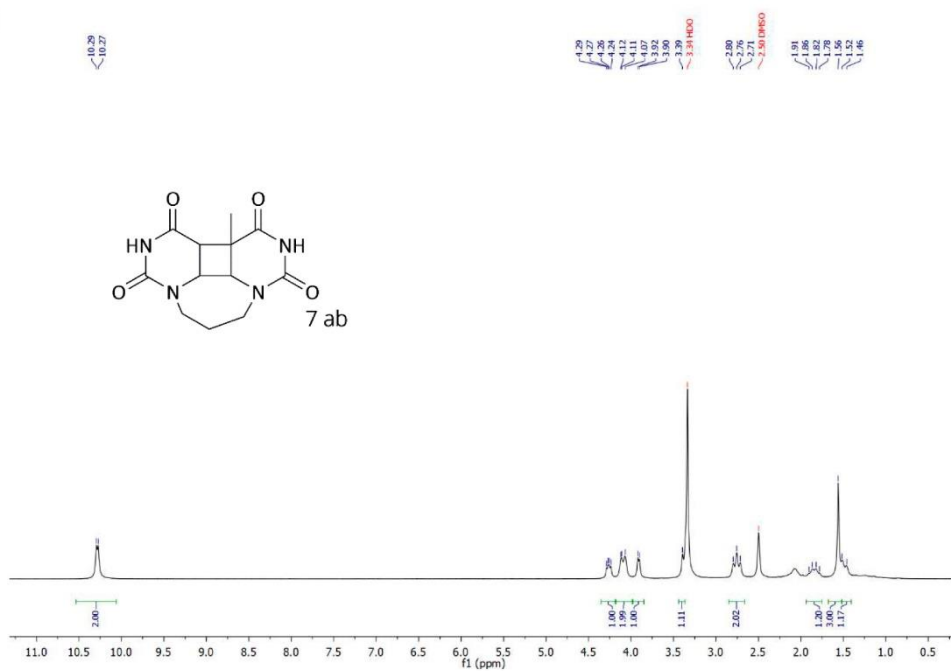
 $^{13}\text{C}$ 

HSQC

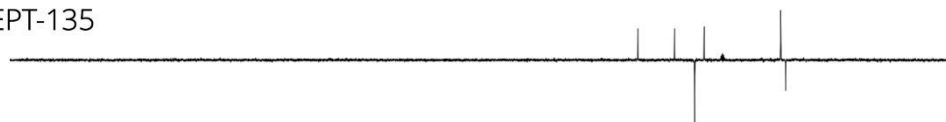
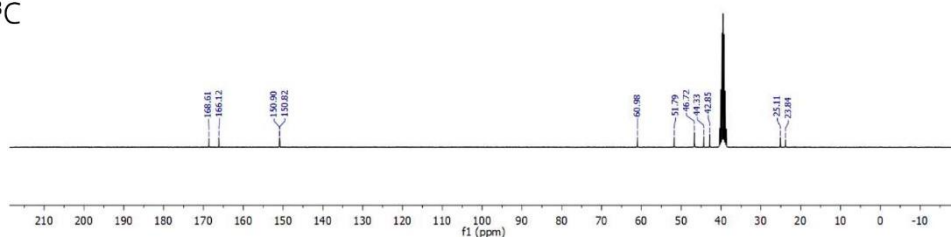


NOESY

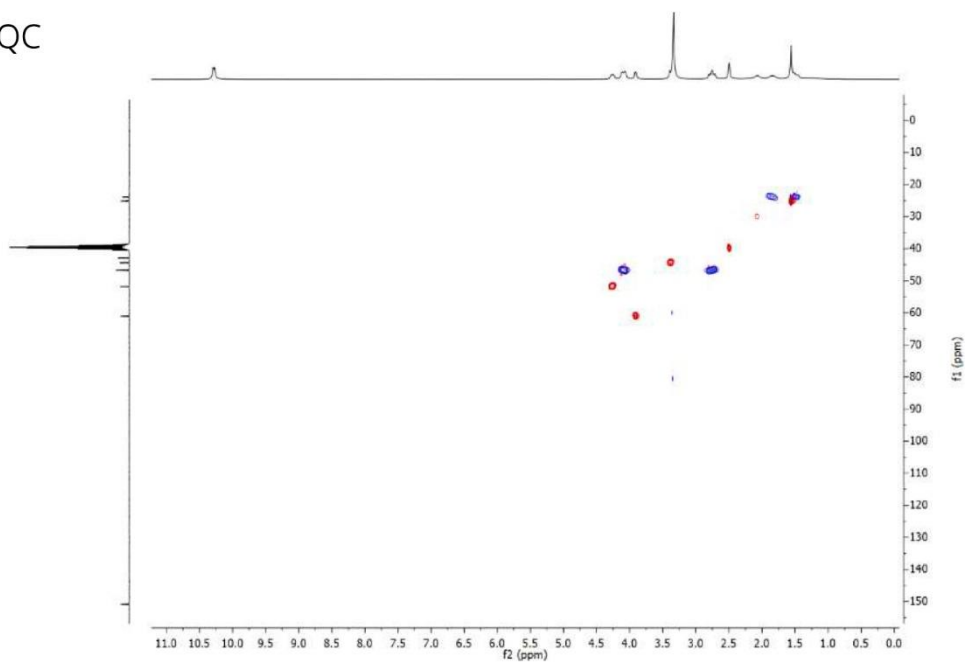


$^1\text{H}$ 

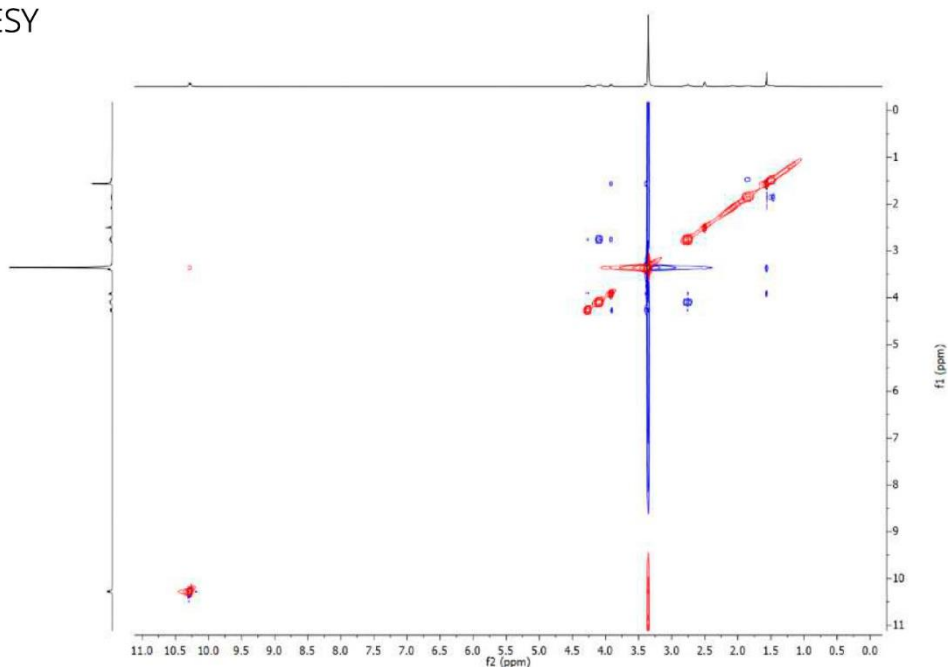
DEPT-135

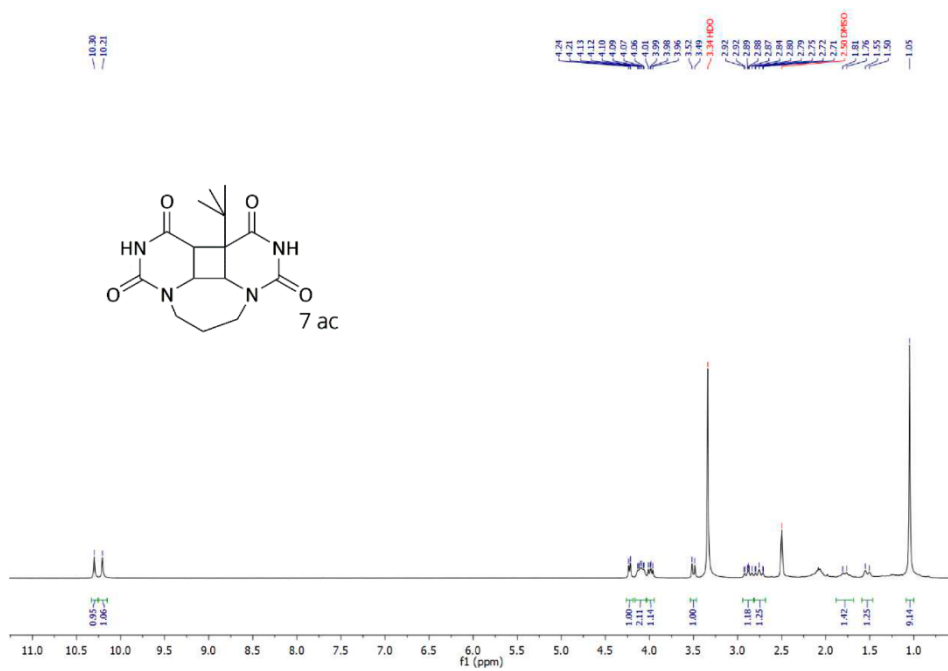
 $^{13}\text{C}$ 

HSQC

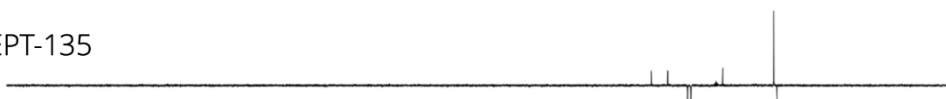
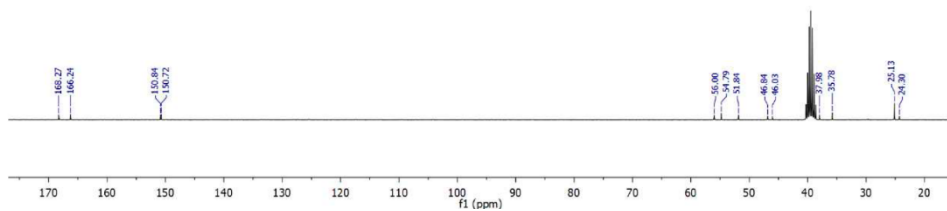


NOESY

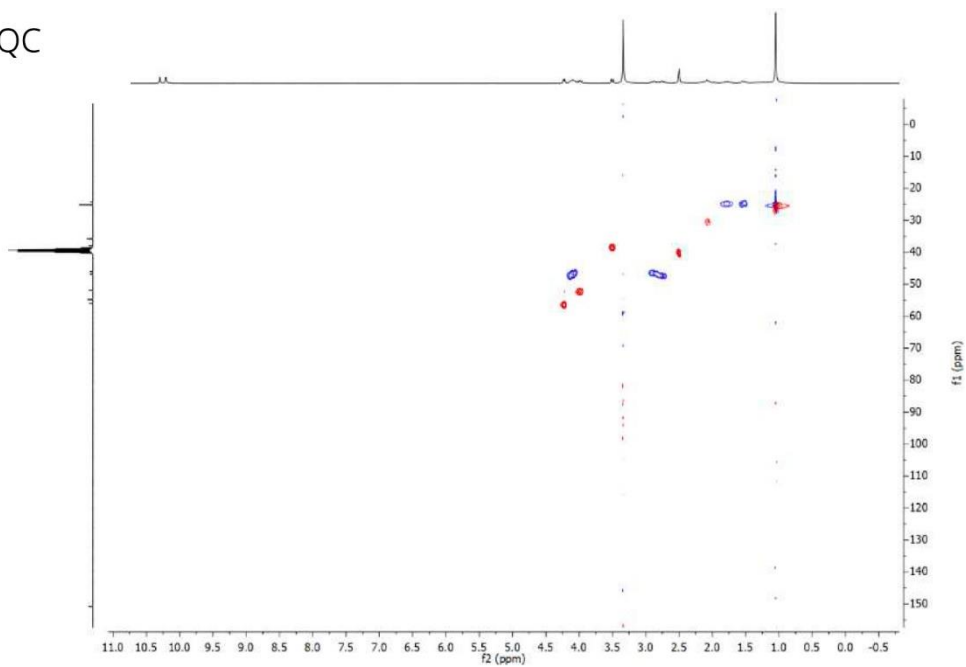


$^1\text{H}$ 

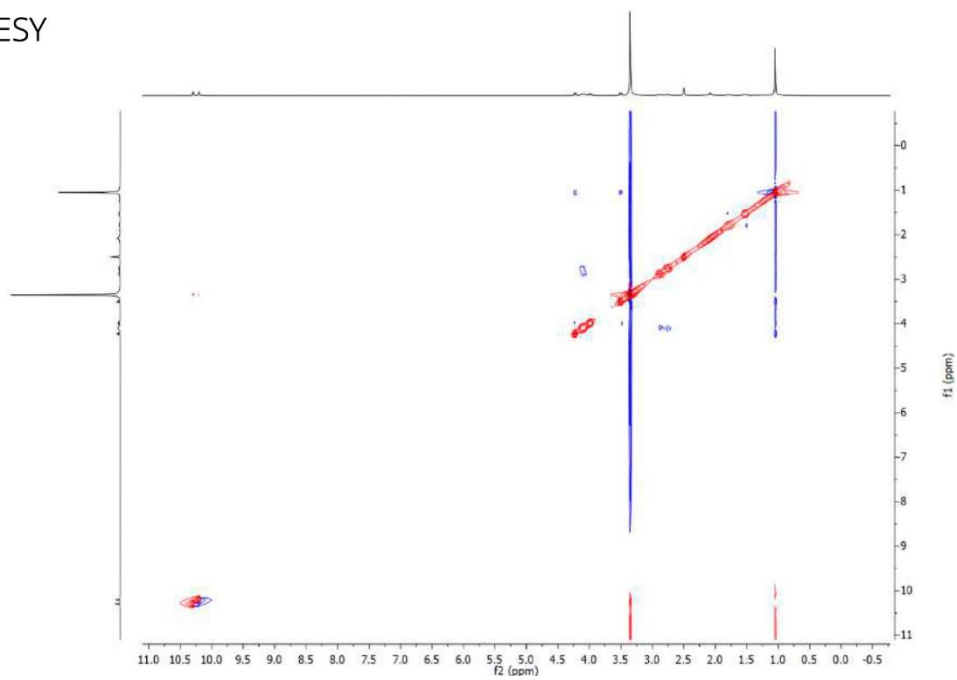
DEPT-135

 $^{13}\text{C}$ 

HSQC

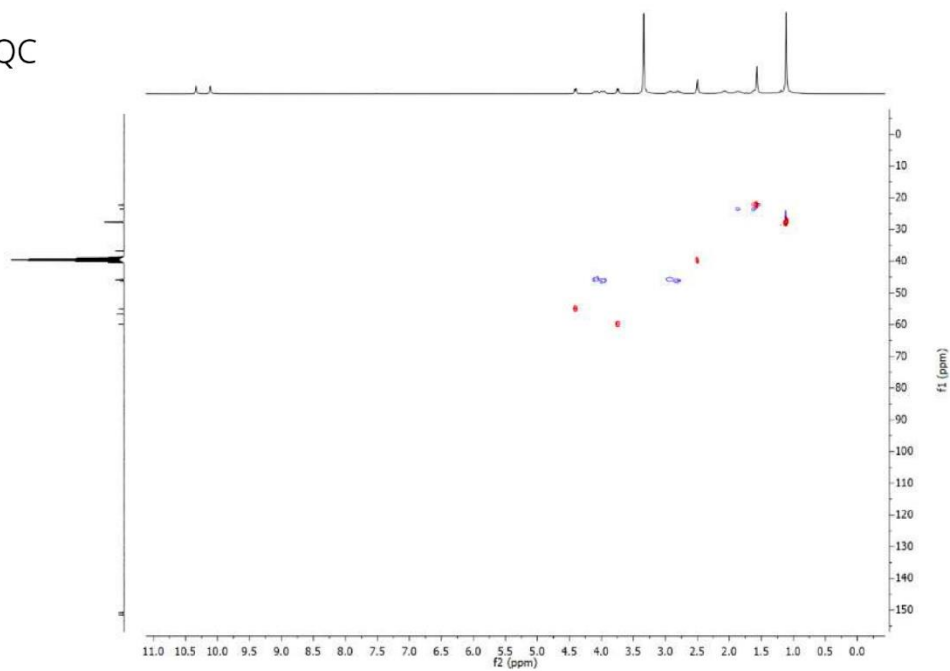


NOESY

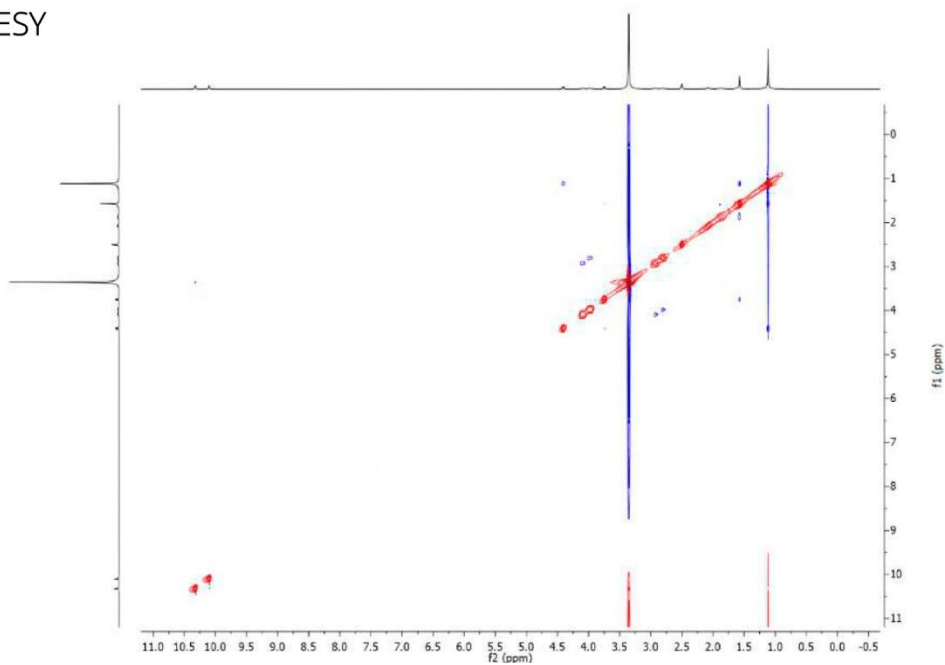




HSQC



NOESY



#### 4.4.2.2. Analytical 2'-Methoxyacetophenone Photosensitised Irradiation

For analytical purposes, irradiations were performed in quartz cuvettes with two opposing lamps (Luzchem lamps, LZC-UVA centered at approx. 350 nm, 8 Watt). A 0.04 mM solution of **2M** in PB 10 mM was prepared and compounds **3**, **5** or **6** added to 172 mL of this solution in order to have the same concentration as **2M**. All the solutions were bubbled with N<sub>2</sub> prior to light exposure during 10 min and the progress of the reaction was monitored by using a UV-Vis spectrophotometer. 2'-Methoxyacetophenone stock solution was used as a reference.

#### 4.4.2.3. Preparative 2'-Methoxyacetophenone Photosensitised Irradiation

Preparative irradiations were accomplished in a pyrex erlenmeyer flask using six opposing (Luzchem lamps, LZC-UVA centered at approx. 350 nm, 8 Watt). To 500 mL of miliQ water compounds **3** or **6** were added (0.02 mmol) and the solution boiled. Then it was cooled bubbling N<sub>2</sub> and **2M** added (3.2 μL, 0.02 mmol). The progress of the reaction was monitored by using a UV-Vis spectrophotometer (1.5 h) and the solvent removed under vacuum. <sup>1</sup>H-NMR spectra were recorded for each photomixture and compared with those of the isolated CPDs.

#### 4.4.3. Absorption Spectra

UV-vis absorption spectra were registered with a simple beam spectrophotometer (see section 6.2.1).

#### 4.4.4. Phosphorescence Spectroscopy

Phosphorescence spectroscopy was performed using a spectrophosphorimeter Photon Technology International (see section 6.2.4).

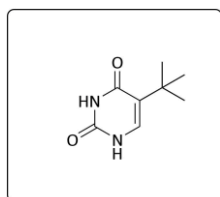
#### 4.4.5. Phosphorescence Spectroscopy

A pulsed Nd: YAG SL404G-10 Spectron Laser Systems, using 355 nm as the excitation wavelength with a pulse duration of 10 ns and an energy lower than 15 mJ pulse<sup>-1</sup> was used to carry out the laser LFP experiments (see section 6.2.3).

For quenching experiments, compounds **3**, **5**, and **6** were dissolved in 0.7 mL of anhydrous DMSO (from 0 to 1.3 mM), added to a solution of **2M** in PB 10 mM with an absorbance of 0.3 at  $\lambda_{\text{exc}} = 355$  nm, and monitored at 420 nm.

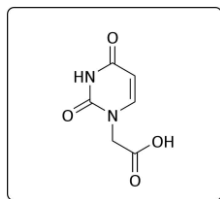
## 4.5. Annex

5-(*tert*-butyl)pyrimidine-2,4(1H,3H)-dione white solid.  $^1\text{H NMR}$  (300 MHz,



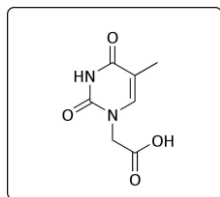
DMSO- $d_6$ )  $\delta_{\text{H}}$ : 10.89 (s, 1H), 10.59 (s, 1H), 6.99 (s, 1H), 1.18 (s, 9H).  $^{13}\text{C NMR}$  (75 MHz, DMSO- $d_6$ ):  $\delta$  163.54 (CO), 151.15 (CO), 135.84 (CH), 119.32 (C), 32.09 (C), 28.48 (3CH $_3$ ). HRMS (ESI-TOF)  $m/z$ :  $[\text{M} + \text{H}]^+$  calcd for C $_8$ H $_{13}$ N $_2$ O $_2$ ; 169.0977 found 169.0973.

2-(2,4-dioxo-3,4-dihydropyrimidin-1(2H)-yl)acetic acid white solid.  $^1\text{H NMR}$



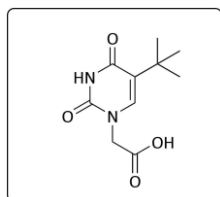
(300 MHz, DMSO- $d_6$ )  $\delta_{\text{H}}$ : 11.35 (s, 1H), 7.61 (d,  $J = 7.8$  Hz, 1H), 5.59 (dd,  $J = 7.8, 2.1$  Hz, 1H), 4.41 (s, 2H).  $^{13}\text{C NMR}$  (75 MHz, DMSO- $d_6$ ):  $\delta$  169.52 (CO), 163.75 (CO), 150.96 (CO), 146.01 (CH), 100.81 (CH), 48.55 (CH $_2$ ). HRMS (ESI-TOF)  $m/z$ :  $[\text{M} + \text{H}]^+$  calcd for C $_6$ H $_7$ N $_2$ O $_4$  171.0406; found 171.0401.

2-(5-methyl-2,4-dioxo-3,4-dihydropyrimidin-1(2H)-yl)acetic acid white solid.



$^1\text{H NMR}$  (300 MHz, DMSO- $d_6$ )  $\delta_{\text{H}}$ : 11.32 (s, 1H), 7.46 (d,  $J = 1.5$  Hz, 1H), 4.36 (s, 2H), 1.74 (d,  $J = 1.3$  Hz, 3H).  $^{13}\text{C NMR}$  (75 MHz, DMSO- $d_6$ )  $\delta$  169.52 (CO), 163.75 (CO), 150.96 (CO), 146.01 (CH), 100.81 (CO), 48.55 (CH $_2$ ), 39.4 (CH $_3$ ). HRMS (ESI-TOF)  $m/z$ :  $[\text{M} + \text{H}]^+$  calcd for C $_7$ H $_9$ N $_2$ O $_4$  185.0562 found 185.0562.

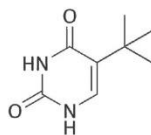
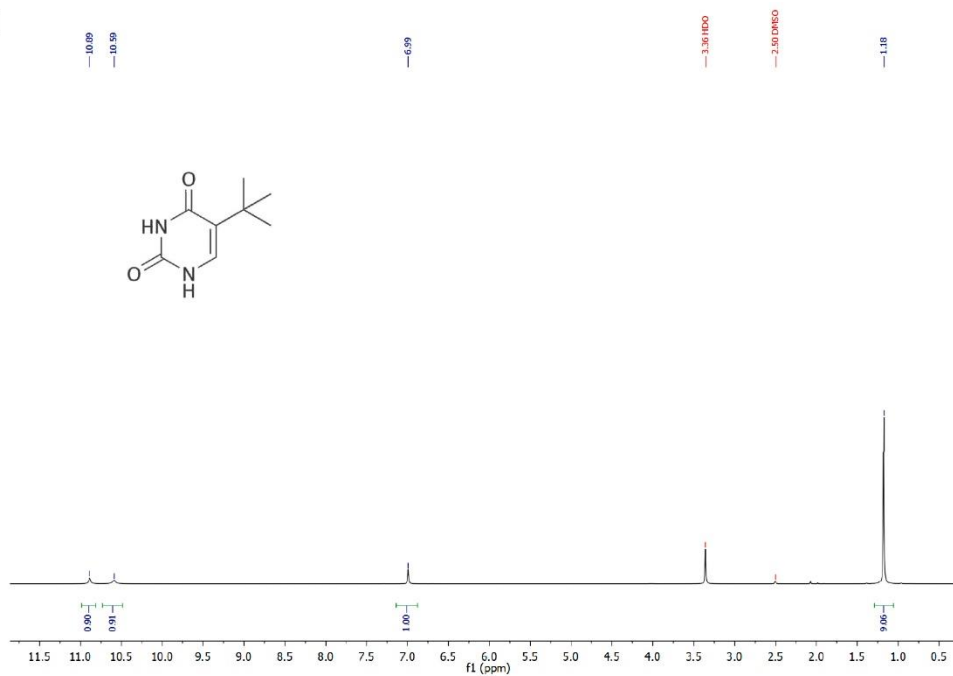
2-(5-(*tert*-butyl)-2,4-dioxo-3,4-dihydropyrimidin-1(2H)-yl)acetic acid white



solid.  $^1\text{H NMR}$  (300 MHz, DMSO- $d_6$ )  $\delta_{\text{H}}$ : 11.20 (s, 1H), 7.38 (s, 1H), 4.41 (s, 2H), 1.20 (s, 9H).  $^{13}\text{C NMR}$  (75 MHz, DMSO- $d_6$ )  $\delta$  169.65 (CO), 163.08 (CO), 150.66 (CO), 140.57 (CH), 119.93 (C), 48.70 (CH $_2$ ), 32.38 (C), 28.59 (3CH $_3$ ). HRMS (ESI-TOF)  $m/z$ :  $[\text{M} + \text{H}]^+$  calcd for C $_{10}$ H $_{15}$ N $_2$ O $_4$  227.1032 found 227.1030.

# Chapter 4

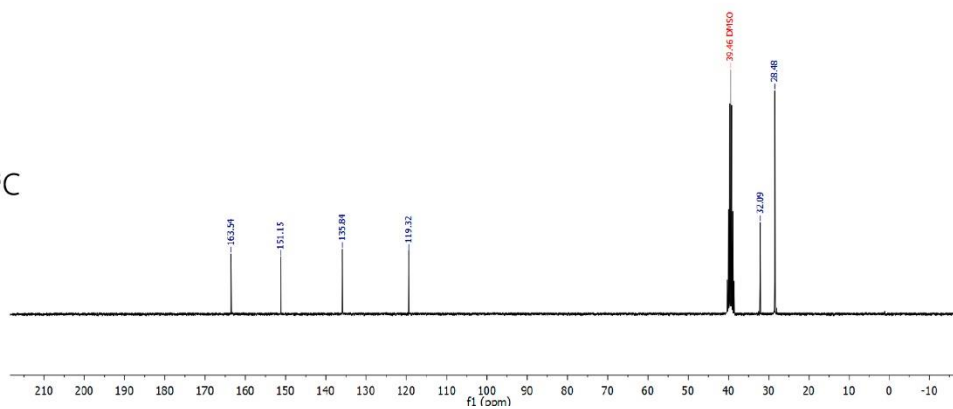
$^1\text{H}$

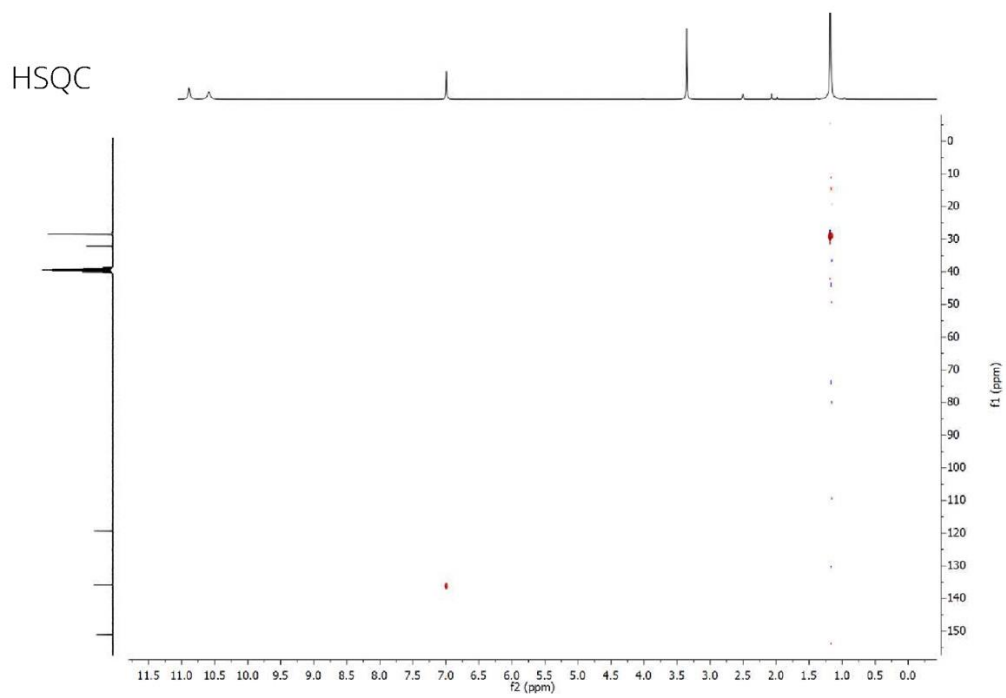


DEPT-135



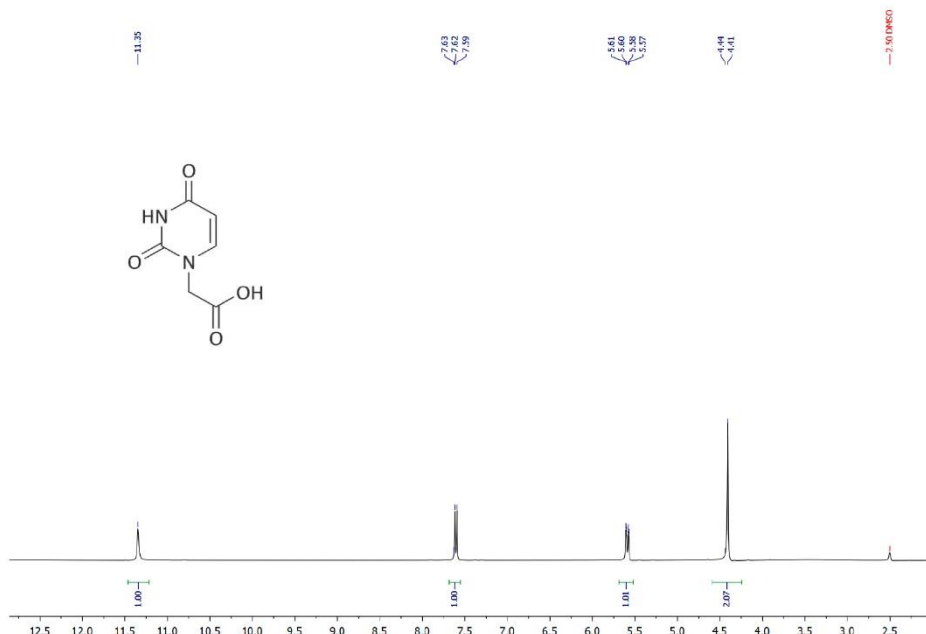
$^{13}\text{C}$



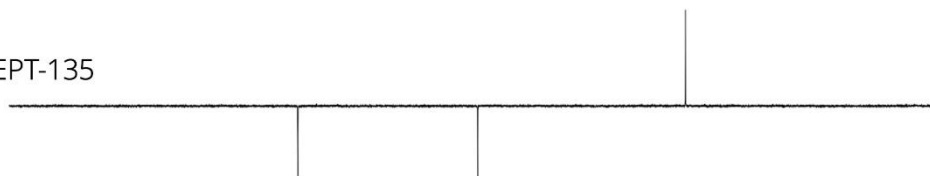


# Chapter 4

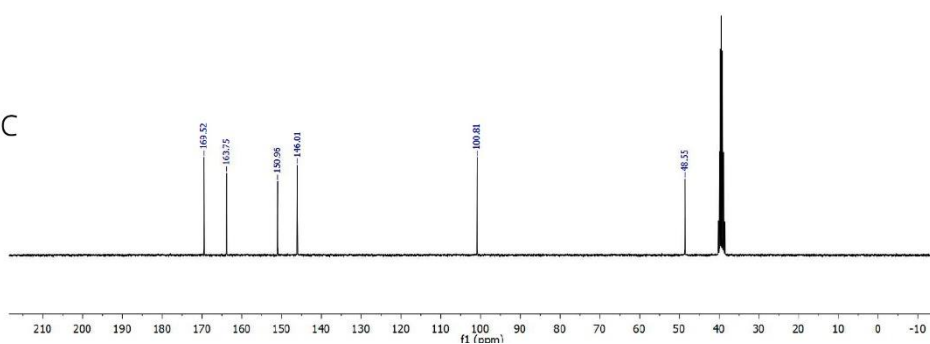
$^1\text{H}$

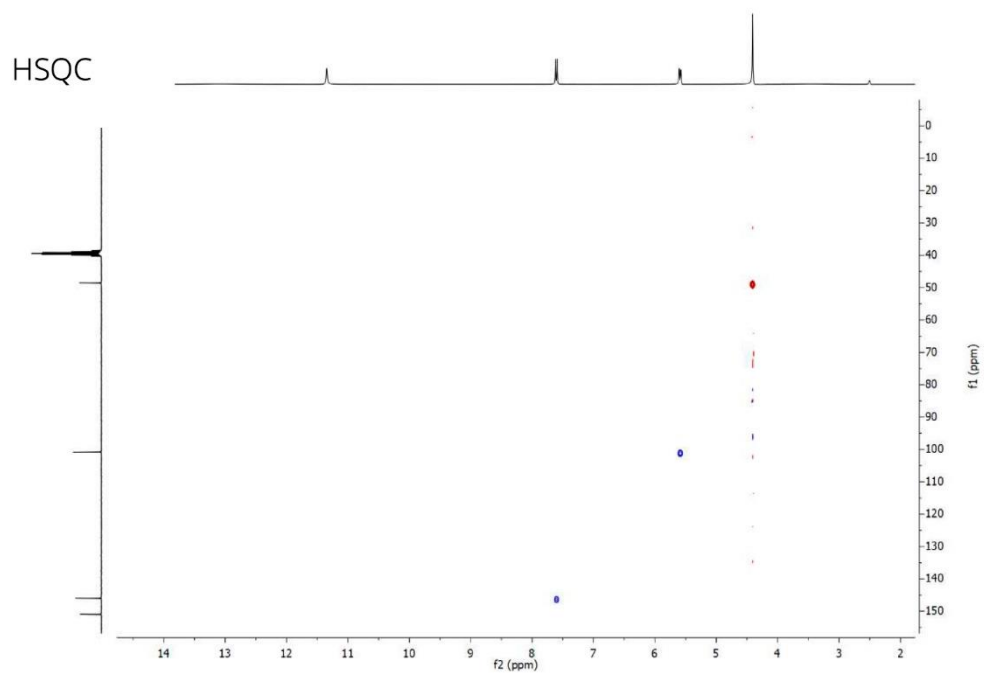


DEPT-135



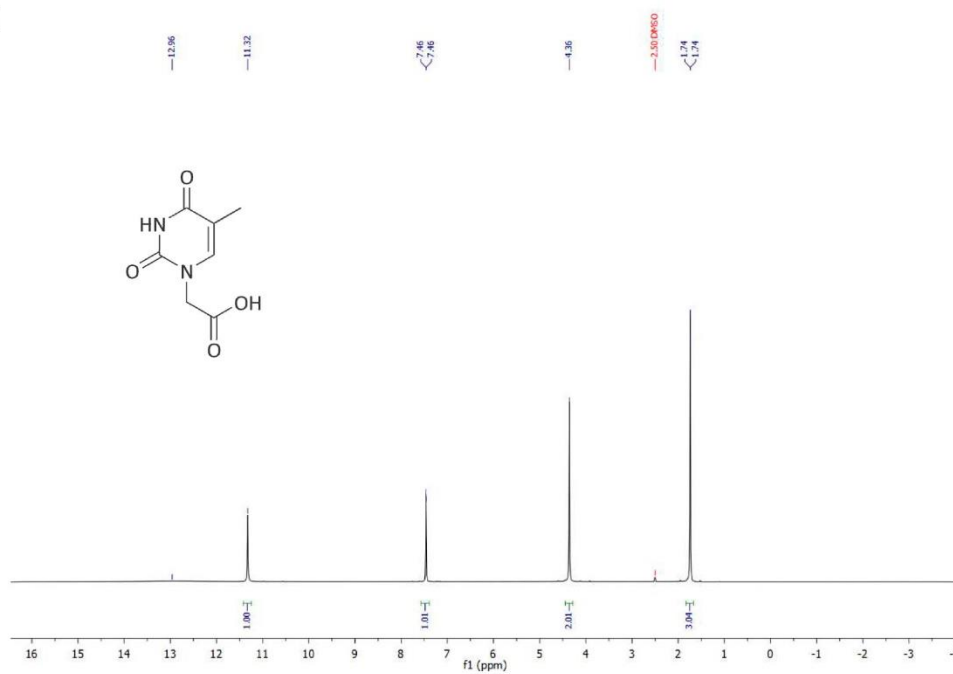
$^{13}\text{C}$



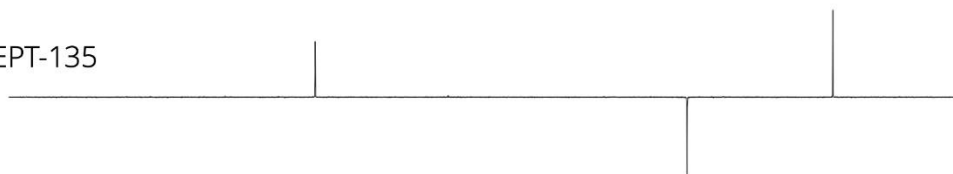


# Chapter 4

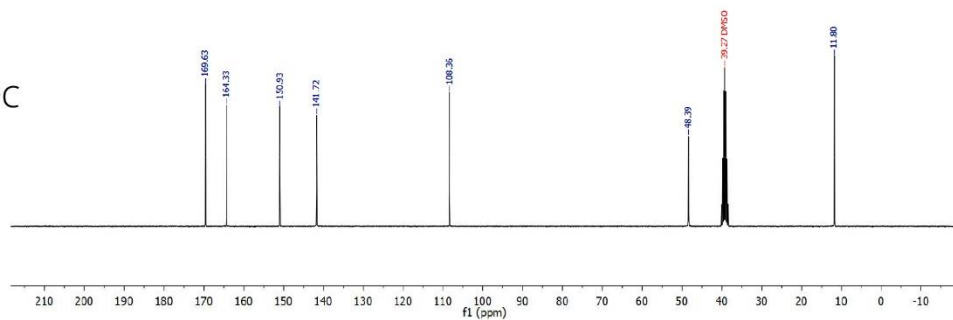
$^1\text{H}$

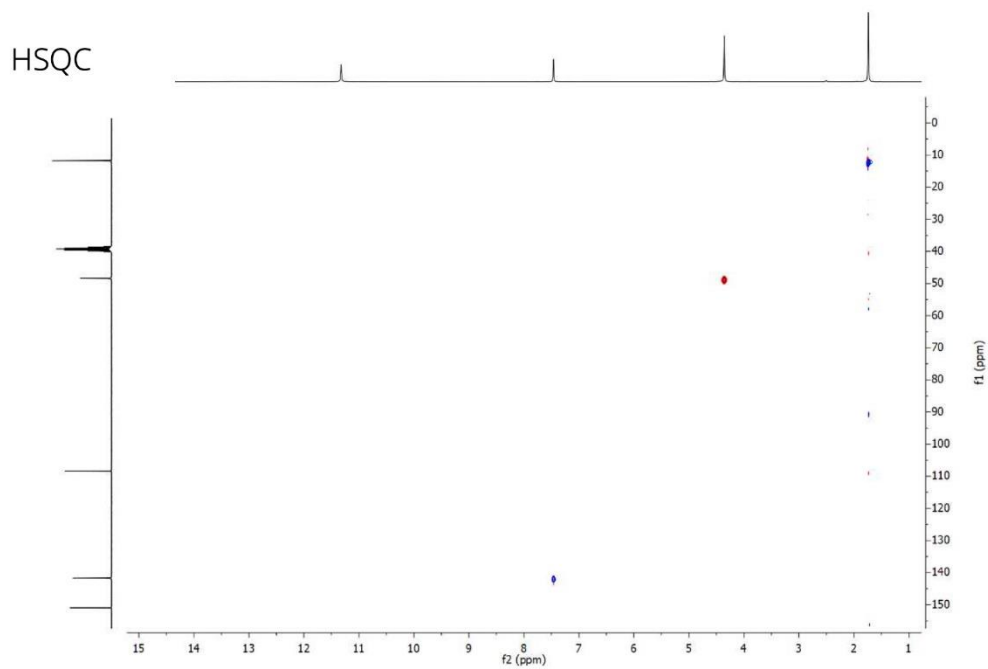


DEPT-135



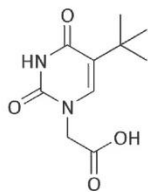
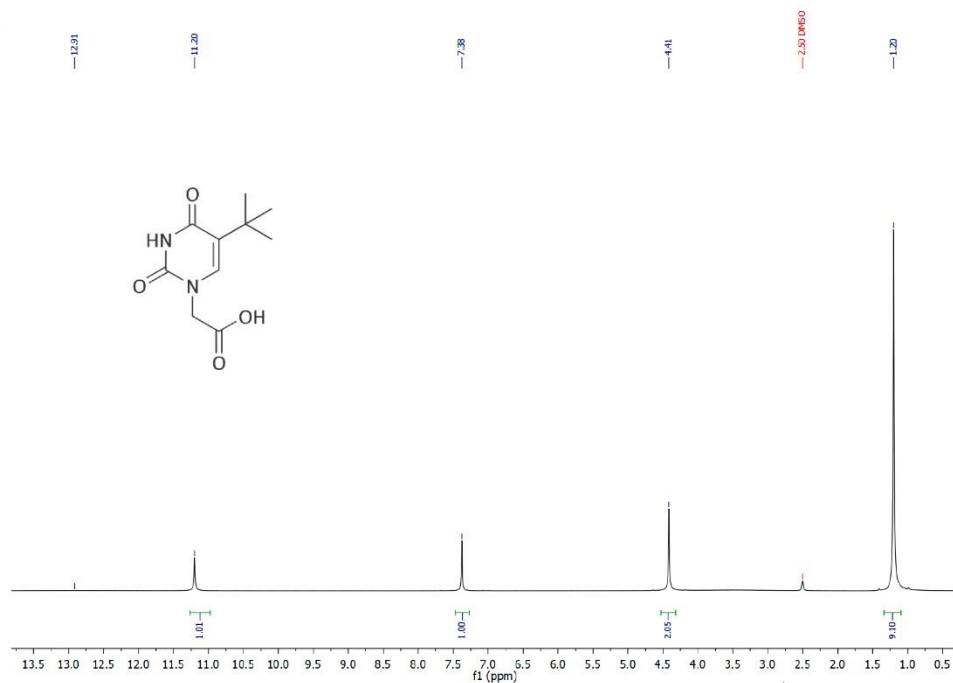
$^{13}\text{C}$



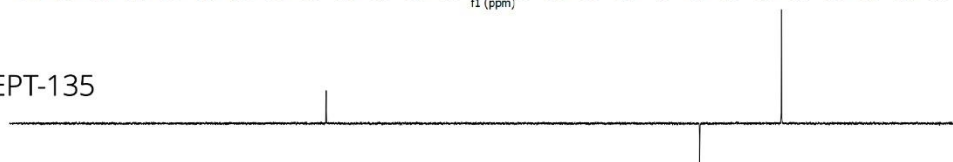


# Chapter 4

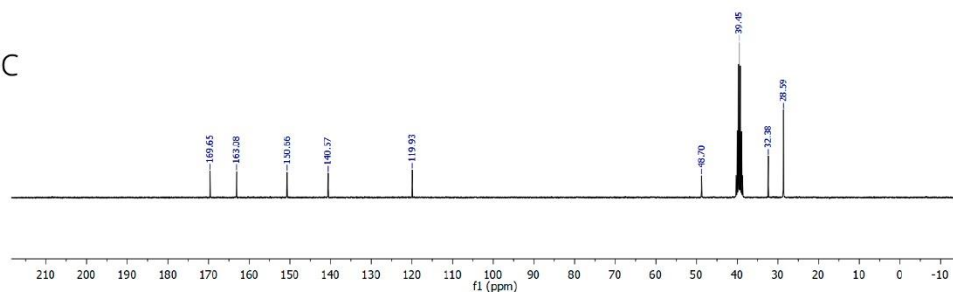
$^1\text{H}$

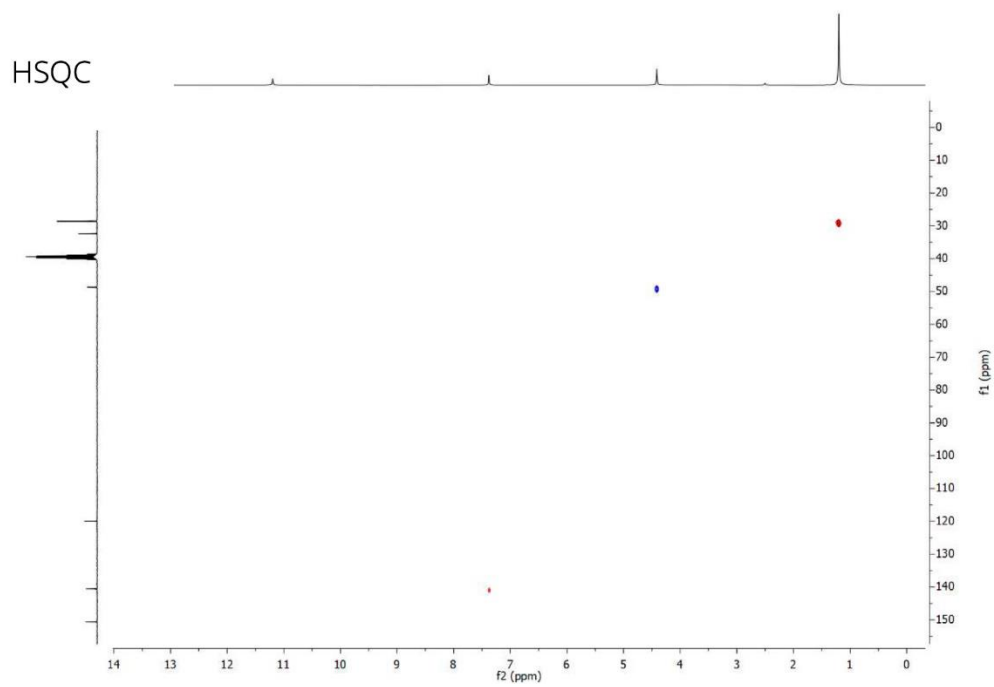


DEPT-135



$^{13}\text{C}$





## 4.6. References

- (1) Marrot, L.; Meunier, J.-R. Skin DNA Photodamage and its Biological Consequences. *J. Am. Acad. Dermatol.* **2008**, *58*, S139-S148.
- (2) Cadet, J.; Douki, T. Formation of UV-Induced DNA Damage Contributing to Skin Cancer Development. *Photochem. Photobiol. Sci.* **2018**, *17*, 1816-1841.
- (3) Mouret, S.; Baudouin, C.; Charveron, M.; Favier, A.; Cadet, J.; Douki, T. Cyclobutane Pyrimidine Dimers Are Predominant DNA Lesions in Whole Human Skin Exposed to UVA Radiation. *Proc. Natl. Acad. Sci. USA* **2006**, *103*, 13765-13770.
- (4) Nishigori, C. Current Concept of Photocarcinogenesis. *Photochem. Photobiol. Sci.* **2015**, *14*, 1713-1721.
- (5) Beukers, R.; Eker, A. P. M.; Lohman, P. H. M. 50 Years Thymine Dimer. *DNA Repair* **2008**, *7*, 530-543.
- (6) Lamola, A. A.; Mittal, J. P. Solution Photochemistry of Thymine and Uracil. *Science* **1966**, *154*, 1560-1561.
- (7) Noonan, F. P.; Zaidi, M. R.; Wolnicka-Glubisz, A.; Anver, M. R.; Bahn, J.; Wielgus, A.; Cadet, J.; Douki, T.; Mouret, S.; Tucker, M. A.; Popratiloff, A.; Merlino, G.; De Fabo, E. C. Melanoma Induction by Ultraviolet A but not Ultraviolet B Radiation Requires Melanin Pigment. *Nat. Commun.* **2012**, *3*, 1-10.
- (8) Cadet, J.; Mouret, S.; Ravanat, J.-L.; Douki, T. Photoinduced Damage to Cellular DNA: Direct and Photosensitized Reactions. *Photochem. Photobiol.* **2012**, *88*, 1048-1065.
- (9) Cuquerella, M. C.; Lhiaubet-Vallet, V.; Bosca, F.; Miranda, M. A. Photosensitized Pyrimidine Dimerisation in DNA. *Chem. Sci.* **2011**, *2*, 1219-1232.

(10) Cuquerella, M. C.; Lhiaubet-Vallet, V.; Cadet, J.; Miranda, M. A. Benzophenone Photosensitized DNA Damage. *Acc. Chem. Res.* **2012**, *45*, 1558-1570.

(11) Cadet, J.; Courdavault, S.; Ravanat, J. L.; Douki, T. UVB and UVA Radiation-Mediated Damage to Isolated and Cellular DNA. *Pure Appl. Chem.* **2005**, *77*, 947-961.

(12) Huix-Rotllant, M.; Dumont, E.; Ferré, N.; Monari, A. Photophysics of Acetophenone Interacting with DNA: Why the Road to Photosensitization is Open. *Photochem. Photobiol.* **2015**, *91*, 323-330.

(13) Liu, L.; Pilles, B. M.; Gontcharov, J.; Bucher, D. B.; Zinth, W. Quantum Yield of Cyclobutane Pyrimidine Dimer Formation Via the Triplet Channel Determined by Photosensitization. *J. Phys. Chem. B* **2016**, *120*, 292-298.

(14) Dumont, E.; Monari, A. Benzophenone and DNA: Evidence for a Double Insertion Mode and Its Spectral Signature. *J. Phys. Chem. Lett.* **2013**, *4*, 4119-4124.

(15) Liu, L.; Pilles, B. M.; Reiner, A. M.; Gontcharov, J.; Zinth, W. 2'-Methoxyacetophenone: an Efficient Photosensitizer for Cyclobutane Pyrimidine Dimer Formation. *ChemPhysChem* **2015**, *16*, 3483-3487.

(16) R. Alzueta, O.; Cuquerella, M. C.; Miranda, M. A. Transient UV-Vis Absorption Spectroscopic Characterisation of 2'-Methoxyacetophenone as a DNA Photosensitiser. *Spectrochim. Acta A Mol. Biomol. Spectrosc.* **2019**, *218*, 191-195.

(17) Antusch, L.; Gaß, N.; Wagenknecht, H.-A. Elucidation of the Dexter-Type Energy Transfer in DNA by Thymine-Thymine Dimer Formation Using Photosensitizers as Artificial Nucleosides. *Angew. Chem. Int. Ed.* **2017**, *56*, 1385-1389.

(18) Itahara, T. NMR and UV Study of 1,1'-( $\alpha,\omega$ -Alkanediyl)bis[thymine] and 1,1'-( $\alpha,\omega$ -Alkanediyl)bis[uracil]. *Bull. Chem. Soc. Jpn.* **1997**, *70*, 2239-2247.

---

(19) Leonard, N. J.; McCredie, R. S.; Logue, M. W.; Cundall, R. L. Synthetic Spectroscopic Models Related to Coenzymes and Base Pairs. XI. Solid State Ultraviolet Irradiation Of 1,1'-Trimethylenebisthymine and Photosensitized Irradiation of 1,1'-Polymethylenebisthymines. *J. Am. Chem. Soc.* **1973**, *95*, 2320-2324.

(20) Sandros, K. Transfer of Triplet State Energy in Fluid Solutions III. Reversible Energy Transfer. *Acta Chem. Scand.* **1964**, *18*, 2355-2374.

(21) Vendrell-Criado, V.; Lhiaubet-Vallet, V.; Yamaji, M.; Cuquerella, M. C.; Miranda, M. A. Blocking Cyclobutane Pyrimidine Dimer Formation by Steric Hindrance. *Org. Biomol. Chem.* **2016**, *14*, 4110-4115.

(22) Vendrell-Criado, V.; Rodríguez-Muñiz, G. M.; Yamaji, M.; Lhiaubet-Vallet, V.; Cuquerella, M. C.; Miranda, M. A. Two-Photon Chemistry from Upper Triplet States of Thymine. *J. Am. Chem. Soc.* **2013**, *135*, 16714-16719.

(23) Basnak, I.; Balkan, A.; Coe, P. L.; Walker, R. T. The Synthesis of Some 5-Substituted and 5,6-Disubstituted 2'-Deoxyuridines. *Nucleosides & Nucleotides* **1994**, *13*, 177-196.

CHAPTER **5**

Chapter 5. Photosensitised Biphotonic  
Chemistry of Pyrimidine Derivatives

---



## 5.1. Introduction

It is well known that direct solar (or lamp) UV irradiation of pyrimidine bases (Pyr) results in the formation of Pyr dimers as the most abundant lesions. In addition, the use of lasers in surgery, therapy, dermatology, immunology and a variety of medical or aesthetic treatments is steadily increasing over the years. However, the effects of high intensity direct irradiation on DNA has been scarcely investigated.<sup>1-10</sup> Typically, a UVC laser (248 or 266 nm) is used as excitation source leading to biphotonic processes. In general, the photolesions found after high intensity UVC irradiation arise from photoionisation, since the ionisation potential (IP) of the bases is by far exceeded under these experimental conditions (for example 2 x 266 nm photons equals 9.4 eV, whereas the IP of Pyr bases is around 9 eV). Therefore, formation of oxidised bases and guanine-thymine cross-links through the transient generation of highly reactive base radical cations has been observed in both isolated and cellular DNA as endpoints.<sup>11,12</sup>

In this context, the aim of this Chapter is to study the processes where a first photon generates an initial transient that in turn absorbs a second photon giving rise to a more energetic species from which new reactions can occur. It is important to note that these are two consecutive steps and that the initially produced transients act as real chemical entities in spite of their ultrashort lifetimes (in the order of ps for  $S_1$  and in the  $\mu$ s timescale for  $T_1$ ). Biphotonic photosensitisation of DNA remains practically unexplored, with the exception of a few oxidations mediated by dyes through the generation of reactive oxygen species, such as hydroxyl radical.<sup>5,13-15</sup>

Photosensitised Pyr biphotonic chemistry has been addressed by our research group following a different approach,<sup>16</sup> in which an upper triplet excited state ( $T_n$ ) of benzophenone (BP)<sup>17,18</sup> is populated upon its selective

irradiation using the third harmonic of a Nd-YAG laser (355 nm). In this approach, the first step is biphotonic and proceeds through excitation of the sensitiser to the singlet BP  $S_1$ , followed by intersystem crossing (ISC); a second excitation of the resulting BP  $T_1$  leads to BP  $T_n$ . This allows for a *triplet-triplet energy transfer* from BP  $T_n$  to Pyr  $T_2(n\pi^*)$ .<sup>19,20</sup> Experimentally, since  $T_n$  are ultrashort-lived entities, it is mandatory to locate the triplet donor (BP) and the acceptor (a Pyr chromophore) spatially close to each other by synthesising a dyad to circumvent the relatively slow diffusion step. The concept was proven by the Norrish-Yang photoreaction of a *tert*-butyluracil (**tBU**), a modified Pyr base with an abstractable H in  $\gamma$  position with respect to the carbonyl moiety.

Thus, in this Chapter, a more general photoexcitation scheme has been proposed to investigate biphotonic DNA photosensitisation, which does not require the synthetic effort associated with linked dyads and would allow for a large structural variability in the systems to be challenged. This approach involves absorption of a first photon by an adequate sensitiser followed by triplet energy transfer to a Pyr unit. Subsequently, a second photon would be absorbed by the resulting Pyr  $T_1$  giving rise to Pyr  $T_2$ , from which new chemistry would ensue (Figure 5.1). Here, as the  $T_1$  of the sensitiser is long lived, it does not have to be covalently linked to the Pyr unit.

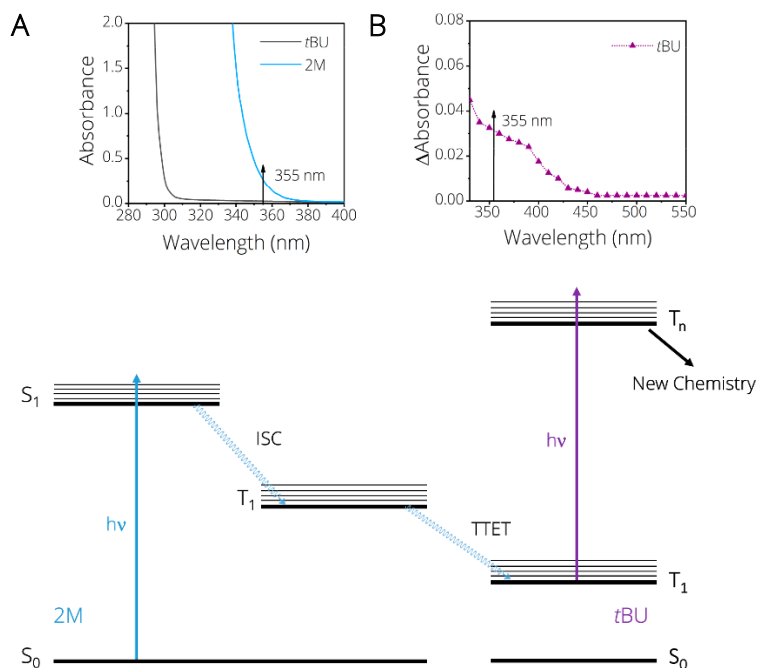
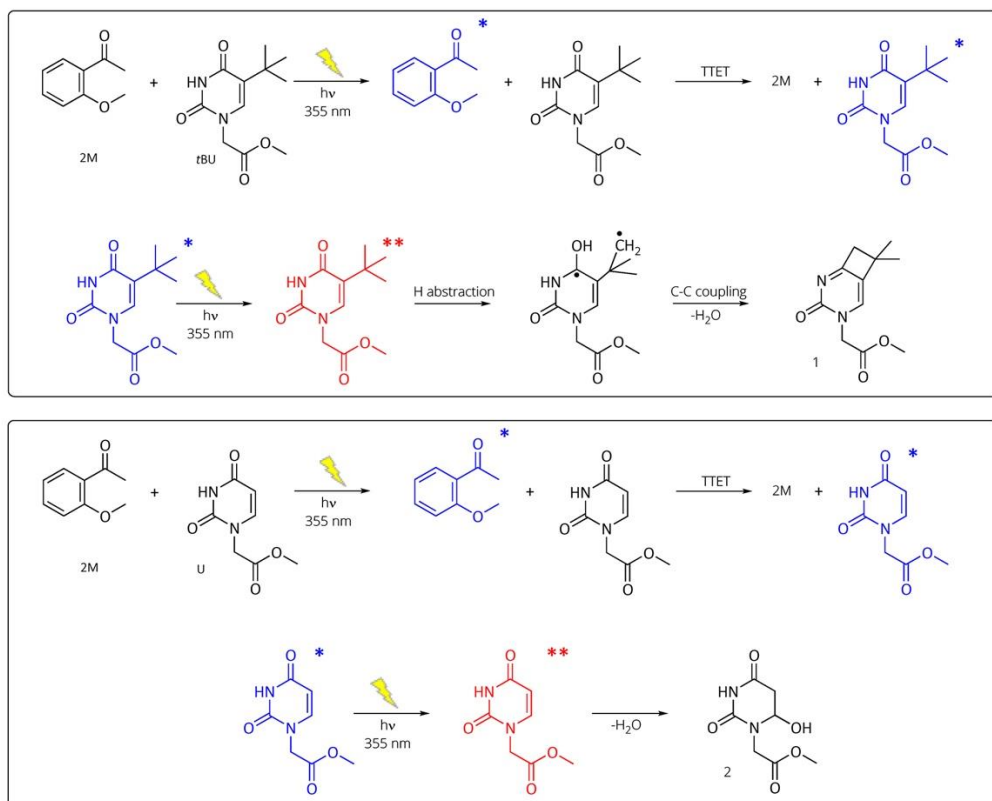


Figure 5.1 Biphotonic **2M**-photosensitised intermolecular strategy to generate **tBU** upper triplet excited state. A) UV-Vis spectra of **2M** (blue) and **tBU** (black) at irradiation conditions (0.3 abs at 355 nm under  $N_2$  in 10 mm quartz cuvettes). B) **tBU** triplet excited state absorption spectrum.

In order to check the feasibility of the proposed strategy, two model reactions have been chosen (Scheme 5.1): a) the Norrish-Yang photoreaction of **tBU** as a prototype of Pyr photoreactions occurring through a  $n\pi^*$  triplet excited state and b) the photohydration of its analogue **U**, lacking the *tert*-butyl substituent, in connection with photonucleophilic additions to nucleobases. The former could be involved in the Paternò-Büchi photoreaction leading to 6,4 photoproducts whereas the latter might be relevant to the formation of nucleic acid-protein cross-links.



Scheme 5.1 Biphotonic photoreaction of the **2M** + **tBU** or **U** systems leading to the Norrish-Yang photoproduct **1** (up) and the hydrated uracil **2** (down).

In both cases, 2'-methoxyacetophenone (**2M**) has been chosen as photosensitiser since it allows for selective excitation in the presence of nucleobases and presents a  $\Phi_{\text{ISC}}$  *ca.* 1.<sup>21,22</sup> In addition, **2M** minimises side reactions like H abstraction and Paternò-Büchi cycloadditions, in contrast with the paradigmatic benzophenone (BP). For comparison, BP and the related compound fenofibrate (FB), have also been included in the study.

## 5.2. Results and Discussion

The normalised UV absorption spectra of **2M**, BP and FB are shown in Figure 5.2, whereas the spectra under the employed experimental conditions are displayed in the inset.

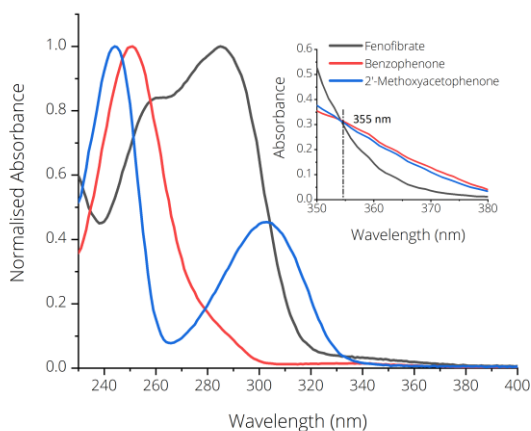


Figure 5.2 UV spectra of photosensitisers: fenofibrate (black), benzophenone (red) and 2'-methoxyacetophenone (blue). Inset) UV spectra of the mentioned photosensitisers at the biphotonic irradiation concentration, with 0.3 absorbance at 355 nm.

Irradiation of **2M** in the presence of **tBU** was performed using the third harmonic of a Nd-YAG laser (355 nm, 10 Hz) operating at 45 mJ/pulse, and the photomixtures were analysed by UPLC coupled with tandem mass spectrometry. Selected ion monitoring revealed the presence of a compound with molecular ion  $MH^+$  at  $m/z$  value of 223.1073 corresponding to the formula  $C_{11}H_{15}N_2O_3$  (Figure 5.3A). It was safely assigned to the Norrish-Yang photoproduct (**1**, Scheme 5.1) by comparison of its retention time and fragmentation pattern with those of an authentic sample independently synthesised in our lab.<sup>16,23</sup> The conversion was intentionally kept very low to

minimise secondary photolysis of **1**. From the calibration with known amounts of compounds, an upper yield for **1** of *ca.* 1% was estimated. The amount of photoproduct formed increased with increasing irradiation times (Figure 5.3 B). Remarkably, when the experiment was performed in the absence of the photosensitiser, compound **1** was hardly detected (Figure 5.3 B). Likewise, no reaction was observed in the presence of **2M** using as light source a Xe lamp equipped with a monochromator to ensure selective irradiation at 355 nm. Equivalent photon fluxes were secured in this control experiment as detailed in the experimental section.

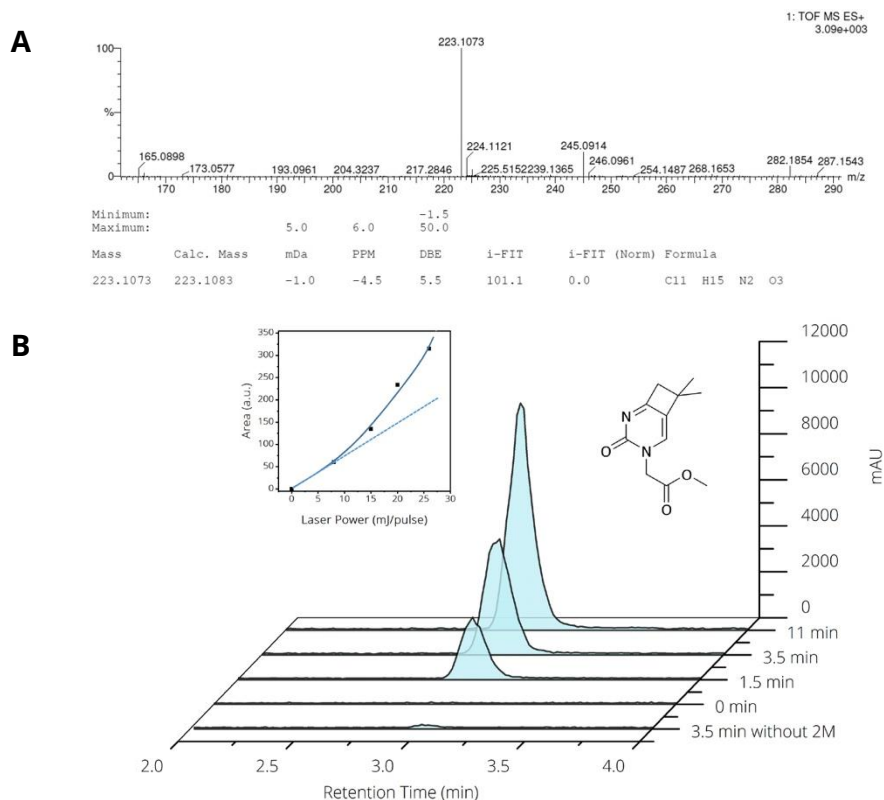


Figure 5.3 A) Mass spectra of photoinduced product **1**. B) Chromatograms registered after injection of the photolysates obtained upon two-photon irradiation of **2M**

in the presence of **tBU**. Selected ion monitoring at 223.1073 [M+H]<sup>+</sup>. Inset) plot of the amount of **1** versus the employed laser power.

When the **2M** photosensitised reaction was done at different laser energies, a clear upward curvature was observed in the formation of product **1** (Figure 5.3 B, inset); by contrast, a linear plot would have been obtained for a monophotonic process. This is clearly in agreement with the occurrence of the Norrish-Yang photoreaction through a two-photon sensitisation process under the employed experimental conditions. Replacing **2M** with BP or FB led to similar results; however, the reaction yields were markedly lower (Figure 5.4). This is probably due to the occurrence of side reactions with BP and FB, such as the Paternò-Büchi photocycloaddition between their carbonyl groups and the Pyr C5-C6 double bond.<sup>24</sup>

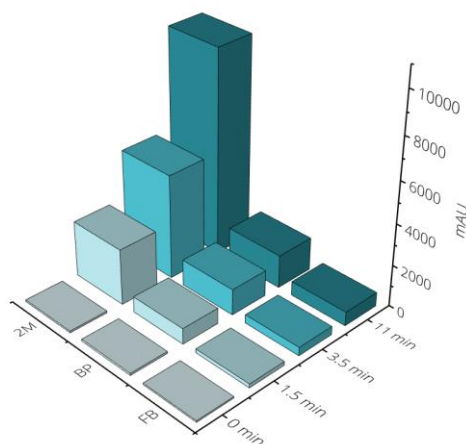


Figure 5.4 Relative amounts of Norrish-Yang photoproduct obtained after two-photon sensitisation of **tBU** with **2M**, BP or FB at increasing irradiation times (0-11 min).

Biphotonic photosensitisation of the unsubstituted uracil chromophore was also investigated. Analysis of the photolysates obtained from **U** by means of UPLC-MS/MS revealed the appearance of a photoproduct whose

concentration increased with irradiation time (Figure 5.5). This product was identified as a 6-hydroxy-5,6-dihydrouracil (**2**, Scheme 5.1), formally arising from photohydration of the nucleobase. Its structure was safely assigned by comparison with a true sample obtained through an alternative synthesis (see in the experimental section). To further secure that formation of **2** occurs through a biphotonic sensitised process, control experiments were performed where irradiation was carried out in the absence of **2M** or using a Xe lamp coupled with a monochromator ( $\lambda_{\text{exc}} = 355 \text{ nm}$ ) as light source. In both cases, no production of **2** was observed.

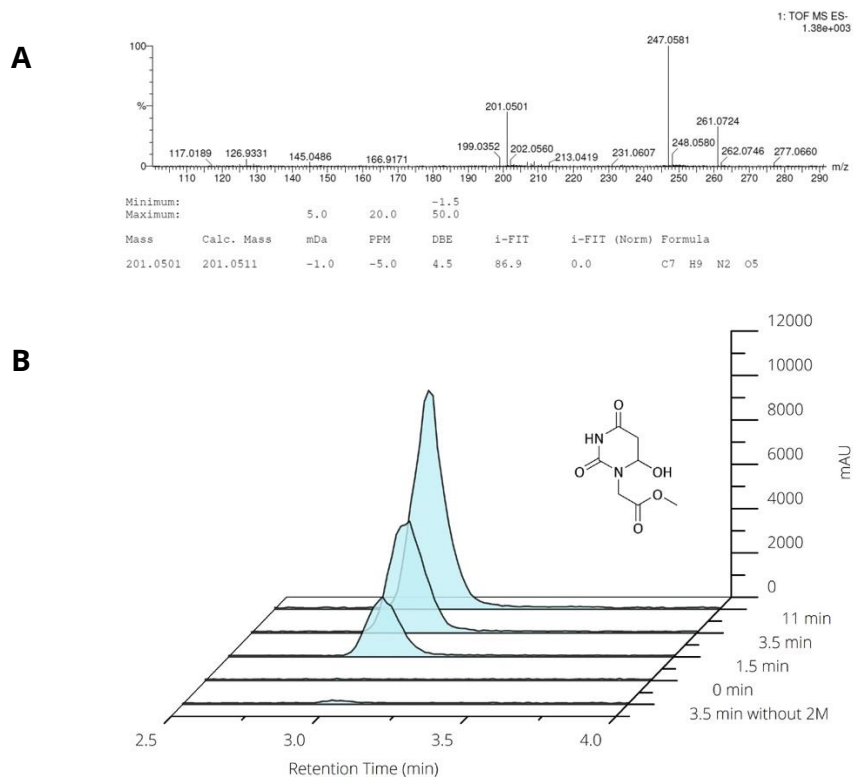


Figure 5.5 A) Mass spectra of photoinduced product **2**. B) Chromatograms registered after injection of the photolysates obtained upon two-photon irradiation of **2M** in the presence of **U**. Selected ion monitoring at 201.0501 [M-H].

Interestingly, photohydration of Pyr bases has been the first identified photoreaction of nucleic acid components in aqueous solutions.<sup>25-27</sup> At this point, it is important to note that ionisation of a Pyr base can not be achieved along two-photon 355 nm laser irradiation, and thus formation of radical cation  $U^{\bullet+}$  can be ruled out as the origin of **2**.

Actually, the IP of Pyr bases is around 9 eV<sup>5</sup> far higher than that reachable by two 355 nm pulses ( $2 \times 3.5$  eV, Figure 5.6). Moreover,  $U^{\bullet+}$  in aerated aqueous solutions would lead to the predominant formation of 5,6-dihydroxy-5,6-dihydrouracil.

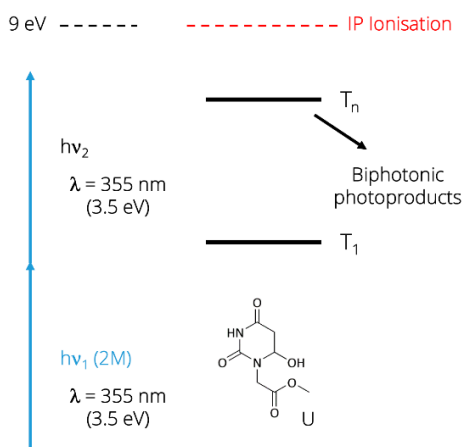
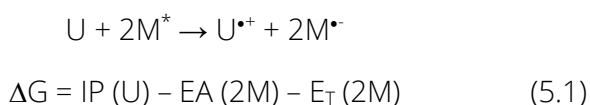


Figure 5.6 Schematic energy diagram showing the key excited states involved in biphotonic photo reaction in our design.

The possibility of an electron transfer between **U** and the excited photosensitiser has also been considered by estimating the free energy changes, based on the IP, electron affinity (EA) and triplet energy ( $E_T$ ) values as in Equation 5.1



Thus, taking IP (**U**) as 9.6 eV,<sup>28</sup> EA (**2M**) as 0.33 eV<sup>29</sup> and  $E_T(\mathbf{2M})$  as *ca* 3.3 eV,<sup>30</sup>  $\Delta G$  results to be clearly positive. This is not compatible with the feasibility of an electron transfer reaction.

Hence, the triplet biphotonic activation remains as the only plausible photohydration pathway explaining formation of **2**. The process can occur directly from the  $T_n$  or, after intersystem crossing, from the  $S_1$  excited state.<sup>31,32</sup> In fact,  $T_2$  in Pyr bases is nearly isoenergetic with  $S_1$  and lies *ca.* 1 eV above  $T_1$ . This energy gap makes internal conversion in the triplet cascade slow enough to allow other physical or chemical processes to compete.

### 5.3. Conclusions

A new strategy has been developed for biphotonic DNA photosensitisation, which involves absorption of a first 355 nm photon by a sensitiser, followed by triplet energy transfer to a Pyr derivative and absorption of a second 355 nm photon by the resulting Pyr triplet excited state. The feasibility of the concept has been demonstrated by means of two model reactions, namely the Norrish-Yang photocyclisation of a *t*-butyluracil and the photohydration of its parent uracil analogue. Due to the intermolecular nature of this approach, it could in principle allow for a large structural variability in the systems to be challenged.

### 5.4. Experimental Section

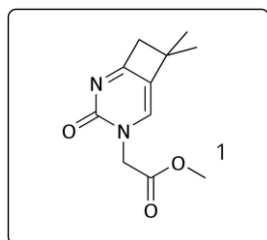
#### 5.4.1. Synthesis and Characterisation

Compounds 5-*tert*-butyl uracil was prepared according to literature procedures (see Chapter 4, Annex 4.5).<sup>16,23</sup> Compounds **1** and **2** were obtained by preparative steady-state direct irradiation of **tBU** and **U**, respectively. A Luzchem photoreactor (see Section 6.2.2) was employed with

lamps emitting light centred at 254 nm (LZC-UVC, 8 Watt) during 6 h, and being the samples located at 18 cm from them.

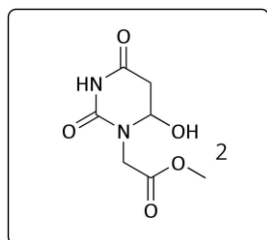
Solutions of **tBU** (79 mg, 0.33 mmol) and **U** (60 mg, 0.33 mmol) in 360 mL of acetonitrile or deionised water were boiled to favour the dissolution and then cooled while bubbling N<sub>2</sub> in quartz flasks. Reactions were monitored by UV-Vis spectrometry (see Section 6.2.1). In the case of **tBU** irradiation, when the band with a  $\lambda_{\text{max}}$  at 355 nm, corresponding to the pyrimidone chromophore, reached its maximum of absorbance, the irradiated solution was evaporated under vacuum. The same procedure was followed for **U** irradiation, but monitoring the disappearance of its main band at 260 nm. The solid residues from both reactions were purified by column chromatography on silica gel, using cyclohexane: ethyl acetate 1:1 as eluents (see Section 6.1.2.1).

**Compound 1 (Norrish-Yang photoproduct).** <sup>1</sup>H NMR (300 MHz, CDCl<sub>3</sub>, 300K)



$\delta_{\text{H}}$  7.12 (s, 1H), 4.52 (s, 2H), 3.75 (s, 3H), 3.14 (s, 2H), 1.45 ppm (s, 6H). <sup>13</sup>C NMR (75 MHz, CDCl<sub>3</sub>)  $\delta$  181.76 (CO), 167.13 (C), 156.84 (CO), 136.42 (CH), 128.43 (C), 51.71 (CH<sub>3</sub>), 51.09 (CH<sub>2</sub>), 49.89 (CH<sub>2</sub>), 40.54 (C), 26.04 ppm (2CH<sub>3</sub>). HRMS (ESI-TOF) :m/z calcd for C<sub>11</sub>H<sub>15</sub>N<sub>2</sub>O<sub>3</sub> [M+H]<sup>+</sup> 223.1083, found 223.1073.

**Compound 2 (Hydrated uracil).** <sup>1</sup>H NMR (300 MHz, Methanol-*d*<sub>4</sub>, 300K)  $\delta_{\text{H}}$  5.12

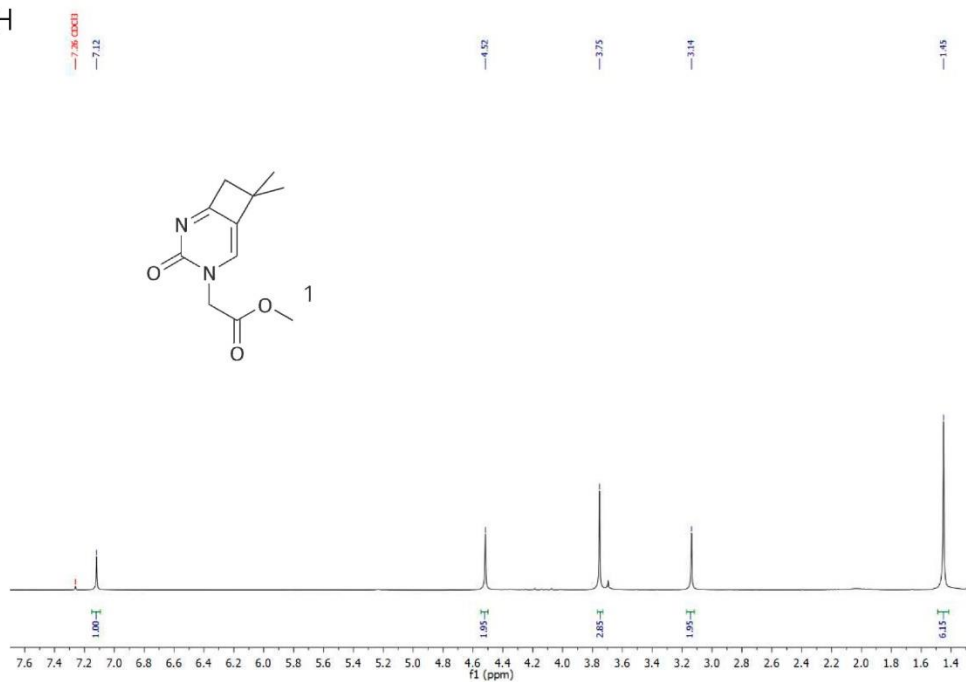


(dd, *J* = 4.4, 2.4 Hz, 1H), 4.44 (d, *J* = 17.7 Hz, 1H), 4.09 (d, *J* = 17.7 Hz, 1H), 3.77 (s, 3H), 3.36 (s, 1H), 3.04 (dd, *J* = 16.7, 4.4 Hz, 1H), 2.66 (dd, *J* = 16.7, 2.4 Hz, 1H). <sup>13</sup>C NMR (300 MHz, Methanol-*d*<sub>4</sub>, 300K)  $\delta$  171.84 (CO), 171.42(CO), 154.28(CO), 78.97(CH), 52.90(CH<sub>3</sub>), 47.88(CH<sub>2</sub>), 39.94(CH<sub>2</sub>). HRMS (ESI-TOF) :m/z calcd for

C<sub>7</sub>H<sub>9</sub>N<sub>2</sub>O<sub>5</sub> [M-H]<sup>-</sup> 201.0511, found 201.0501.

# Chapter 5

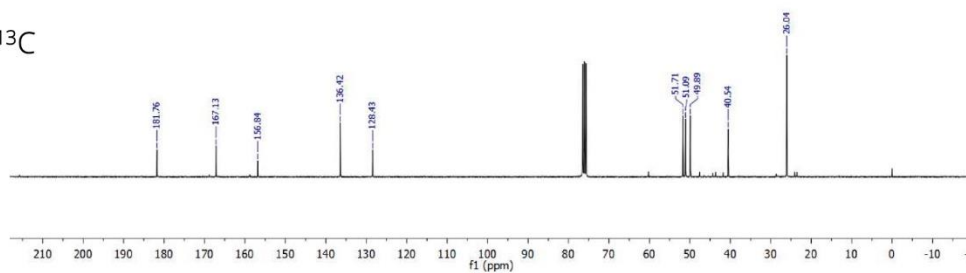
$^1\text{H}$

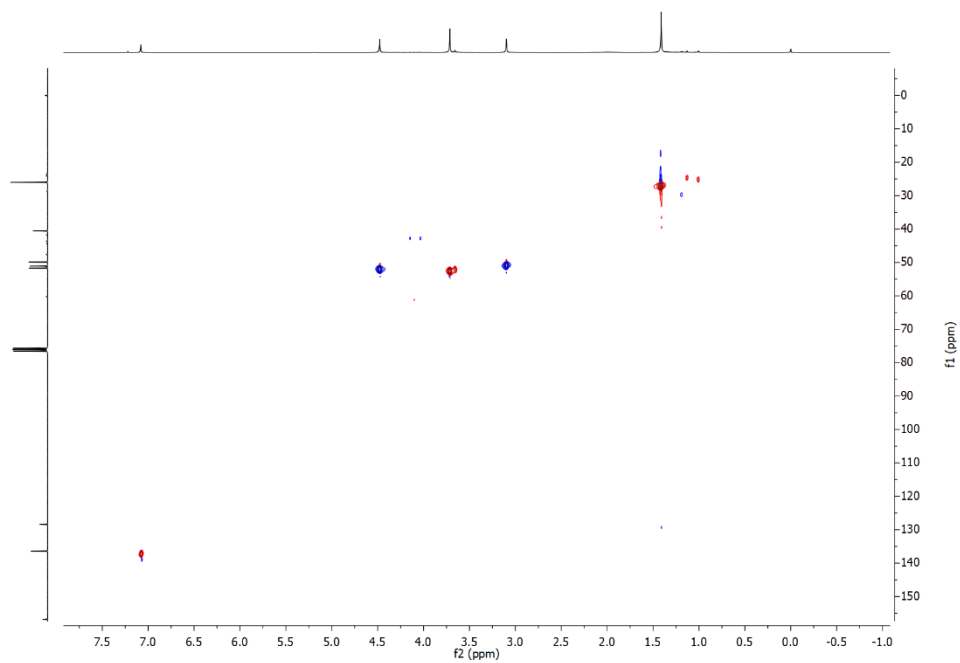


DEPT-135



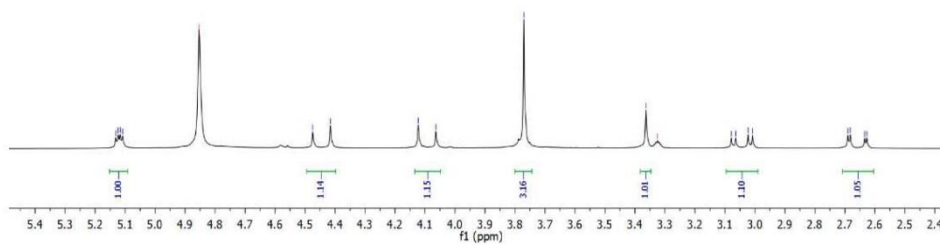
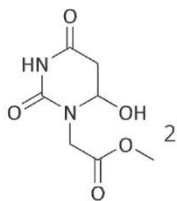
$^{13}\text{C}$





# Chapter 5

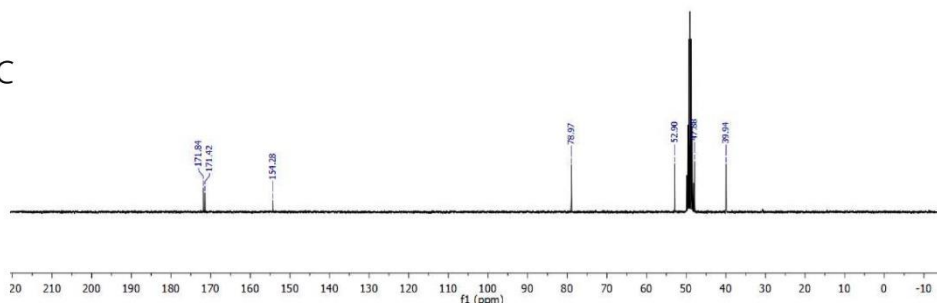
$^1\text{H}$

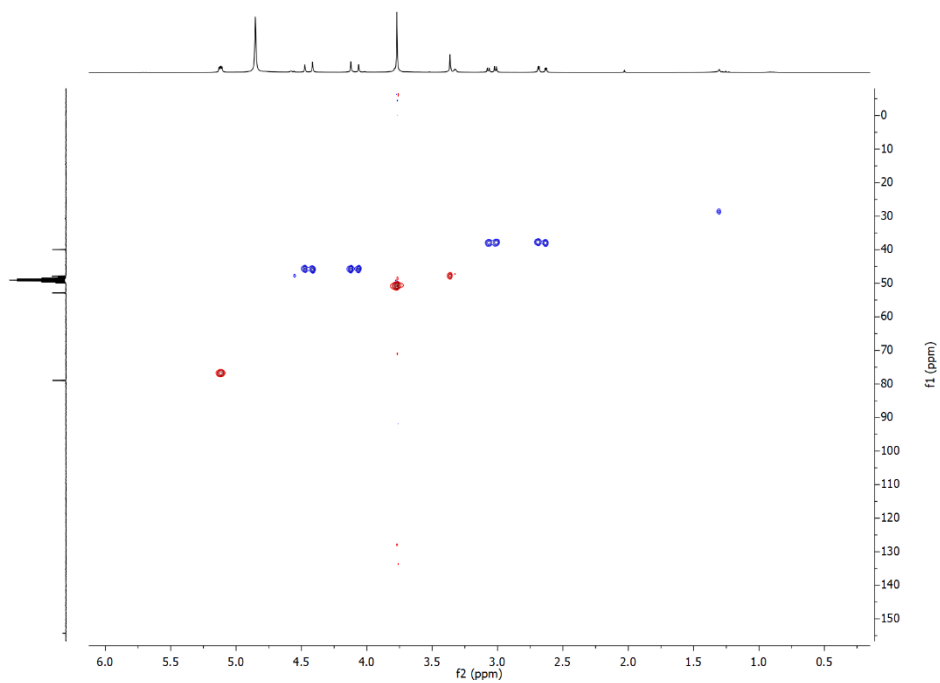


DEPT-135



$^{13}\text{C}$





## 5.4.2. Irradiation Procedures and Spectral Measurements

### 5.4.2.1. High Energy Photosensitised Irradiations

Biphotonic irradiations were performed using a Nd: YAG laser exciting at 355 nm with high energy pulses (see Section 6.2.2). Samples containing **tBU** and **U**, with a photosensitiser's absorbance of 0.2 at 355 nm were prepared using respectively acetonitrile and deionised water as solvents and bubbled with N<sub>2</sub>, prior to irradiation in quartz cuvettes.

In the case of **tBU** samples, photosensitisers' solutions (**2M**, **FB** and **BP** with an absorbance of 0.2 at 355 nm), were prepared using acetonitrile. Then, to 10 mL of each solution 64 mg (0.27 mmol) of **tBU** were added.

Similarly, **U** solution in **2M** solutions with an absorbance of 0.3 at 355 nm were prepared using deionised water. To 5 mL of the solution 21.7 mg (0.13 mmol) of **U** were added.

### 5.4.2.2. Control experiment: Irradiation in the absence of photosensitiser

A control experiment under equal experimental conditions was run, irradiating the same **tBU** and **U** concentration samples in acetonitrile and deionised water without photosensitiser. The irradiation times were 0, 1.5, 3.5 and 11 min, and the photomixtures were submitted to UPLC-MS/MS analysis (see Section 6.1.2.2) to establish **1** and **2** formation. This was accomplished by comparison of its retention time and fragmentation pattern with authentic samples of **1** and **2** independently synthesised.

### 5.4.2.3. Steady-State Monochromatic Irradiations

A Xenon lamp equipped with a monochromator (see Section 6.2.2) was used to irradiate solutions containing **tBU** and **U** in **2M** solutions (0.3 absorbance at 355 nm) at 355 nm. They were prepared in acetonitrile (for **tBU** mixtures) and deionised water (for **U** mixtures), in the same proportion as in the ones used in high energy photosensitised irradiations, and purged with N<sub>2</sub>, prior to irradiation in quartz cuvettes during 25 min. Photomixtures were submitted to UPLC-MS/MS analysis (see Section 6.1.2.2) to establish 1 and 2.

### 5.4.2.4. Securing equivalent photon fluxes in the laser and Xe-lamp irradiation

Equivalent photon fluxes must be secured for both laser and Xe-lamp irradiations, in order to make meaningful comparisons. To achieve this goal, **2M** photosensitisation of the thymine model (**Thy-C<sub>3</sub>-Thy**) previously studied in this Thesis, yielding thymine cyclobutane dimers has been chosen as reaction model (Figure 5.7).

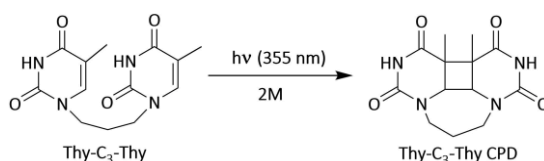


Figure 5.7 2M photosensitised cyclobutane thymine dimerisation.

Thus, a solution containing 0.04 mM of both, **2M** and **Thy-C<sub>3</sub>-Thy** in PB 10 Mm was prepared. Then two aliquots (2 mL) of this solution were treated separately. One of them was irradiated with the laser beam (Nd/YAG at 355nm, see Section 6.2.2) during 1.5 min, and its UV spectrum absorbance registered. The other one was irradiated with the Xe-lamp equipped with a

monochromator (see Section 6.2.2), and the progress of the reaction periodically monitors by UV spectroscopy (see Section 6.2.1). The results are shown in Figure 5.8.

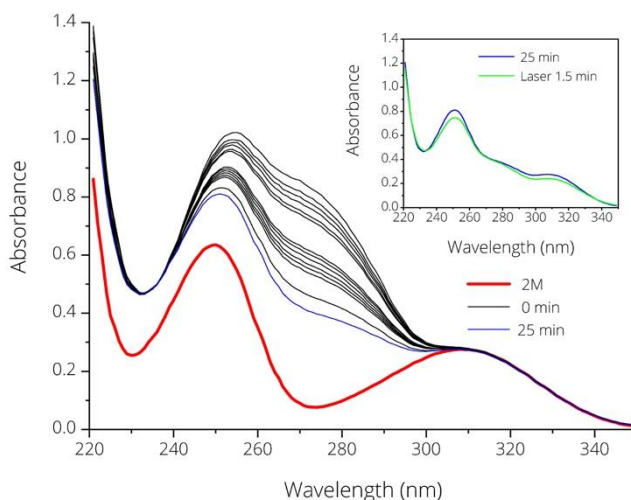


Figure 5.8 Xe lamp irradiation of a solution containing equimolar quantities of **2M** and **Thy-C<sub>3</sub>-Thy** (0.04 mM) in PB 10 mM, monitored by UV spectroscopy. Inset) Comparison of the UV spectra of the sample irradiated with 355 nm laser light (1.5 min) with the 25 min Xe lamp irradiation. Under these conditions, the absorbance of the samples was 0.01 at 355 nm.

### 5.4.3. Spectral Measurements

Analysis of the irradiation of **tBU** and **U** in the presence or in the absence of **2M** was achieved under the same ESI conditions (see Section 6.1.2.2). However, in this case of the **tBU** photolysates, an isocratic elution was performed using 70% water and 30% methanol (both containing 0.01% formic acid) as the mobile phase during the first 10 min followed by a gradient to reach 100% of methanol at 15 min. For the **U** containing mixtures, the isocratic elution was performed using 95% water and 5% acetonitrile (both containing 0.01% formic acid) as the mobile phase during the first 10

---

min followed by a gradient to reach 100% of acetonitrile at 15 min. In both cases, the flow was maintained at 0.3 mL/min, and the injection volume were 3 and 10  $\mu$ L for **tBU** and **U** mixtures, respectively.

## 5.5. References

(1) Rubin, L. B.; Menshonkova, T. N.; Simukova, N. A.; Budowsky, E. I. The Effects of High-Intensity UV-Radiation on Nucleic Acids and their Components - I. Thymine. *Photochem. Photobiol.* **1981**, *34*, 339-344.

(2) Budovskii, E. I.; Simukova, N. A.; Tikhonova, A. M.; Men'shonkova, T. N.; Rubin, L. B. Two-Photon Photochemistry of Nucleic Acid Components. *Sov. J. Quantum Electron.* **1981**, *11*, 1602-1606.

(3) Kryukov, P. G.; Letokhov, V. S.; Nikogosyan, D. N.; Borodavkin, A. V.; Budowsky, E. I.; Simukova, N. A. Multiquantum Photoreactions of Nucleic Acid Components in Aqueous Solution by Powerful Ultraviolet Picosecond Radiation. *Chem. Phys. Lett.* **1979**, *61*, 375-379.

(4) Khoroshilova, E. V.; Nikogosyan, D. N. Photochemistry of Uridine on High Intensity Laser UV Irradiation. *J. Photochem. Photobiol. B* **1990**, *5*, 413-427.

(5) Angelov, D.; Berger, M.; Cadet, J.; Getoff, N.; Keskinova, E.; Solar, S. Comparison of The Effects of High-Power UV-Laser Pulses and Ionizing-Radiation on Nucleic-Acids and Related-Compounds. *Radiat. Phys. Chem.* **1991**, *37*, 717-727.

(6) Menshonkova, T. N.; Simukova, N. A.; Budowsky, E. I.; Rubin, L. B. The Effect Of High-Intensity Ultraviolet-Irradiation On Nucleic-Acids And Their Components - Cleavage Of N-Glycosidic Bond In Thymidine, Adenosine And 2'-Deoxyadenosine. *FEBS Lett.* **1980**, *112*, 299-301.

(7) Cadet, J.; Wagner, J. R.; Angelov, D. Biphotonic Ionization of DNA: From Model Studies to Cell. *Photochem. Photobiol.* **2019**, *95*, 59-72.

(8) Douki, T.; Angelov, D.; Cadet, J. UV Laser Photolysis of DNA: Effect of Duplex Stability on Charge-Transfer Efficiency. *J. Am. Chem. Soc.* **2001**, *123*, 11360-11366.

(9) Masnyk, T. W.; Nguyen, H. T.; Minton, K. W. Reduced Formation of Bipyrimidine Photoproducts in DNA UV Irradiated at High Intensity. *J. Biol. Chem.* **1989**, *264*, 2482-2488.

(10) Nikogosyan, D. N.; Angelov, D. A.; Oraevsky, A. A. Determination of Parameters of Excited States of DNA and RNA Bases by Laser UV Photolysis. *Photochem. Photobiol.* **1982**, *35*, 627-635.

(11) Douki, T.; Ravanat, J.-L.; Pouget, J.-P.; Testard, I.; Cadet, J. Minor Contribution of Direct Ionization to DNA Base Damage Induced by Heavy Ions. *Int. J. Radiat. Biol.* **2006**, *82*, 119-127.

(12) Madugundu, G. S.; Wagner, J. R.; Cadet, J.; Kropachev, K.; Yun, B. H.; Geacintov, N. E.; Shafirovich, V. Generation of Guanine–Thymine Cross-Links in Human Cells by One-Electron Oxidation Mechanisms. *Chem. Res. Toxicol.* **2013**, *26*, 1031-1033.

(13) Benimetskaya, L. Z.; Bulychev, N. V.; Kozionov, A. L.; Lebedev, A. V.; Nesterikhin, Y. E.; Novozhilov, S. Y.; Rautian, S. G.; Stockmann, M. I. 2-Quantum Selective Laser Scission of Polyadenilic Acid in the Complementary Complex with a Dansyl Derivative of Oligothymidilate *FEBS Lett.* **1983**, *163*, 144-149.

(14) Gantchev, T. G.; Grabner, G.; Keskinova, E.; Angelov, D.; Vanlier, J. E. Hematoporphyrin-Sensitized Degradation of Deoxyribose and DNA in High-Intensity Near-UV Picosecond Pulsed-Laser Photolysis. *Radiat. Phys. Chem.* **1995**, *45*, 111-119.

(15) Gantchev, T.; Keskinova, E.; Kaltchev, M.; Angelov, D. Photoproducts Generated from Hematoporphyrin under High-Intensity Picosecond Flash-Photolysis - Evidences for Involvement of Biphotonic Processes. *Radiat. Environ. Biophys.* **1990**, *29*, 225-239.

(16) Vendrell-Criado, V.; Rodríguez-Muñiz, G. M.; Yamaji, M.; Lhiaubet-Vallet, V.; Cuquerella, M. C.; Miranda, M. A. Two-Photon Chemistry from Upper Triplet States of Thymine. *J. Am. Chem. Soc.* **2013**, *135*, 16714-16719.

(17) Cai, X.; Sakamoto, M.; Fujitsuka, M.; Majima, T. Higher Triplet Excited States of Benzophenones and Bimolecular Triplet Energy Transfer Measured by Using Nanosecond–Picosecond Two-Color/Two-Laser Flash Photolysis. *Chem. Eur. J.* **2005**, *11*, 6471-6477.

(18) Cai, X.; Sakamoto, M.; Hara, M.; Sugimoto, A.; Tojo, S.; Kawai, K.; Endo, M.; Fujitsuka, M.; Majima, T. Benzophenones in The Higher Triplet Excited States. *Photochem. Photobiol. Sci.* **2003**, *2*, 1209-1214.

(19) González-Luque, R.; Climent, T.; González-Ramírez, I.; Merchán, M.; Serrano-Andrés, L. Singlet–Triplet States Interaction Regions in DNA/RNA Nucleobase Hypersurfaces. *J. Chem. Theory Comput.* **2010**, *6*, 2103-2114.

(20) Harada, Y.; Okabe, C.; Kobayashi, T.; Suzuki, T.; Ichimura, T.; Nishi, N.; Xu, Y.-Z. Ultrafast Intersystem Crossing of 4-Thiothymidine in Aqueous Solution. *J. Phys. Chem. Lett.* **2010**, *1*, 480-484.

(21) R. Alzueta, O.; Cuquerella, M. C.; Miranda, M. A. Transient UV–Vis Absorption Spectroscopic Characterisation of 2'-Methoxyacetophenone as a DNA Photosensitizer. *Spectrochim. Acta A Mol. Biomol. Spectrosc.* **2019**, *218*, 191-195.

(22) Liu, L.; Pilles, B. M.; Reiner, A. M.; Gontcharov, J.; Zinth, W. 2'-Methoxyacetophenone: an Efficient Photosensitizer for Cyclobutane Pyrimidine Dimer Formation. *ChemPhysChem* **2015**, *16*, 3483-3487.

(23) Vendrell-Criado, V.; Lhiaubet-Vallet, V.; Yamaji, M.; Cuquerella, M. C.; Miranda, M. A. Blocking Cyclobutane Pyrimidine Dimer Formation by Steric Hindrance. *Org. Biomol. Chem.* **2016**, *14*, 4110-4115.

(24) Cuquerella, M. C.; Lhiaubet-Vallet, V.; Cadet, J.; Miranda, M. A. Benzophenone Photosensitized DNA Damage. *Acc. Chem. Res.* **2012**, *45*, 1558-1570.

(25) Heyroth, F. F.; Loofbourow, J. R. Changes in The Ultraviolet Absorption Spectrum of Uracil and Related Compounds under The Influence of Radiations. *J. Am. Chem. Soc.* **1931**, *53*, 3441-3453.

(26) Sinsheimer, R. L.; Hastings, R. A Reversible Photochemical Alteration of Uracil and Uridine. *Science* **1949**, *110*, 525-526.

(27) Wacker, A.; Dellweg, H.; Träger, L.; Kornhauser, A.; Lodemann, E.; Türck, G.; Selzer, R.; Chandra, P.; Ishimoto, M. Organic Photochemistry of Nucleic Acids. *Photochem. Photobiol.* **1964**, *3*, 369-394.

(28) Padva, A.; LeBreton, P. R.; Dinerstein, R. J.; Ridyard, J. N. A. UV Photoelectron Studies of Biological Pyrimidines: The Electronic Structure of Uracil. *Biochem. Biophys. Res. Commun.* **1974**, *60*, 1262-1268.

(29) Wentworth, W. E.; Chen, E. Experimental Determination of the Electron Affinity of Several Aromatic Aldehydes and Ketones. *J. Phys. Chem.* **1967**, *71*, 1929-1931.

(30) Yang, N.-C.; McClure, D. S.; Murov, S.; Houser, J. J.; Dusenbery, R. Photoreduction of Acetophenone and Substituted Acetophenones. *J. Am. Chem. Soc.* **1967**, *89*, 5466-5468.

(31) Burr, J. G.; Gordon, B. R.; Park, E. H. The Mechanism of Photohydration of Uracil and n-Substituted Uracils. *Photochem. Photobiol.* **1968**, *8*, 73-78.

(32) Wang, S. Y.; Nnadi, J. C. Mechanism for the Photohydration of Pyrimidines. *Chem. Commun.* **1968**, *19*, 1160-1162.

# CHAPTER 6

## Chapter 6. Instrumentation

---



## 6.1. General Instrumentation

### 6.1.1. Nuclear Magnetic Resonance (NMR)

The one-dimensional ( $^1\text{H}$ ,  $^{13}\text{C}$ , DEPT-135) and two-dimensional (HSQC and NOESY) NMR spectra were measured by a 300 MHz Varian Bruker instrument, using DMSO- $d_6$  and  $\text{CDCl}_3$  as solvents. The corresponding solvent signals were taken as the reference (chemical shift of  $\delta$  of *ca* 2.50 ppm and 7.26 ppm for  $^1\text{H}$  NMR and 39.52 and 77.16 ppm for  $^{13}\text{C}$  NMR, respectively). Coupling constants ( $J$ ) are given in hertz (Hz).

### 6.1.2. Chromatography

#### 6.1.2.1. Thin-Layer Liquid Chromatography (TLC) and Liquid Chromatography (LC)

Thin-layer liquid analysis were performed using  $\text{SiO}_2$  (silica gel F<sub>254</sub>) as the stationary phase. In the case of Liquid Chromatography silica gel 60, SDS, 230-400 mesh ASTM was used.

#### 6.1.2.2. Ultra Performance Liquid Chromatography Tandem Mass Spectrometer (UPLC-MS/MS)

A QToF spectrometer coupled with a liquid chromatography system, with a conditional autosampler at 10°C, was used to determine the exact mass values. The separation was carried out on an UPLC with a BEC C18 column (50 mm Å ~ 2.1 mm i.d., 1,7 μm). The ESI source was operated in positive or negative ionisation mode with the capillary voltage at 1.9 kV or 2.4 kV, respectively. The source's temperature was set at 80°C (positive mode) and 400°C (negative mode), and the cone and desolvation gas flows were 20 and 800 L h<sup>-1</sup>, respectively. All data were collected in centroid mode, and

Leucine-enkephalin was used as the lock mass generating and  $[M+H]^+$  ion ( $m/z$  556.2771) or  $[M-H]^-$  ion ( $m/z$  556.2771) at a concentration of 250 pg/mL and flow rate of 50  $\mu\text{L min}^{-1}$  to ensure accuracy during the MS analysis.

## 6.2. Photochemical Instrumentation

### 6.2.1. UV-VIS Absorption Spectroscopy

All UV-Vis absorption spectra were registered with a simple beam Varian Cary 50 spectrophotometer, using quartz cells of 1 cm optical path length.

### 6.2.2. Steady-State Photolysis

Irradiation of the samples was performed under anaerobic conditions in quartz cuvettes of 1 cm optical path length, quartz flasks or pyrex vessels, using three different systems:

- A Luzchem photoreactor (model LZV-4V) with a variable number of lamps (maximum output at 350 nm), for UVA irradiations.
- A Xenon lamp (75 W) equipped with a monochromator from Photon Technology International (PTI) for monochromatic irradiations.
- A Nd: YAG SL404G-10 Spectron Laser Systems, operating at 10 Hz, with a  $\lambda_{\text{exc}} = 355$  nm and an energy pulse of 45 mJ pulse<sup>-1</sup>, for the biphotonic irradiations.

### 6.2.3. Laser Flash Photolysis Spectroscopy (LFP)

For the LFP a pulsed Nd: YAG SL404G-10 Spectron Laser Systems, was used at 355 nm (3<sup>rd</sup> harmonic) as the excitation wavelength, and the energy of the single pulses (*ca* 10 ns duration) was setted under 15 mJ pulses. The apparatus consisted of the pulsed laser, a pulsed Lo255 Oriel Xenon lamp, a

77200 Oriel monochromator, an 70705 Oriel photomultiplier tube (PMT) housing, a 70705 PMT power supply and a TDS-640A Tektronix oscilloscope. The output signal from the oscilloscope was transferred to a personal computer and all experiments were performed in quartz cuvettes of 1 cm optical path.

#### 6.2.4. Phosphorescence Emission Measurements

The phosphorescence spectra were recorded using a spectrophosphorimeter Photon Technology International (PTI, TimeMater TM/2003) equipped with a pulsed Xenon lamp. Compounds were dissolved in ethanol, adjusting their absorbance at ca. 0.8 at the excitation wavelength, with cuvettes of 1cm optical pathway. Measurements were carried out in a quartz tube (0.5 mm diameter) at 77 K.

Singlet oxygen emission lifetime was recorded at 1270 nm by means of a Hamamatsu NIR detector coupled to a laser photolysis cell in a right angle geometry. Samples were excited with the above described Nd-YAG laser at 355 nm, and using acetophenone as a reference compound (absorbance ca. 0.6 at  $\lambda_{exc} = 355$  nm). The output current of the photodiode was amplified and sent to a TDS-640A Tektronix oscilloscope, being the resulting signal transferred to a personal computer.



# CHAPTER 7

## Chapter 7. General Conclusions

---



In this Doctoral Thesis, photosensitised DNA damage has been investigated, with special emphasis on the formation of cyclobutane pyrimidine dimers (CPD) from their triplet excited states. Thus, a thorough research work has been carried out to get a deeper insight into the nature of the molecular processes involved.

In this context, photosensitisation is a convenient tool to investigate triplet mediated chemistry, as in this way the formation of singlet excited states is circumvented, facilitating the mechanistic analysis. In general, aromatic ketones are appropriate triplet photosensitisers. Among them, 2'-methoxyacetophenone has been selected in the present work because it presents an enhanced UVA absorption as compared with other acetophenone derivatives, which allows its selective excitation in the presence of pyrimidine bases.

With this background, a full transient UV-Vis absorption spectroscopic characterisation of 2'-methoxyacetophenone has been performed in Chapter 3, which has:

- *Confirmed its potential as DNA photosensitiser, not only for CPD formation, but also for oxidative damage.*
- *Permitted to determine photophysical parameters of its triplet excited state, such as its lifetime, singlet oxygen quantum yield or rate constants for quenching by thymine derivatives, supporting its suitability for mechanistic studies.*

Next, this photosensitiser has been used in Chapter 4 to unveil the nature of the rate controlling step in the photosensitised dimerisation of a more extensive family of homo- and hetero- bipyrimidine polymethylene linked models. They have been synthesised varying their substitution at C5 as well as the length of the linking bridge, subsequently, their 2M

photosensitised reaction has been performed and monitored by UV spectroscopy. The recorded spectra have shown the complete disappearance of the enone chromophore of the pyrimidine bases which, in agreement with CPD formation. After evaluation of the photoreaction kinetics for all compounds, the following tendencies have been established:

- *The photosensitised intramolecular CPD formation in the model bipyrimidine compounds is efficient. All the photoproducts obtained have been isolated and identified as the corresponding CPD by means of NMR spectroscopic analysis.*
- *The process is faster when the bipyrimidine model contains a thymine unit.*
- *Elongation of the polymethylene bridge between the two bases results in a decrease of the photoreaction rate.*
- *By modification of the substitution pattern at C5, the length of the linking bridge or the substrate concentration it is possible to switch from a reaction governed by the intrinsic excited state dimerisation process to an energy transfer controlled process.*

Finally, 2'-methoxyacetophenone has been used in Chapter 5 to explore the possibility of producing photosensitised pyrimidine biphotonic chemistry by means of high energy laser pulses. A new approach has been followed, which involves absorption of a first photon by the photosensitiser followed by a triplet energy transfer to the pyrimidine unit. The resulting pyrimidine triplet excited state absorbs the second photon to populate a higher triplet state from which new chemistry occurs. The importance of this new strategy resides in:

- *Reduction of the synthetic effort compared to the intramolecular biphotonic approach, which requires the synthesis of dyads where the photosensitiser is covalently bound to the pyrimidine unit.*

- *A large structural variability in the systems to be challenged.*

The concept has been tested in two model reactions, the Norrish-Yang photoreaction of a 5-*tert*-butyl uracil and the photohydration of its non-substituted analogue. In both cases the feasibility of the new approach has been demonstrated, as analysis of the photomixtures after high intensity irradiation reveals formation of the biphotonic photoproducts only in the presence of the photosensitiser 2'-methoxyacetophenone.



# CHAPTER 8

## Chapter 8. Summary-Resumen-Resum

---



## 8.1. Summary

Solar light is necessary for life on Earth and its beneficial effects are beyond any doubt. However, ultraviolet radiation (UV), which is part of the solar spectrum, can be harmful to living beings, as it is capable of generating mutations in DNA, which are closely related to the appearance of skin cancer.

DNA damage can be produced both by direct absorption of UV radiation by this biomolecule and through photosensitised processes. Specially important in the case of the UVA range, which represents 90% of the solar UV radiation that reaches the Earth's surface. Although this light is barely absorbed by DNA, it is able to produce damage to the genetic material due to the presence of UVA-absorbing photosensitising compounds in its vicinity.

This Doctoral Thesis is focused on photosensitised DNA damage, more concretely, on the mechanistic understanding of the processes involved in the formation of pyrimidine dimers through the triplet excited state.

For this purpose, the photochemistry of DNA models of increasing complexity has been studied, using 2'-methoxyacetophenone as photosensitiser.

Initially, the complete characterisation of this photosensitiser has been carried out in Chapter 3 by means of UV-Vis transient absorption spectroscopy. Its triplet excited state has been investigated in-depth, determining its spectrum, lifetime, rate constant for quenching by a thymine model, and capability to produce  $^1\text{O}_2$ . The aim was to demonstrate its potential as a DNA photosensitiser, not only for cyclobutane pyrimidine dimer (CPD) formation, but also for oxidative damage.

From the obtained results, the suitability of 2'-methoxyacetophenone as a DNA photosensitiser for mechanistic studies has been confirmed. Hence, it has been used in Chapter 4 to determine the nature of the rate controlling reaction step in the photosensitised cyclodimerisation of homo- and hetero- bipyrimidine models, where the nucleobases are linked by polymethylene bridges of different length and present different substitution patterns at the C5 position.

In all cases, selective irradiation of 2'-methoxyacetophenone in the presence of the bipyrimidine models results in the formation of the corresponding CPD, demonstrating the efficiency of the photosensitised process. Analysis of the reaction kinetics for all compounds has allowed establishing the reactivity order, which is rationalised on the basis of a thorough photophysical study. Thus, it has been found that upon variation of the substitution pattern and the length of the linking bridge it is possible to switch from a process governed by the intrinsic excited state cyclodimerisation to a process controlled by the energy transfer from the photosensitiser to the base.

Finally, the biphotonic photosensitisation of pyrimidine derivatives has been explored in Chapter 5, following a new and more general approach than the one recently reported in the literature. This approach does not require the synthetic effort associated with the preparation of covalently linked photosensitiser and pyrimidine units. It is based on the absorption of a first photon by 2'-methoxyacetophenone, followed by triplet energy transfer to the pyrimidine, which then receives a second photon to reach a higher triplet state that gives rise to new chemistry. The feasibility of this approach has been demonstrated through the study of two model reactions, namely the Norrish-Yang photoreaction and the photohydration of uracil derivatives.

## 8.2. Resumen

La luz solar es necesaria para la vida en la Tierra y sus efectos beneficiosos están fuera de toda duda. Sin embargo, la radiación ultravioleta (UV), que forma parte del espectro solar, puede resultar dañina para los seres vivos dado que es capaz de producir mutaciones en el ADN, íntimamente relacionadas con la aparición de cáncer de piel.

El daño al ADN puede producirse tanto por absorción directa de la radiación UV por parte de esta biomolécula como mediante procesos fotosensibilizados, principales responsables en el caso del rango de radiación UVA, que representa el 90% de la radiación ultravioleta que llega a la superficie terrestre. De este modo, pese a que el ADN apenas absorbe este tipo luz, se pueden producir daños en el material genético debido a la presencia de compuestos fotosensibilizantes en su entorno que sí absorben en la zona UVA.

En este contexto, la presente Tesis Doctoral se centra en el daño fotosensibilizado al ADN, y más concretamente en la elucidación de los mecanismos de los procesos involucrados en la formación de dímeros de pirimidina en el estado excitado triplete. Para ello se ha estudiado la fotoquímica de distintos modelos de ADN de complejidad creciente, usando como fotosensibilizador 2'-metoxiacetofenona (2M).

En primer lugar, se ha llevado a cabo la caracterización completa de este fotosensibilizador mediante espectroscopía de absorción transitoria UV-Vis (Capítulo 3 de la Tesis). Se ha estudiado en profundidad su estado excitado triplete, determinándose su espectro, tiempo de vida, constante de desactivación por un modelo de timina y capacidad para producir  $^1\text{O}_2$ . Con ello se pretende demostrar su potencial como fotosensibilizador del ADN, no

solo para la formación de dímeros ciclobutánicos (DCB), sino también de daño oxidativo.

En base a los resultados obtenidos se ha confirmado la idoneidad de 2M como fotosensibilizador del ADN y su idoneidad para estudios mecanísticos, por lo que se ha empleado en el Capítulo 4 para determinar la naturaleza del paso dominante de la velocidad de reacción en la ciclodimerización fotosensibilizada de modelos homo- y hetero-bipirimidínicos unidos por puentes polimetilénicos y con distinta sustitución en la posición C5.

La irradiación selectiva de 2M en presencia de estos modelos da lugar en todos los casos a la formación de sus correspondientes DCB, demostrando la eficiencia del proceso fotosensibilizado. El análisis de la cinética de reacción para cada compuesto ha permitido establecer su orden relativo de reactividad, que se ha justificado a través de un estudio fotofísico en el que variando la sustitución y la longitud del puente se ha demostrado que ocurre un cambio desde un proceso gobernado por el proceso de dimerización intrínseca en el estado excitado a un proceso controlado por la transferencia de energía entre el fotosensibilizador y la nucleobase.

Finalmente, en el Capítulo 5 se explora la fotosensibilización bifotónica de derivados pirimidínicos, siguiendo una nueva aproximación más general que la existente en la bibliografía y que evita el esfuerzo sintético de unir covalentemente el fotosensibilizador al modelo estudiado. Esta aproximación se basa en la absorción de un primer fotón por la 2M, seguida de una transferencia de energía triplete-triplete a una pirimidina, que recibe un segundo fotón para alcanzar un estado triplete superior que da lugar a una nueva química, desde este estado de alta energía. La viabilidad de dicha aproximación se ha demostrado mediante el estudio de dos reacciones

modelo, la fotorreacción Norrish-Yang y la fotohidratación de dos derivados de uracilo.

### 8.3. Resum

La llum solar és necessària per a la vida a la Terra i els seus efectes beneficiosos estan fora de tot dubte. No obstant això, la radiació ultraviolada (UV), que forma part de l'espectre solar, pot resultar nociva per als éssers vius atés que és capaç de produir mutacions en l'ADN que estan íntimament relacionades amb l'aparició de càncer de pell.

El dany a l'ADN pot produir-se tant per absorció directa de la radiació UV com mitjançant processos de fotosensibilització. Aquests tenen especial importància en el cas de la radiació UVA, que representa el 90% de la radiació ultraviolada que arriba a la superfície terrestre. Malgrat que l'ADN gairebé no absorbeix aquest tipus de llum, aquesta és capaç de modificar el material genètic amb la presència de compostos fotosensibilitzadors al seu voltant, els quals sí absorbeixen la radiació UVA.

Aquesta Tesi Doctoral s'ha centrat en el dany fotosensibilitzat a l'ADN, i més concretament, en la comprensió mecanística dels processos involucrats en la formació de dímers de pirimidina a través de l'estat excitat. Per fer això, s'ha estudiat la fotoquímica de diferents models d'ADN de complexitat creixent, utilitzant la 2'-metoxiacetofenona (2M) com a fotosensibilitzador.

Inicialment s'ha dut a terme la caracterització completa d'aquest fotosensibilitzador en el Capítol 3, mitjançant espectroscòpia d'absorció transitòria UV-Vis. S'ha estudiat en profunditat el seu estat excitat triplet mitjançant la determinació del seu espectre, temps de vida i constant de desactivació per amb un model de timina sintetitzat *ex professo*, i també la seua capacitat per a produir  $^1\text{O}_2$ . Amb això s'ha pretés demostrar el seu

potencial com a fotosensibilitzador de l'ADN, tant per a la formació de dímers ciclobutànics (DCBs), com per al dany oxidatiu.

Dels resultats obtinguts s'ha confirmat la idoneïtat de la 2M com a fotosensibilitzador d'ADN per a estudis mecanístics. Per fer-ho, s'ha emprat en el Capítol 4 per a determinar la naturalesa del pas dominant de reacció en la ciclodimerització fotosensibilitzada de models homo- i hetero-bipirimidínics, en els quals les bases s'han unit per ponts metilènics i amb diferent substitució en la posició C5.

La irradiació selectiva de la 2M en presència d'aquests models ha donat lloc en tots els casos a la formació dels seus corresponents DCBs, cosa que demostra l'eficiència del procés fotosensibilitzador. L'anàlisi de la cinètica de reacció per a cada compost ha permès establir l'ordre de reactivitat, que ha estat justificat a través d'un estudi fotofísic. En ell s'ha constatat que, variant la substitució i la longitud del pont d'unió, és possible passar d'un procés governat per la dimerització intrínseca a un de controlat per la transferència d'energia entre el fotosensibilitzador i la base.

Finalment, s'ha explorat la fotosensibilitació bifotònica de derivats pirimidínics al Capítol 5 a través d'una nova aproximació més generalista que l'existent en la bibliografia. Aquesta nova estratègia evita l'esforç sintètic d'unir covalentment el fotosensibilitzador a les unitats de pirimidina. Es basa en l'absorció d'un primer fotó per la 2-metoxiacetofenona seguida d'una transferència d'energia del triplet a la pirimidina que, en rebre el segon fotó, és capaç d'aconseguir un estat triplet superior que dona lloc a una nova química. La factibilitat d'aquesta aproximació s'ha demostrat mitjançant l'estudi de dues reaccions model: la fotorreacció Norrish-Yang i la fotohidratació de dos derivats d'uracil.

# CHAPTER 9

## Chapter 9. Scientific Contribution

---



## 9.1. Contribution to Congresses

- Alzqueta, O. R.; Cuquerella, M. C.; Miranda, M. A. "Biphotonic Chemistry of Pyrimidine Derivatives". 17th International Congress on Photobiology and 18th Congress of the European Society for Photobiology, Barcelona, Spain, 25th-30th August, **2019**. Oral communication.
- Alzqueta, O. R.; Cuquerella, M. C.; Miranda, M. A. "Photochemical Approach to 2'-Methoxyacetophenone as CPDs Photosensitiser". 27<sup>th</sup> Congress of the PhotoIUPAC, Dublin, Ireland, 8<sup>th</sup>-13<sup>th</sup> July, **2018**. Poster.
- Alzqueta, O. R.; Cuquerella, M. C.; Miranda, M. A. "Direct and Photosensitised Photochemistry of Linked Uracil and Thymine Dimers". 17<sup>th</sup> Congress of the European Society for Photobiology, Pisa, Italy, 4<sup>th</sup>-8<sup>th</sup> September, **2017**. Poster.

## 9.2. Publications

- Alzqueta, O. R.; Cuquerella, M. C.; Cadet, J.; Miranda, M. A. "Photosensitised Biphotonic Chemistry of Pyrimidine Derivatives" *Org. Biomol. Chem.* **2020**, *18*, 2227-2232.
- Alzqueta, O. R.; Cuquerella, M. C.; Miranda, M. A. "Triplet Energy Transfer versus Excited State Cyclization as the Controlling Step in Photosensitized Bypyrimidine Dimerization" *J. Org. Chem.* **2019**, *21*, 13329-13335.
  - Alzqueta, O. R.; Cuquerella, M. C.; Miranda, M. A. "Transient UV-Vis Absorption Spectroscopic Characterisation of 2'-Methoxyacetophenone as a DNA Photosensitiser". *Spectrochim. Acta A Mol. Biomol. Spectrosc.* **2019**, *218*, 191-195.